NEESR-II: SYSTEM BEHAVIOR FACTORS FOR COMPOSITE AND MIXED STRUCTURAL SYSTEMS

Work Plan for Testing Composite CFT Beam-Columns Specimens at MAST Laboratory (Part I)

Submitted to MAST Laboratory

by

Roberto T. Leon [1]
Jerome F. Hajjar [2]
Tiziano Perea [3]

[1] Project PI, Georgia Institute of Technology
[2] Project co-PI, University of Illinois
[3] Graduate Student, Georgia Institute of Technology

Contact Information:

Georgia Institute of Technology
Civil & Environmental Engineering
790 Atlantic Drive N.W.
Atlanta, GA 30332-0355
Room: Mason 308
Phone: 404/894-2220
roberto.leon@ce.gatech.edu

April, 2008

Table of Contents

1 Project Summary and Critical Information

1.1 Project Overview

This project is a NEESR-II award with the aim of developing system behavior factors for special and ordinary moment frames with steel beams and composite beam-columns (composite frame system). The system behavior factors to be developed in this research include the structural system factor (R), lateral displacement amplification factor (C_δ), and the system overstrength factor (Ω_0). This research also intends to provide practical guidelines for the analysis and design of this kind of composite system based on results of studies similar to those proposed by the ATC-63 guidelines.

In order to reach these goals, analytical and experimental studies will be conducted. The analytical studies will include parametric studies using fiber and finite element models. The experimental part to be conducted at MAST (Figure 1) includes testing of 24 full-scale slender composite beam-columns (10 CFT, 8 RCFT and 6 SRC) to evaluate their strength, ductility and stiffness under large lateral displacements (Figure 2 and Figure 3).

Figure 1. General view of the MAST system

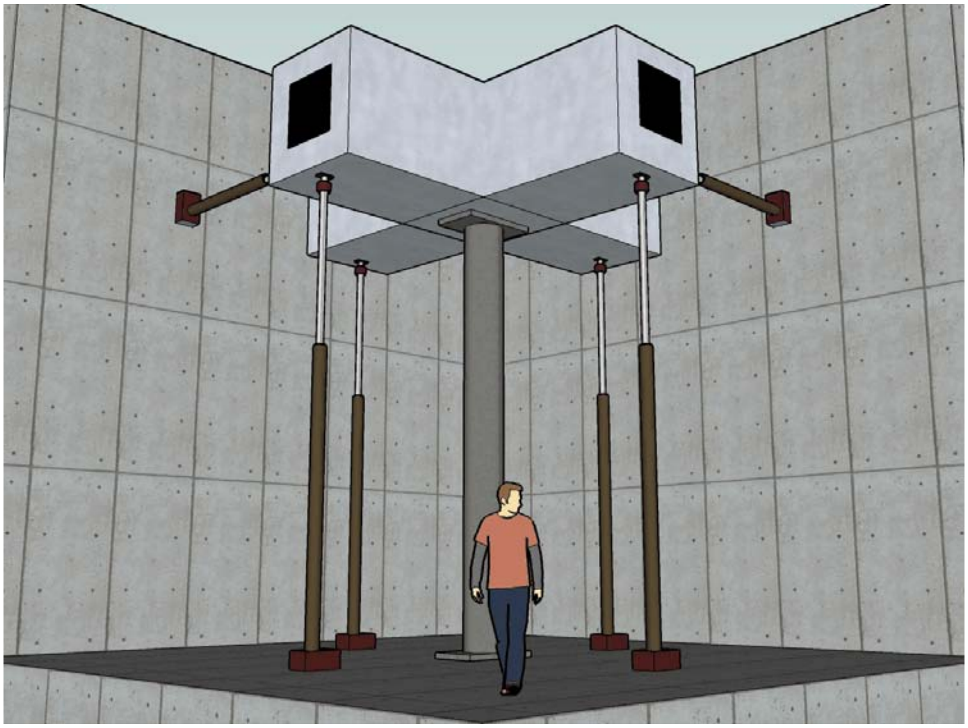

Figure 2. View of the MAST with a circular CFT specimen

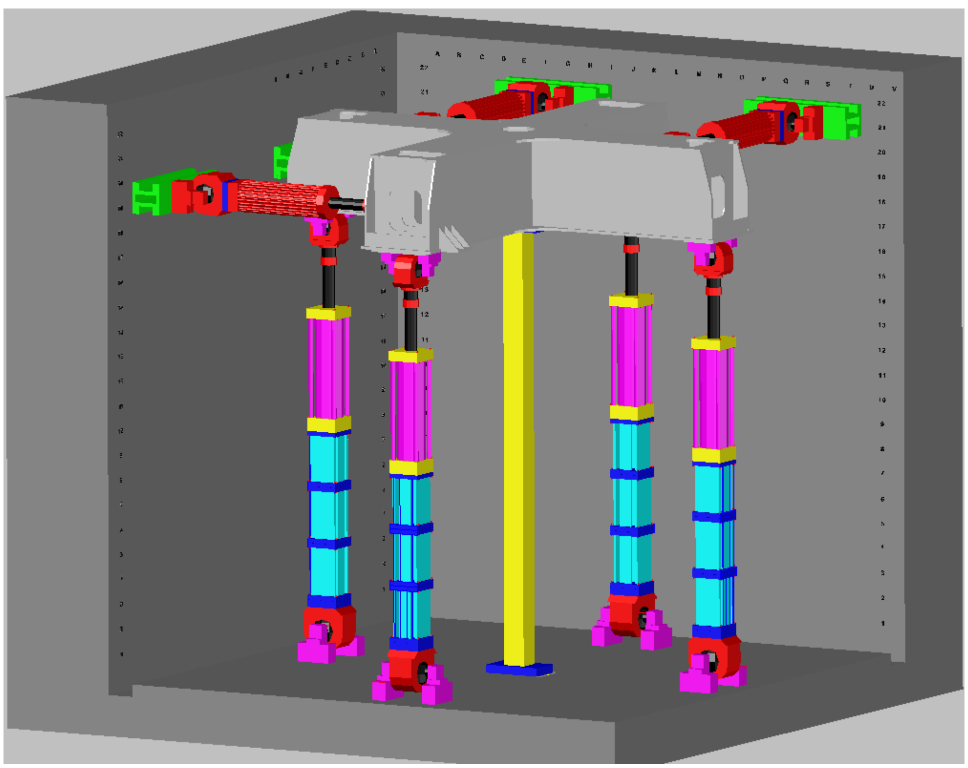

Figure 3. View of the MAST with a rectangular CFT specimen

1.2 Master Schedule

This research project duration is 3 years, with a starting date of August, 2006. Use of the MAST facility at the University of Minnesota is scheduled for the second and third years of the project. The steel will be fabricated and shipped to the MAST laboratory from LeJeune Steel (a local fabricator in Minneapolis) in the middle of May. The concrete infill or encasement will then be cast at MAST. Completion of test setup and initial instrumentation installation will take approximately one month. Testing is estimated to take place over a period of one week per specimen at the outset. A faster schedule is foreseen as experience is gained. Dismantling of the test setup and instrumentation is estimated to take 1 week. Removal of the specimens from the lab floor is estimated to take 1 day. Considering unforeseen delays even in this idealistic estimate, the PIs estimate that the proposed specimens will require use of the facility for two periods of two to three months. The planned schedule and duration of use of the MAST facility for the CFT portion of the tests is summarized in Table 1. Some important dates are listed below.

Table 1. Planned Schedule for use of MAST NEES Facility

TASK	2008												2009											
	1	2	3	4	5	6	7	8	9	10	11	12	1	2	3	4	5	6	7	8	9	10	11	12
Work Plan																								
Shipping steel for CFT specimens to MAST																								
Casting and curing CFT specimens																								
Instrumentation of the CFT specimens																								
Testing 18' long CFT's (set 1, 9 specimens)																								
Demolition of set 1																								
Testing 26' long CFT's (set 2, 9 specimens)																								
Demolition of set 2																								
Interpreting data for sets 1 & 2																								

Important dates (approximate):

- May 21, 2008 (M): First day at MAST. Access to staging area, casting and instrumentation
- June 23, 2008 (M): Testing of the first shorter (L=18ft) CFT specimen

- August 1, 2008 (F): Testing of the first high (L=26ft) CFT specimen
- November 30, 2008 (T): Last day at MAST. Testing and demolition completed.

1.3 Researcher Personnel

The researcher personnel involved at the activities at MAST are enlisted below. The time out schedules of each one is also mentioned.

Roberto T. Leon, Ph.D. (PI), Georgia Institute of Technology

- April 25-25: ASCE Structures
- May 25-31: Jornadas Sudamericanas
- June 2-4: International Bridge Conference
- June 16 -22: NEES Annual Meeting
- June 23-27: Connections Workshop and AISC TC Meetings
- June 30-July 8: Family vacation
- July 20-25: CCVI

Jerome F. Hajjar, Ph.D., P.E. (Co-PI), University of Illinois

- May 10-11: Busy that weekend
- May 16-18: Krawinkler Symposium
- May 23-26: Busy that weekend
- June 16 or 17-20: NEES Annual Meeting
- June 23-27: Connections Workshop and AISC TC Meetings
- June 27-July 14: Busy; little to no E-mail, little phone
- July 20-28: CCVI (returning July 28)

Tiziano Perea (Ph.D. Graduate Student), Georgia Institute of Technology

- May 2: End of classes and exams at GT
- July 20 – July 25: CCVI

Mark Denavit (Ph.D. Graduate Student), University of Illinois

2 Specimen details

2.1 General description of the specimens

This section gives a general description of the specimens to be tested at the MAST Lab. Table 2 and Table 3 show general information for the circular and rectangular CFT specimens. As seen in these tables, the parameters chosen in these specimens intend to develop data on the behavior of slender composite beam-columns (high λ) with the highest slenderness available from commercial steel cross-sections (high b/t or D/t). The behavior of these specimens will be evaluated with two concrete strengths (5ksi and 12ksi) associated to two lengths (18ft and 26ft).

Table 2. Circular CFT specimens

Specimen	Steel section	D/t	Fy (ksi)	f'c (ksi)	L (ft)	λ
CCFT20x0.25	HSS20x0.25	86	42	5	18.0	1.03
					26.0	1.49
		86	42	12	18.0	1.25
					26.0	1.81
CCFT12.75x0.25	HSS12.75x0.25	55	42	5	18.0	1.56
					26.0	2.25
		55	42	12	18.0	1.85
					26.0	2.68
CCFT5.563x0.134	HSS5.563x0.134	45	42	5	18.0	0.88
					26.0	1.27

Table 3. Rectangular CFT specimens

Specimen	Steel section	b/t	Fy (ksi)	f'c (ksi)	L (ft)	λ
RCFT20x12x0.3125w (M at weak axis)	HSS20x12x0.3125	67	46	5	18.0	1.38
					26.0	2.00
		67	46	12	18.0	1.61
					26.0	2.33
RCFT12x20x0.3125s (M at strong axis)	HSS20x12x0.3125	67	46	5	18.0	0.89
					26.0	1.28
		67	46	12	18.0	1.02
					26.0	1.47

All the details and information regarding the SRC specimens will be discussed in a second part of the work plan (*Work Plan for Testing Composite SRC Beam-Columns Specimens*).

The following of testing is initially proposed:

Table 4. Testing Sequence

#	Specimen	L	fc'	K	End Conditions
1	CCFT5.563x0.134	18'	5ksi	0.5	(double fixed)
2	CCFT12.75x0.25	18'	5ksi	2	(fixed-pinned)
3	CCFT12.75x0.25	18'	12ksi	2	"
4	CCFT20x0.25	18'	5ksi	2	"
5	CCFT20x0.25	18'	12ksi	2	"
6	RCFT20x12x0.3125w	18'	5ksi	2	"
7	RCFT20x12x0.3125w	18'	12ksi	2	"
8	RCFT20x12x0.3125s	18'	5ksi	2	"
9	RCFT20x12x0.3125s	18'	12ksi	2	"

The same sequence may be used for the long specimens (L=26')

2.2 Steel requirements

The CFT specimens will be built using HSS cross-sections with A500 Gr. B steel (F_y=42ksi for round HSS, F_y=46ksi for rectangular HSS, F_u=58ksi for both). White-wash painting of the steel specimens will be made. As listed in Table 5, all the 18 CFT specimens have a total weight of about 20 kips.

Table 5. Summary of the total weight of the steel

Cross Section	Weight (kip)
HSS20x0.25	4.64
HSS12.75x0.25	2.94
HSS5.563x0.134	0.34
HSS20x12x0.3125	11.74
	19.67

Stress-strain tests (ASTM E8 - 6.9.2 - Type I) will be conducted at Georgia Tech in order to establish the real properties of the steel used in the specimens to calibrate all the analytical models (Figure 4). The stress-strain tests will be performed on coupons cut from stubs provided by Atlas tubes or from the long specimens. In addition, mill certificates provided by Atlas tube will be considered; a summary of the mill certification data is shown in Table 6. So far, all the analytical results shown in this work plan are based on typical over-strength factors proposed by Liu at al. (2005), which gave R_y=1.4 for A500 Gr. B steel. Thus, calculations are based on R_yF_y=64.4ksi for RCFTs and R_yF_y=58.8ksi for CCFTs.

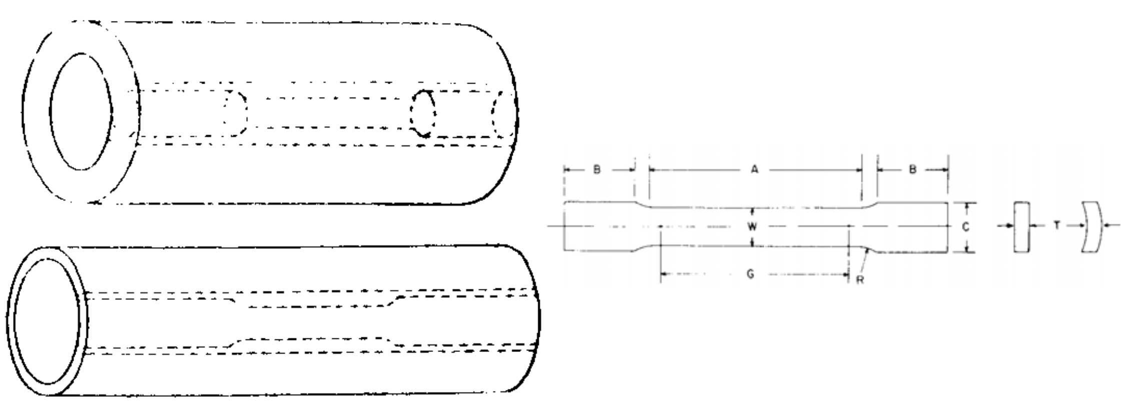

Figure 4. Steel coupons: 10in length (ASTM E8 – 6.9.2 – Type I)

Table 6. Summary of mill certifications from Atlas Tube

TUBE	Heat No.	Fy	Ry	Fu	Ru	Eln.2in
HSS 5.563x0.134x18	680796	61.008	1.453	72.880	1.257	25.0%
HSS 5.563x0.134x26	680796	61.008	1.453	72.880	1.257	25.0%
HSS 12.75x0.25x18	481426	56.571	1.347	71.860	1.239	34.6%
HSS 12.75x0.25x18	481426	56.571	1.347	71.860	1.239	34.6%
HSS 12.75x0.25x26	750789	51.068	1.216	69.680	1.201	28.4%
HSS 12.75x0.25x26	750789	51.068	1.216	69.680	1.201	28.4%
HSS 20x0.25x18	D43542	50.550	1.204	71.380	1.231	39.0%
HSS 20x0.25x18	D43542	50.550	1.204	71.380	1.231	39.0%
HSS 20x0.25x26	D43542	50.550	1.204	71.380	1.231	39.0%
HSS 20x0.25x26	T43452	48.330	1.151	73.170	1.262	37.0%
HSS 20x12x0.3125x18	47212	57.640	1.253	75.620	1.304	38.0%
HSS 20x12x0.3125x18	47212	57.640	1.253	75.620	1.304	38.0%
HSS 20x12x0.3125x18	47212	57.640	1.253	75.620	1.304	38.0%
HSS 20x12x0.3125x18	47212	57.640	1.253	75.620	1.304	38.0%
HSS 20x12x0.3125x26	47212	57.640	1.253	75.620	1.304	38.0%
HSS 20x12x0.3125x26	47212	57.640	1.253	75.620	1.304	38.0%
HSS 20x12x0.3125x26	46839	53.940	1.173	71.980	1.241	40.0%
HSS 20x12x0.3125x26	46839	53.940	1.173	71.980	1.241	40.0%

2.3 Concrete requirements

The estimates for the amount of concrete needed to fill the tubes are 10 cubic yards and 9.8 cubic yards for the 5ksi (10 specimens) and 12ksi (8 specimens), respectively. This volume does not consider the concrete for cylinders and waste. At least thirty cylinders (0.22 cubic yard) will be cast from each truck to ascertain the real strength of the concrete in each specimen and to calibrate the analytical results. The required amounts of concrete for each series are shown in Table 7. The amount of concrete for each strength type will be transported by one truck as either a 5 or 7 cubic yard batch, so the casting of all the specimens with the same strength and length can be completed at the same time.

Table 7. Volumes of concrete

Truck #	Strength (ksi)	Length (ft.)	Volume required (yds.^{3})	Volume ordered (yds.^{3})
1	5	18	4.1	5.0
2	12	18	4.0	5.0
3	5	26	5.9	7.0
4	12	26	5.8	7.0

In practice, the concrete filling procedure can be made pumping or dropping the concrete from top (as in Figure 5.a) or from bottom (as in Figure 5.b). For the specimens previously discussed, casting will take place at MAST, and the concrete will be pumped to the top of the tubes and dropped from there. The contractor and the research team have to make sure the concrete satisfy all the requirements for strength, fluidity, vibrating, curing, etc. to ensure a good quality and avoid segregation, voids, low strength, or any other problems. Self-consolidating concrete with mix characteristics approximating those shown in Table 8 will be used. The research team has been in contact with Mr. Kevin McDonald from Cemstone Corporation, which will provide the materials.

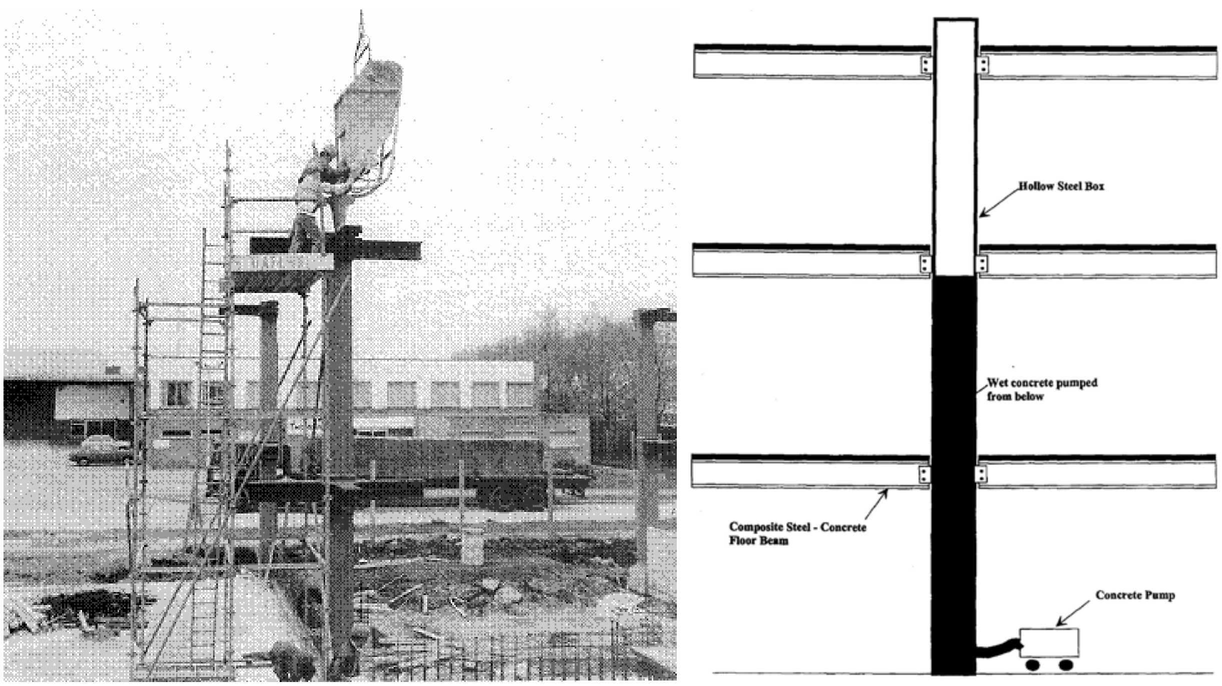

a) CIDECT 5, 1995 b)Uy and Das, 1997)

Figure 5. On-site concrete filling procedures for CFT columns

The following list show some issues/concerns in concrete delivery and placement:

- Delivery very early in the day to have clean trucks
- 4 mixes – 5ksi and 12ksi, ¾ aggregates
- Self-consolidating concrete, with pumping set at lowest practical flow
- Upper 1-2 in. to be filled with no-shrink grout after initial casting to minimize voids
- Additional support for top of columns (see section 2.4, frame support)

2.4 Specimen support during casting and prior to testing (storage)

The frame used to support the specimens while they are casting is shown in Figure 6. This figure shows details in geometry of the frame (plan and elevation), but also testing sequence (from T-1 to T-9) and location of each specimen set; the first set includes all the 18ft long specimens, while the second set contains the 26ft long specimens. The support frame is built with EFCO SuperStuds and will be also used as specimen storage.

Table 8. Preliminary requirements for concrete

Specification	5.563 in. tubes		12.75/ 20.0 in. tubes	
f'_c	5	12	5	12
w/c ratio	0.48	0.27	0.48	0.25
Max aggregate size	3/8	3/8	3/4	3/4
Admixtures		HRWRA		HRWRA
Air content	1%-3%	1%-3%	1%-3%	1%-3%
Slump	4-6 in.	4-6 in.	4-6 in.	4-6 in.
Moisture absorption CA	< 2.0%	< 2.0%	< 2.0%	< 2.0%
Moisture absorption CA	<3.0%	<3.0%	<3.0%	<3.0%
Fineness modulus FA	2.4-2.6	2.4-2.6	2.4-2.6	2.4-2.6

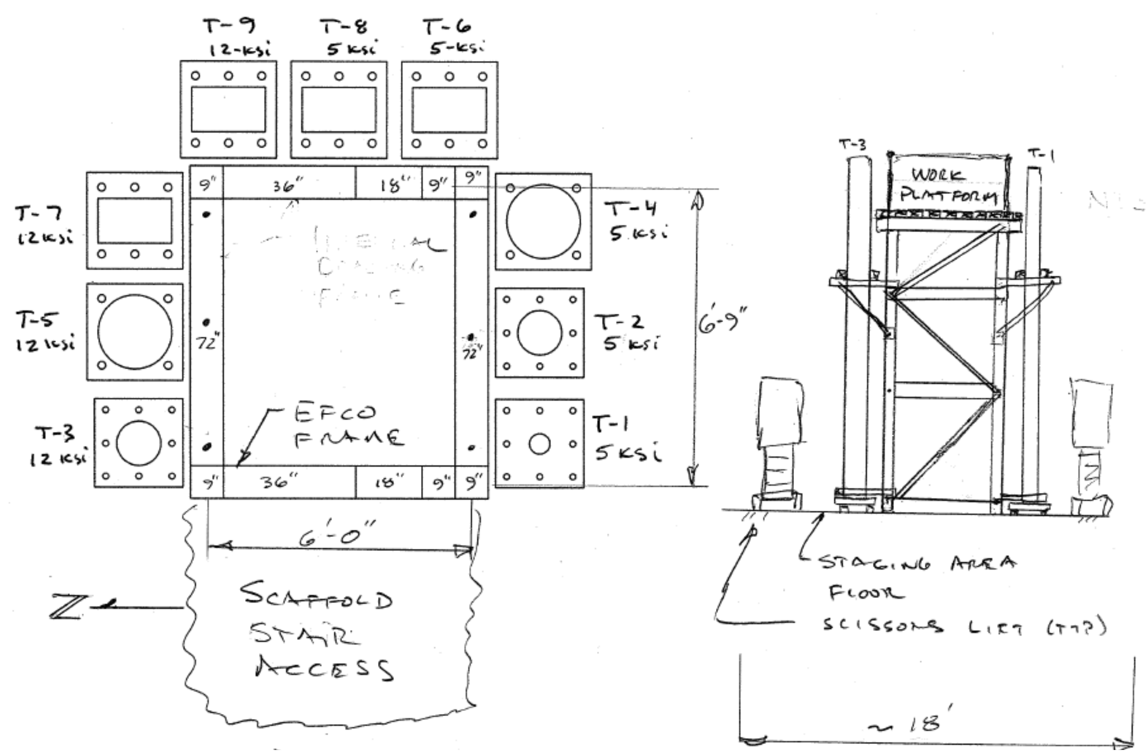

a) Plan view b) Elevation view

Figure 6. Support frame details

2.5 FEA of some longer specimens loaded with hydrostatic pressure

This section summarizes FEA of two long specimens (Figure 7) loaded with hydrostatic pressure, to simulate the condition in the tubes as they are being filling with fluid concrete. The specimens analyzed are:

- CCFT20x0.25x26 – Circular with 20” diameter, 0.25” thickness, 26' long.
- RCFT20x12x0.3125x26 – Rectangular 20x12”, 0.3125” thickness, 26' long.

These analyses assumed that the steel tubes are:

- Initially straight (no initial imperfections)
- Elastic behavior (E=29000ksi, ok since stresses are lower than F_y)
- Loaded only with an hydrostatic pressure

Hydrostatic pressure was obtained assuming a weight per unit volume in concrete equal to 150lb/ft^3. Since these specimens are 26ft long, maximum hydrostatic pressure becomes p=27.1psi at the bottom (p=0 at the top).

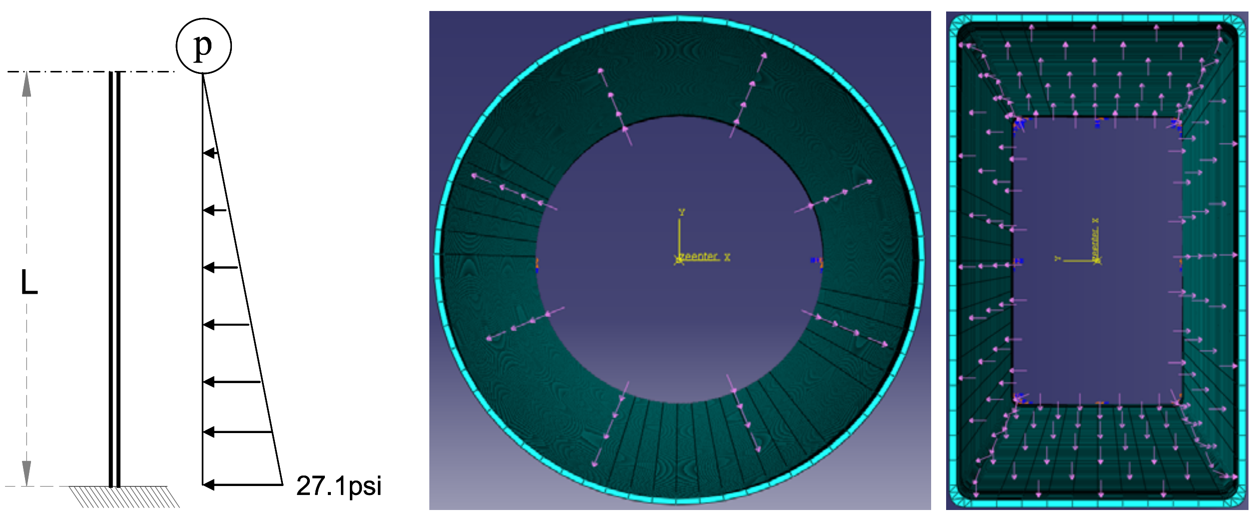

Figure 7. Configuration and FE mesh of some long specimens with hydrostatic pressure

The results obtained with FEA on the circular specimen are very similar to those calculated from the closed-form solution of thin-wall cylindrical pressure vessels. Tangential stresses across the tube thickness remain constant with a value equal to "pr/t" in tension (Figure 8).

The FEA results (Figure 9) on the rectangular specimen showed a big dependency with the mesh. The solution converged with a fine mesh, with the thickness of the tube requiring at least 2 solids. In order to have an acceptable accuracy, the results were obtained with two fine meshes (with 3 and 4 solids across the thickness, respectively) and using isoparametric quadratic solids (20-joint brick elements). Results showed a linear variation of the transversal stresses (s11, s22) across the thickness, and varying from compression to tension. Even though there is no a closed-form solution of pressure vessels with a rectangular cross-sections, simple calculation of stresses across the thickness was obtained assuming bending behavior of the tube walls, unit length, and equal positive and negative moment (Figure 10).

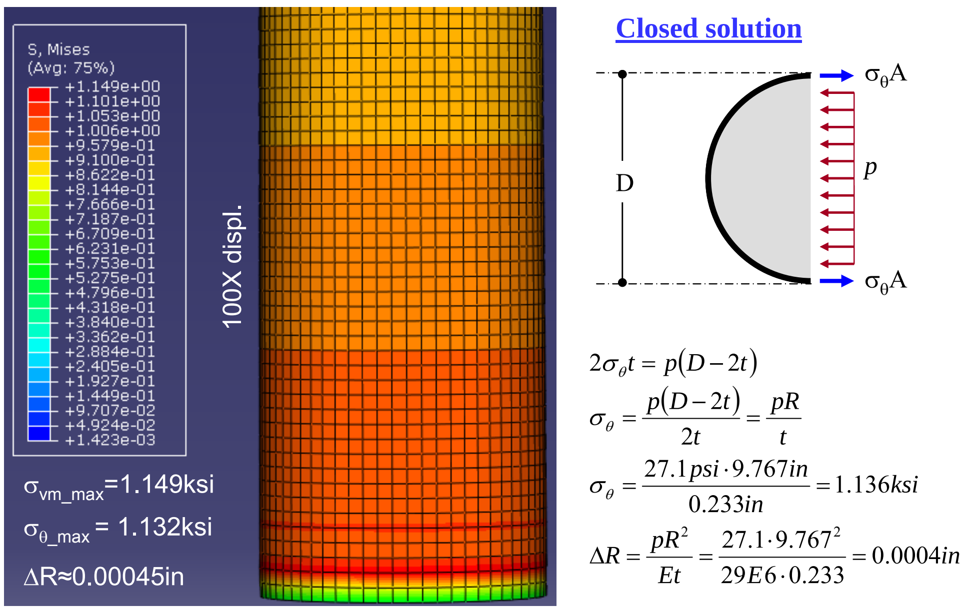

Figure 8. FEA of CCFT20x0.25x26 with hydrostatic pressure

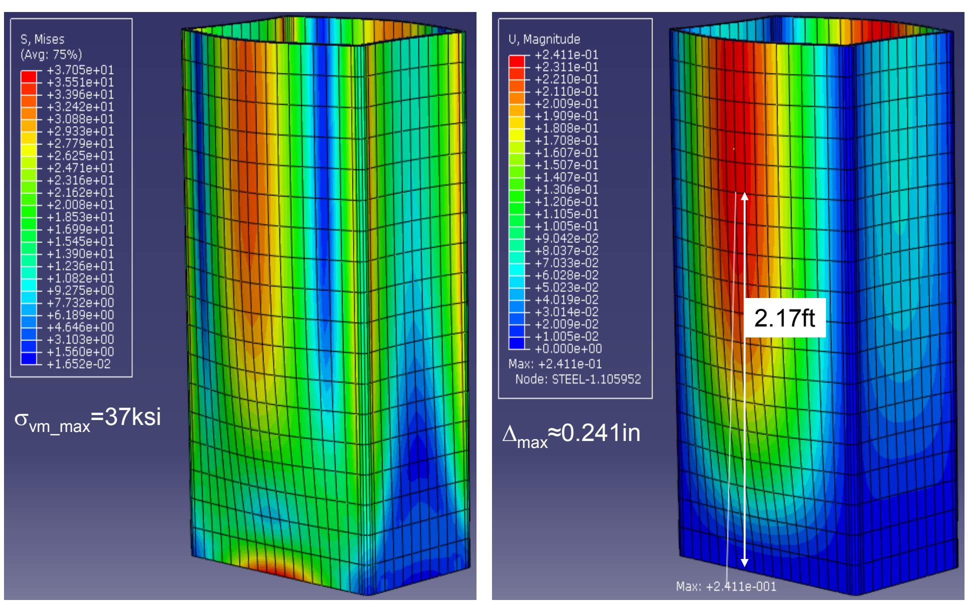

Figure 9. FEA of RCFT20x12x0.3125x26 with hydrostatic pressure

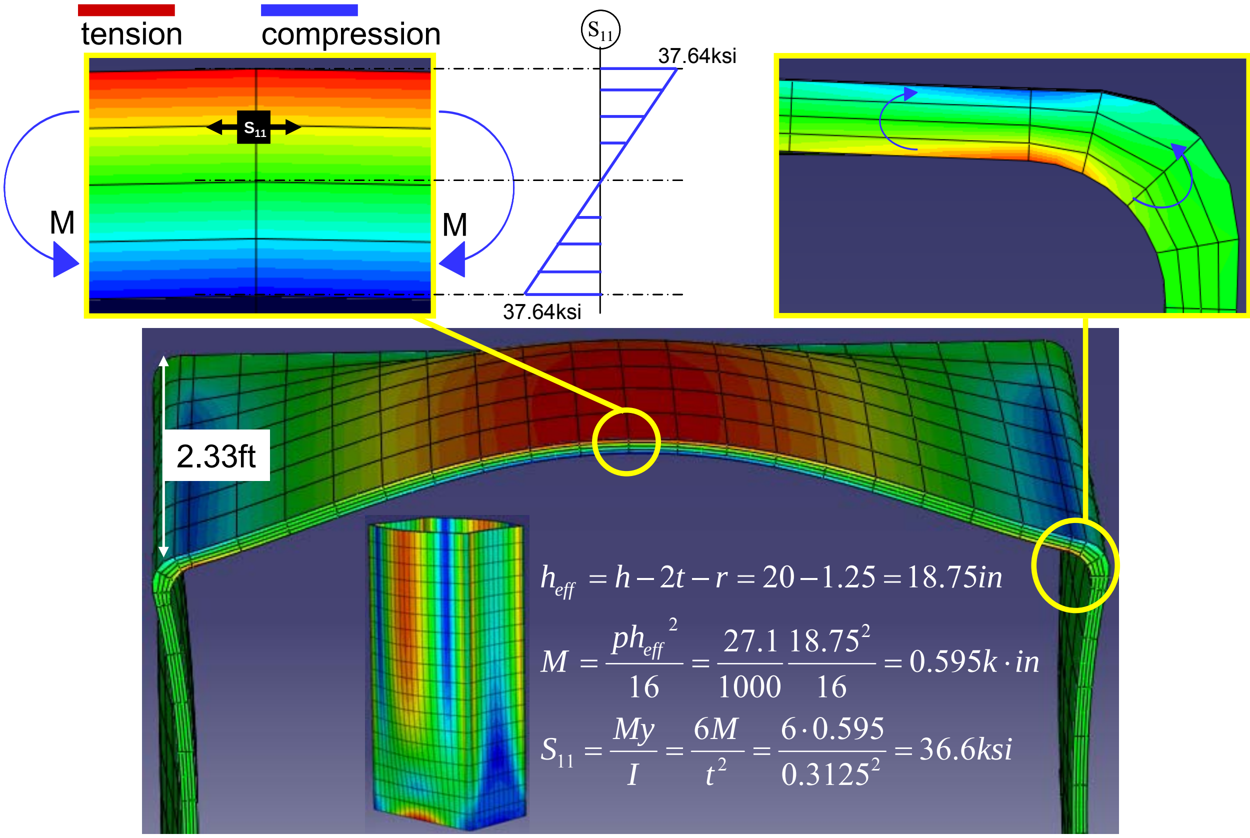

Figure 10. Linear variation of stresses across the thickness in RCFT20x12x0.3125x26

These FE results indicate that hydrostatic pressure in the steel tubes from fluid concrete is not an issue for the circular specimens, even in the longer or the thinner ones since both stresses and displacements are low. However, this is not the case for the rectangular specimens. Since the tube did not yield in any of these two specimens, FEA also showed that there is no residual stress/strain left if the loading is removed (once the concrete has hardened). However, in reality the concrete will be hardened with the deformed shape of the tube, which is in the worst case about 0.24in at 2ft from bottom for the RCFT20x12x0.3125x26 specimen. In order to avoid this situation, the installation of 6 c-clamps (every 2ft from bottom at both sides for a distance of 8 ft. = 6 clamps total) is proposed during the casting process of the rectangular specimens.

2.6 Cross-section strength

Table 9 and Table 10 show some of the cross-section strengths for each circular and rectangular CFT, respectively. These results were obtained with the AISC-05 specification, but an over-strength factor (*$R_y=1.4$*) was assumed in the calculations. In these tables: P_o is the strength of the cross-section in pure compression (short column); P_n is the strength of the slender column in pure compression (Figure 11); P_d and M_d are the compression and bending cross-section strength, respectively, associated with the balanced failure point. The P-M interaction diagrams of the cross-section strength are shown in Figure 12 and Figure 13.

Table 9. Cross section strengths for the Circular CFT specimens

Specimen	D/t	Fy (ksi)	f'c (ksi)	L (ft)	λ	Po (kip)	Pn (kip)	Pd (kip)	Md (k-ft)	Md/Pd (in)
CCFT20x0.25	86	42	5	18.0	1.03	2273	1456	712	691	11.7
				26.0	1.49	2273	897	712	691	11.7
	86	42	12	18.0	1.25	4266	2210	1708	1035	7.3
				26.0	1.81	4266	1141	1708	1035	7.3
CCFT12.75x0.25	55	42	5	18.0	1.56	1101	396	282	240	10.2
				26.0	2.25	1101	190	282	240	10.2
	55	42	12	18.0	1.85	1889	482	676	325	5.8
				26.0	2.68	1889	231	676	325	5.8
CCFT5.563x0.134	45	42	5	18.0	0.88	231	167	53	23	5.2
				26.0	1.27	231	117	53	23	5.2

Table 10. Cross section strengths for the Rectangular CFT specimens

Specimen	b/t	Fy (ksi)	f'c (ksi)	L (ft)	λ	Po (kip)	Pn (kip)	Pd (kip)	Md (k-ft)	Md/Pd (in)
RCFT20x12x0.3125w	67	46	5	18.0	1.38	2118	952	471	594	15.1
				26.0	2.00	2118	466	471	594	15.1
	67	46	12	18.0	1.61	3438	1158	1131	773	8.2
				26.0	2.33	3438	555	1131	773	8.2
RCFT12x20x0.3125s	67	46	5	18.0	0.89	2118	952	471	875	22.3
				26.0	1.28	2118	466	471	875	22.3
	67	46	12	18.0	1.02	3438	1158	1131	1173	12.4
				26.0	1.47	3438	555	1131	1173	12.4

2.7 Stability effects on the strength

One of the primaries concerns of the MAST personnel is the control of the loads and displacements in order to avoid reaching the maximum capacity of the MAST equipment. Thus, the following information will give the expected upper bound results (i.e. with the maximum loading in the specimens). The analytical results are based on the AISC-05 Spec. and fiber-based analyses performed in OpenSees.

Figure 11 shows column curves for the specimens obtained with the AISC-05 Spec. (dashed black curve) and from fiber-based analysis performed in OpenSees (continuous blue curve). These figures illustrate the effect of the length in the strength of columns with pure compression. As seen in these plots, small differences between AISC and fiber analysis can be noticed, mainly in the inelastic buckling range ($\lambda<1.5$). Residual stress, which was neglected in the fiber analysis, is the perhaps the main reason of such differences.

The young's modulus (psi) for the concrete was taken as suggested by ACI 363 (ACI committee for high strength concrete).

$$E_c = 40000\sqrt{f_c'} + 1E6$$

As previously mentioned, Figure 12 and Figure 13 show the P-M interaction diagrams of the cross-section strength according to AISC-05 (with no stability effects included). For design of slender beam-column elements, AISC-05 specifies a simplified bilinear P-M interaction diagrams, which is shown in Figure 12 for (for circular CFT specimens) and Figure 13 (for rectangular CFT specimens). The maximum capacity of the MAST system is also plotted in these figures, considering a reduction in the compression force capacity due to bending moment. According to these figures, only the short CCFT20x0.25 specimens (L=18ft) may exceed the capacity of the MAST system. As a reminder, all these calculation include some over-strength factor, as $R_y=1.4$ for accounting real yield stress in the steel, and $C_3=0.95$ for accounting confinement effects.

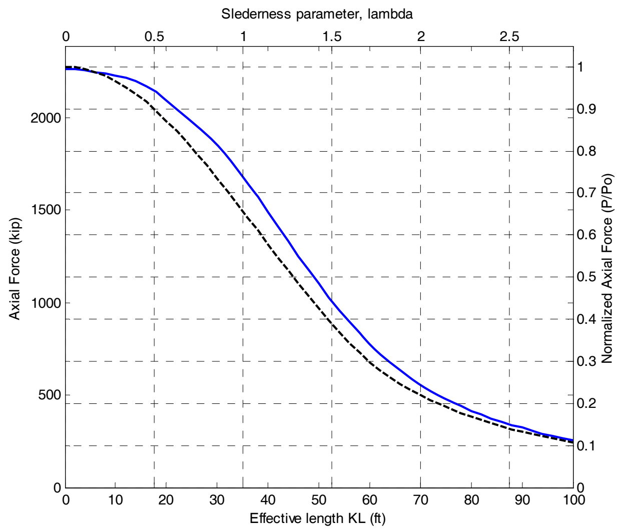

a) CCFT20x0.25, f_c'=5ksi

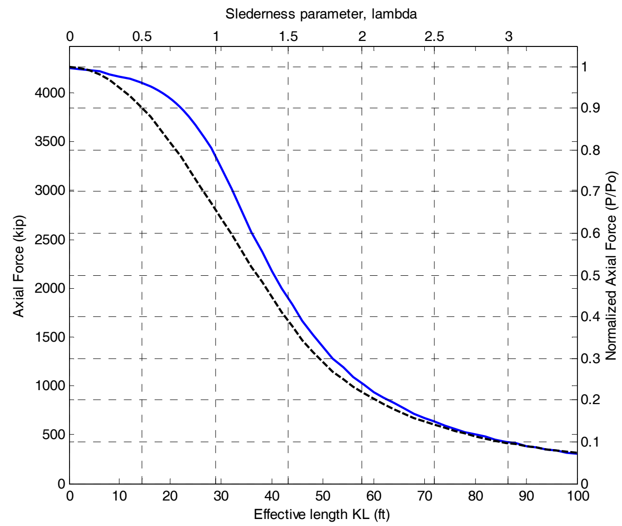

b) CCFT20x0.25, f_c'=12ksi

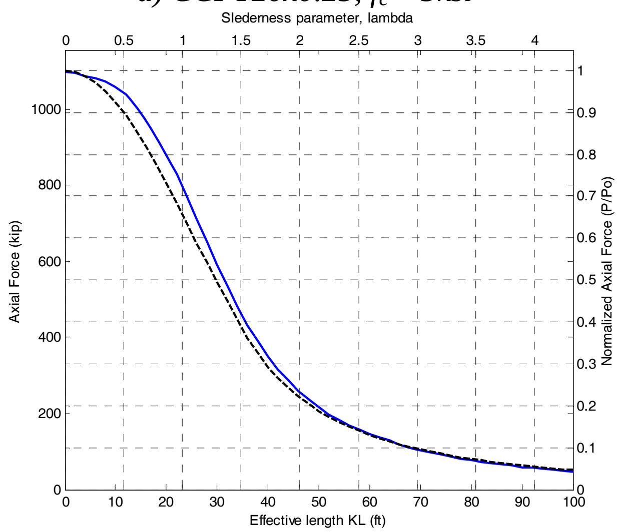

c) CCFT12.75x0.25, f_c'=5ksi

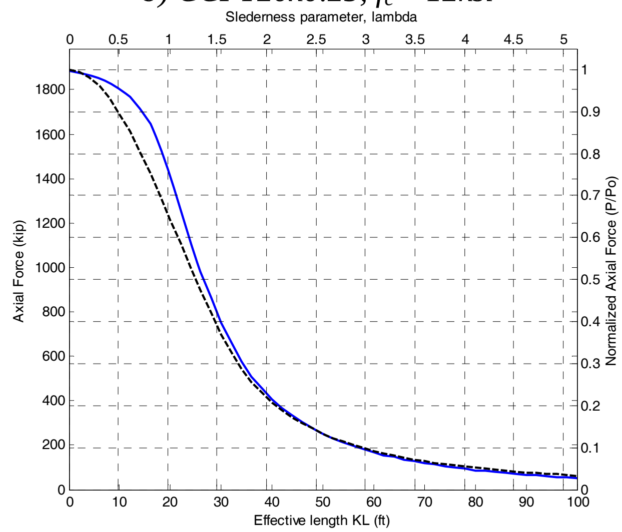

d) CCFT12.75x0.25, f_c'=12ksi

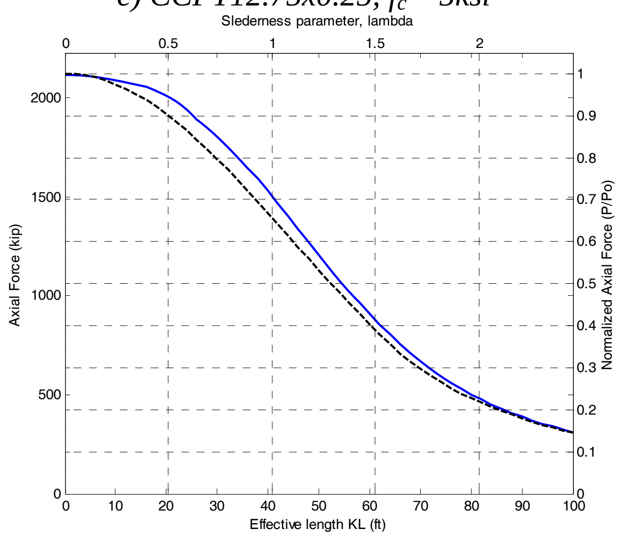

e) RCFT20x12s, f_c'=5ksi

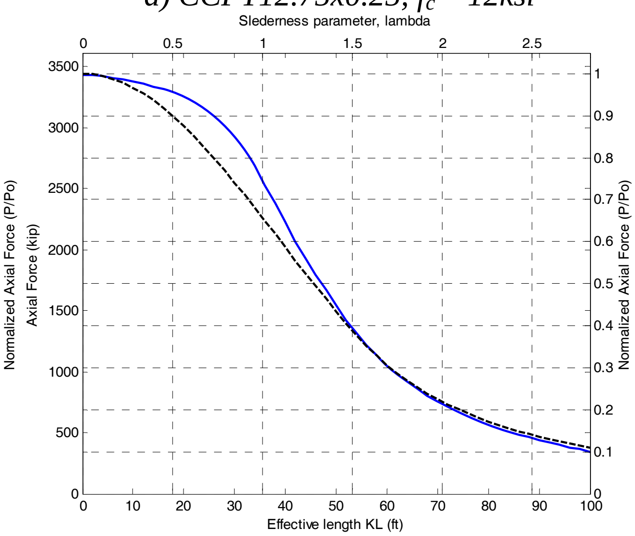

f) RCFT20x12s, f_c'=12ksi

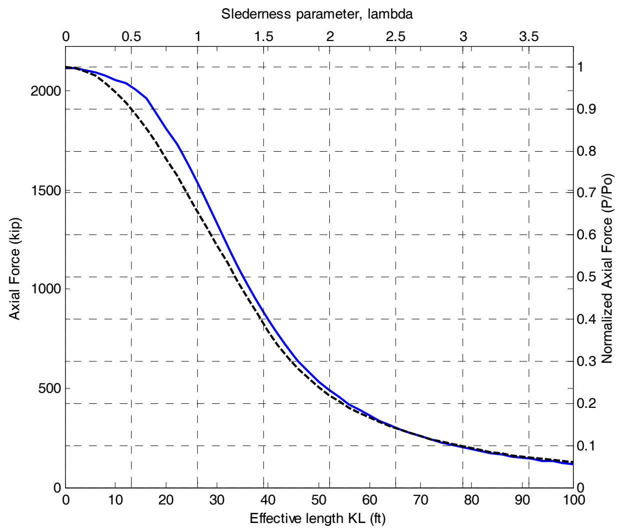

g) RCFT20x12w, f_c'=5ksi

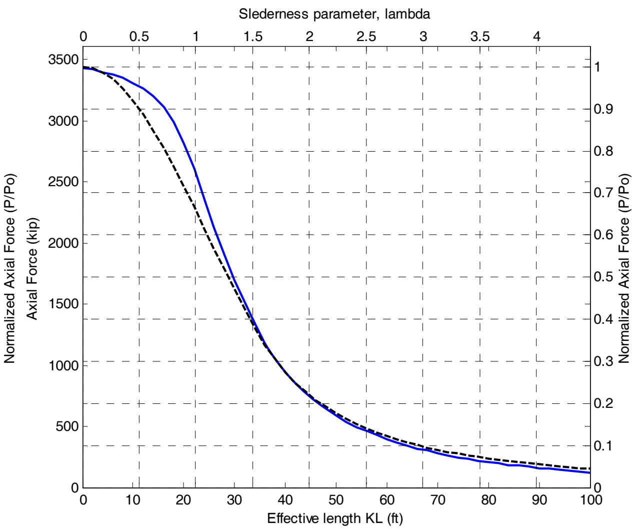

h) CCFT20x12w, f_c'=12ksi

Figure 11. Column curves for CFT specimens with fixed-free conditions (K=2, R_y=1.4) obtained from AISC-05 (dashed black line) and fiber-based analysis (continuous blue line).

However, the AISC-05 simplified bilinear P-M diagram (which is recommended for design purposes) may underestimate the P-M interaction diagram of the real beam-column specimens. Therefore, fiber analyses have been performed in order to capture the stability effects with material and geometric nonlinearity, confinement effects and initial imperfections. Local buckling and residual stresses in the tubes were not considered in the fiber analysis, which overestimate the strength of these specimens. The results of the fiber-based analysis are shown in Figure 14 (for the CCFT20x0.25 specimens) and Figure 15 (for the RFCT20x12x0.3125s specimens). Notice that in these plots both interaction diagrams P-M_1 and P-M_2 are included, where M_1 and M_2 are the bending moments based on first and second order analysis, respectively. The P-M interaction diagrams for the cross-section and the slender beam-column given by AISC-05 are also included. This plots confirm that just the short CCFT20x0.25 specimens (L=18ft) may exceed the capacity of the MAST system.

More information about the experimental load paths (monotonic and cyclic), real demands in the specimens for strength and displacements will be discussed in the next section. Emphasis in the comparison with the MAST limits (loads and displacements) will be also discussed.

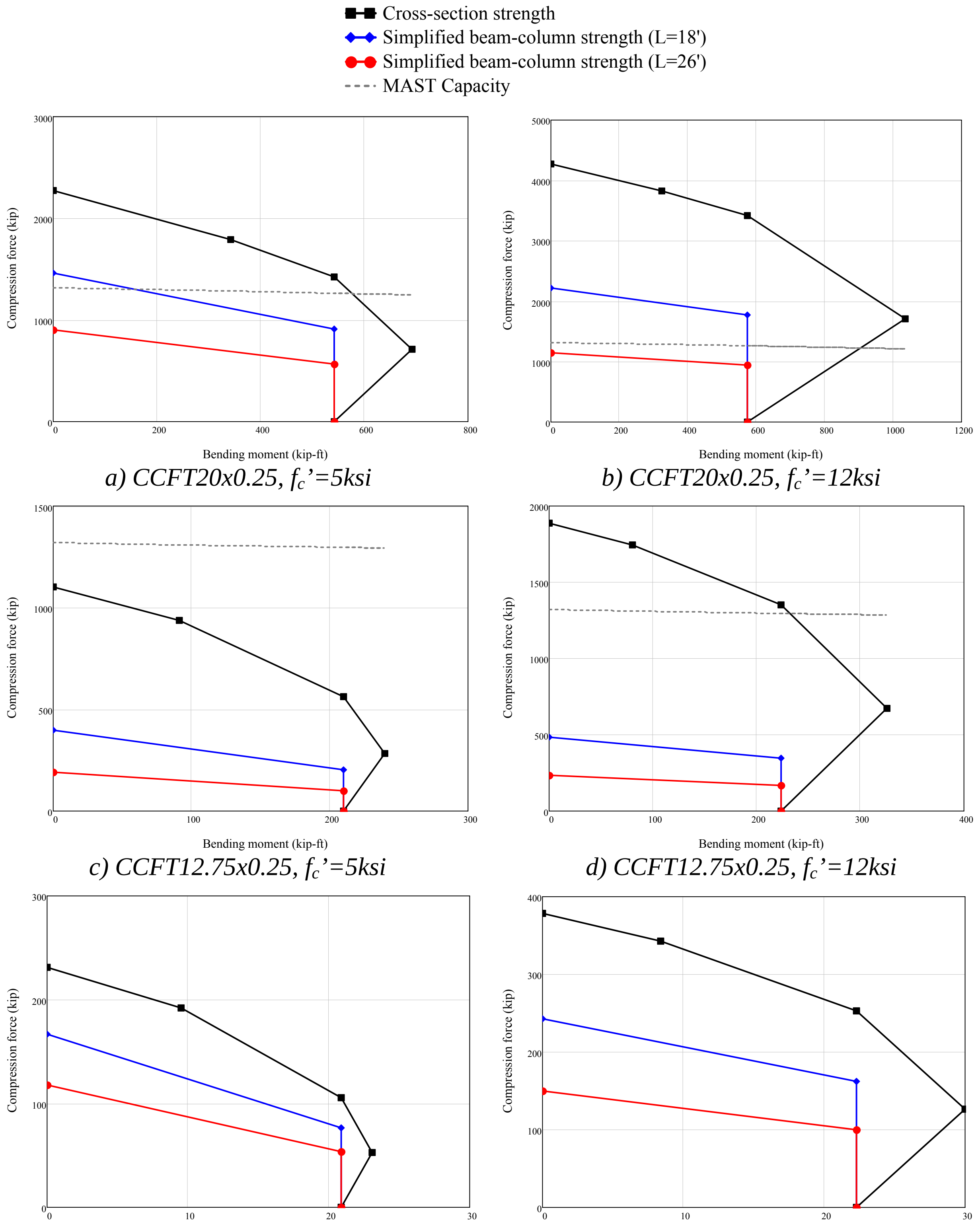

a) *CCFT20x0.25, f_c'=5ksi*

b) *CCFT20x0.25, f_c'=12ksi*

c) *CCFT12.75x0.25, f_c'=5ksi*

d) *CCFT12.75x0.25, f_c'=12ksi*

e) *CCFT5.563x0.134, f_c'=5ksi*

f) *CCFT5.563x0.134, f_c'=12ksi (no test)*

Figure 12. P-M interaction diagrams of the circular CFT specimens (R_y=1.4)

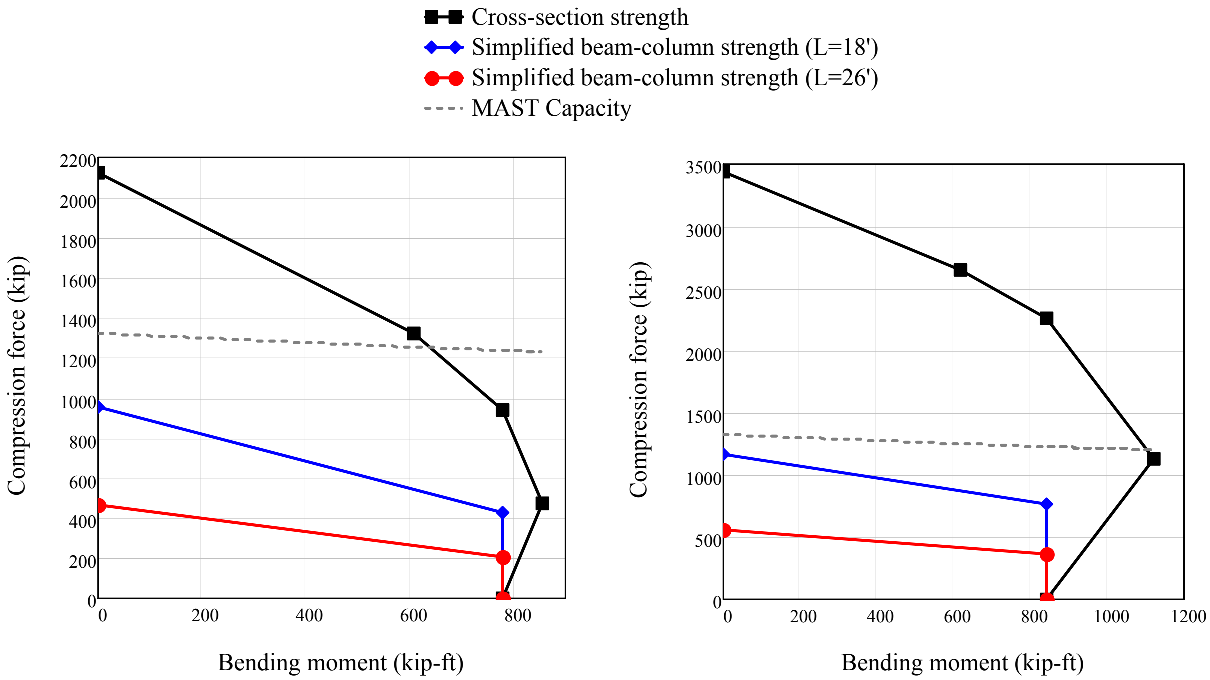

a) f_c'=5ksi *b) f_c'=12ksi*

i) RCFT20x12x0.3125s

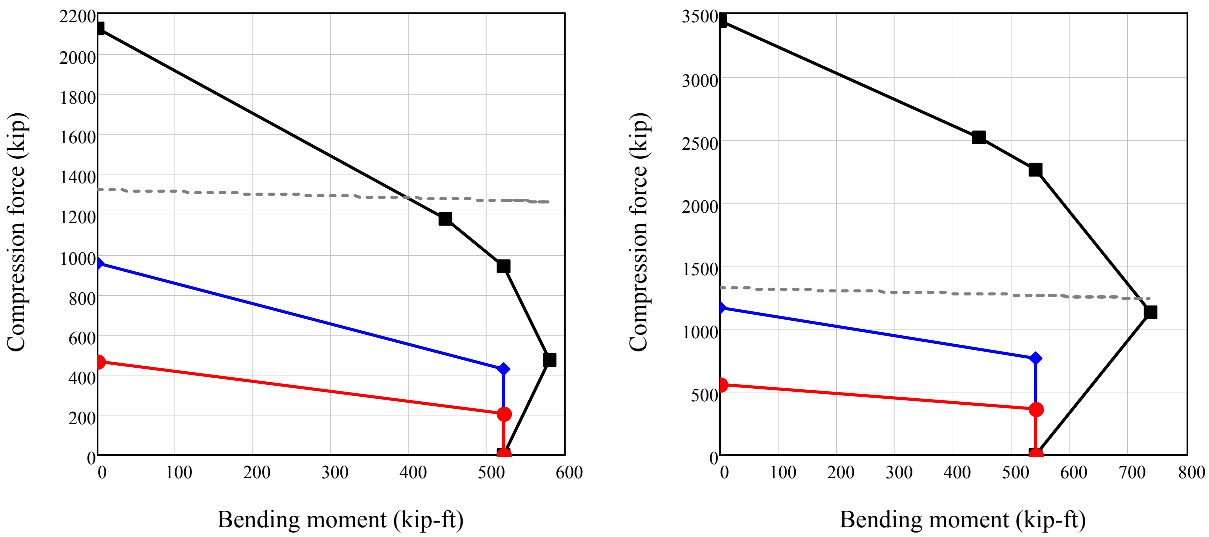

a) f_c'=5ksi *b) f_c'=12ksi*

ii) RCFT20x12x0.3125w

Figure 13. P-M interaction diagrams of the rectangular CFT specimens

(Note: R_y=1.4 in these calculations)

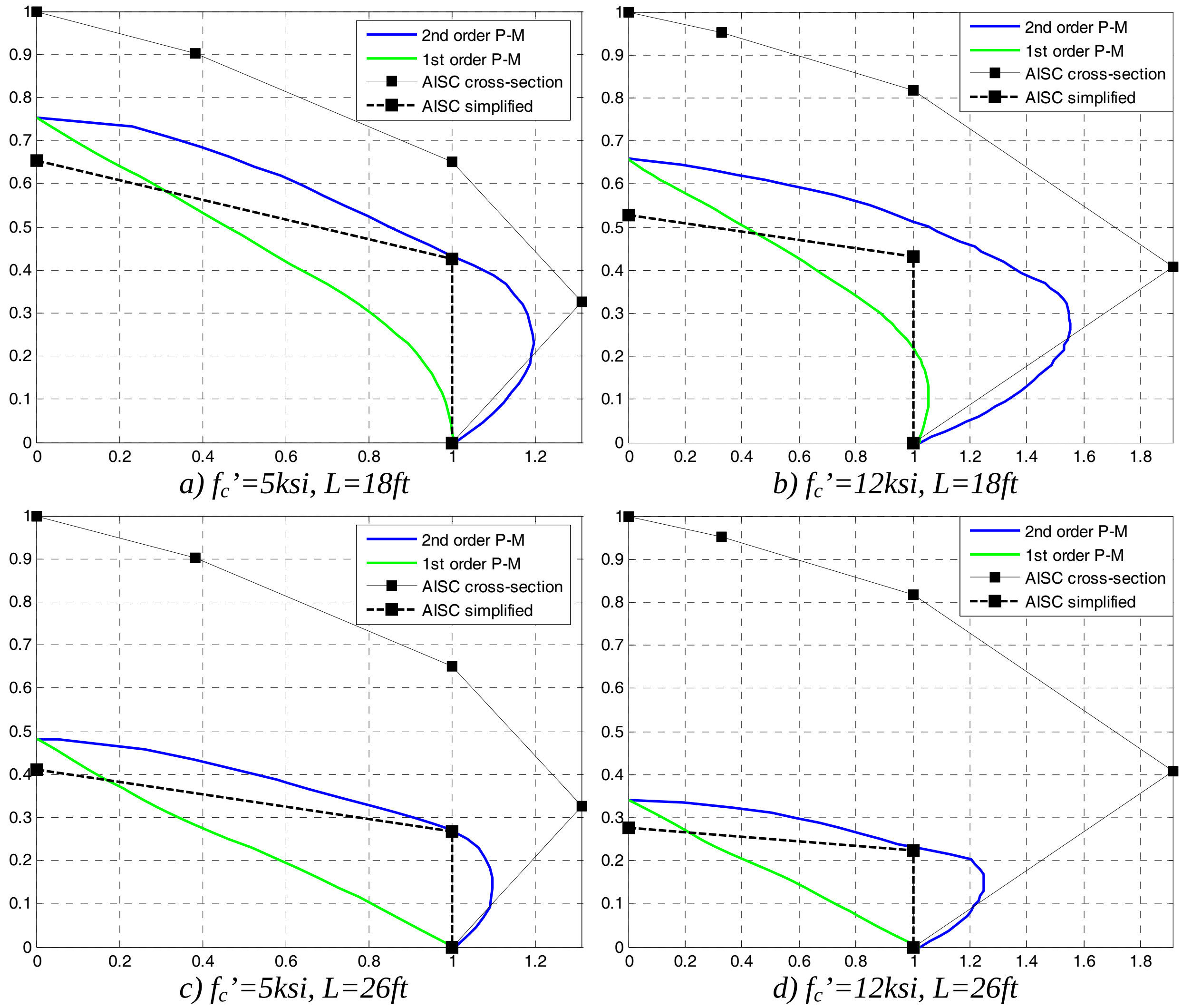

Figure 14. P-M interaction diagrams of the CCFT20x0.25 specimens

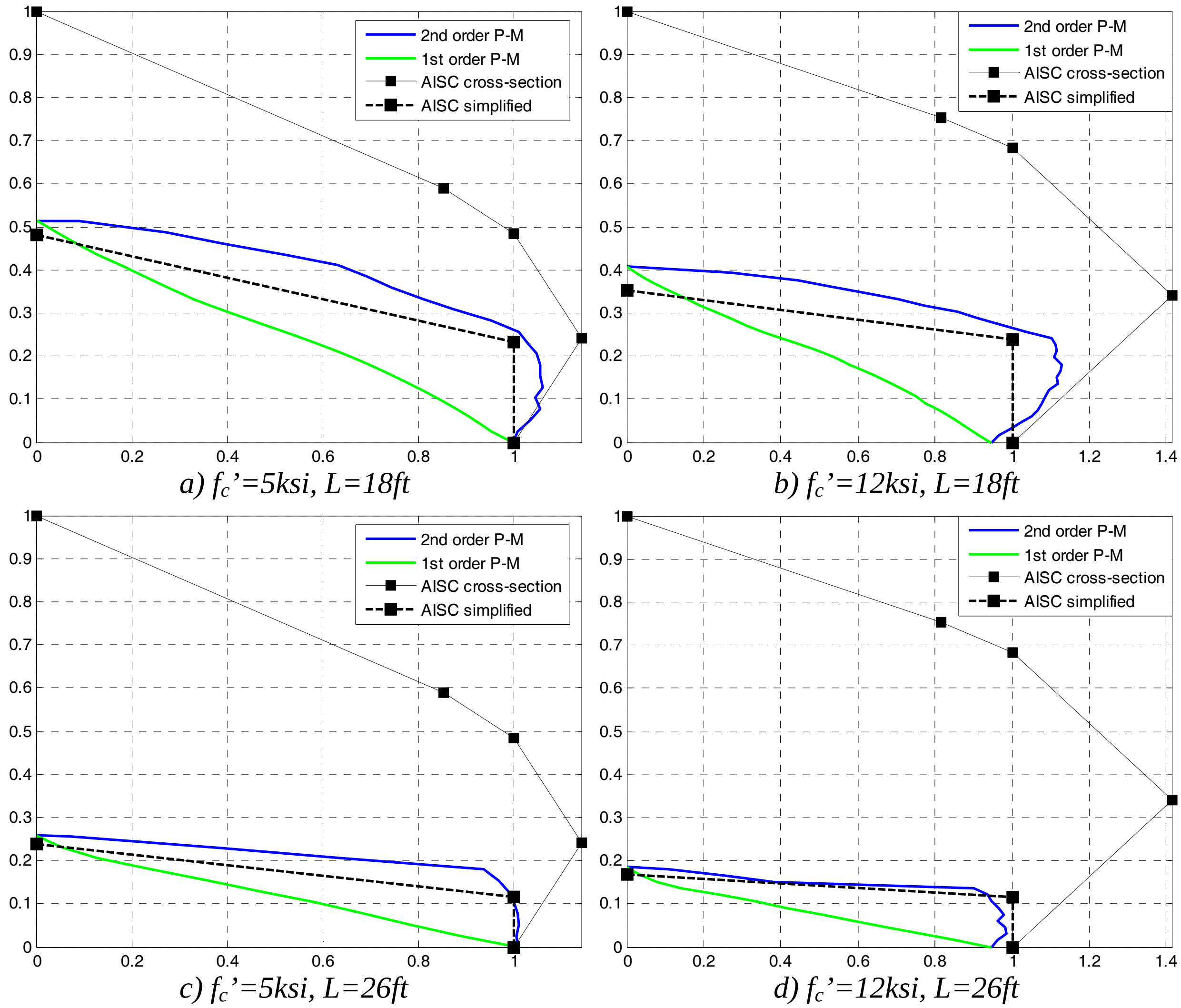

Figure 15. P-M interaction diagrams of the RCFTs20x12x0.3125 specimens

2.8 Base plates requirements

The design of the base plates were based on:

- AISC Steel Design Guide No. 1 (2^{nd} Ed.). Calculations included in attachment 1.
- Finite Element Analysis (performed in ABAQUS)
- Physical constraints to let fit the base plates with the holes layout at the strong-floor and cross-head. Economical issues were also accounted.

Theoretically, the bottom base plates should be strong enough to let the specimens reach the ultimate capacity, which is roughly speaking the P-M cross section strength minus the stability effects. This is, any point defined by P-M_2 (blue curve) as defined in Figure 14 and Figure 15. However, just the critical P-M values were checked for the base plate's design. The critical ultimate values taken for the bottom base plates were:

- AISC pure compression case: $P_u=\chi P_A \leq 1320k$, $M_u=0$
- Compression and max bending moment for the beam-column according to the AISC simplified bilinear curve: $P_u=\chi P_C \leq 1320k$, $M_u=M_C$
- AISC balance point of the P-M cross-section strength: $P_u=P_D \leq 1320k$, $M_u=M_D$

Some notes regarding the last critical values assumed:

- In the three previous cases, an over-strength factor of $R_y=1.4$ was assumed in the steel yield stress (F_y) for the calculations of the ultimate demands (P_u, M_u).
- The ultimate compression load (P_u) cannot exceed the MAST capacity (1320kip).
- The third assumption (where $P_u=P_D$, $M_u=M_D$) govern mostly the base plate's design, since this is the highest bending that the cross-section can reach; the latter is conservative, but a good stiffness and strength is obtained. The second option may be a more reasonable design regarding the strength.
- For the top plates in the fixed-free specimens, only the first of the ultimate-load cases mentioned above was considered since no bending moment will take place.

Figure 16.a shows the results from a finite element analysis (FEA) for the CCFT20x0.25 specimen. In this figure, the P-M Interaction diagrams are shown at the top-left corner; the green line in this plot represents the maximum demand reached by the system (P_u=1240kip, M_u=930.6kip-ft), which did not exceed the MAST capacity. The axial stresses at the base plates (bottom-left), and the Von-Mises (VM) stresses in the specimen (bottom-right) and the bolts are also shown. The stresses values are showing a full plastification in the specimen's cross-section while both bolts (σ<80ksi) and base plate (σ<32ksi) behave elastic.

Similarly, Figure 16.b shows the FEA performed for the RCFT20x12x0.3125 with bending about the strong axis. In this figure, the cross section P-M interaction diagram is shown at the top-left corner; the red line in this plot represents the maximum demand reached by the system (P_u=1150kip, M_u=940kip-ft), which did not exceed the MAST capacity. The axial stresses at the base plates (bottom-left) and the Von-Mises (VM) stresses in the specimen (bottom-right) and the bolts are also shown. The stresses values in this analysis are showing a full plastification in the specimen's cross-section while both bolts (σ<80ksi) and base plate (σ<32ksi) behave elastic.

In conclusion, final results with base plate sizes and weights are shown in the Table 11. Details of all the specimens are shown from Figure 18 to Figure 21.

Table 11. Base plate sizes and weights (A-572 Gr. 50 steel)

SPECIMEN	PLATE SIZE	Qty	Weight (kip)
CCFT20X0.25	26x26x3	4	2.3
	26x26x2	4	1.5
CCFT12.75x0.25	24x24x2.5	4	1.6
	24x24x1.5	4	1.0
CCFT5.563X0.134	24x24x1.5	2	0.5
	24x24x1.5	2	0.5
CCFT20x12x0.3125	26x26x3	8	4.6
	26x26x2	8	3.1
			15.1

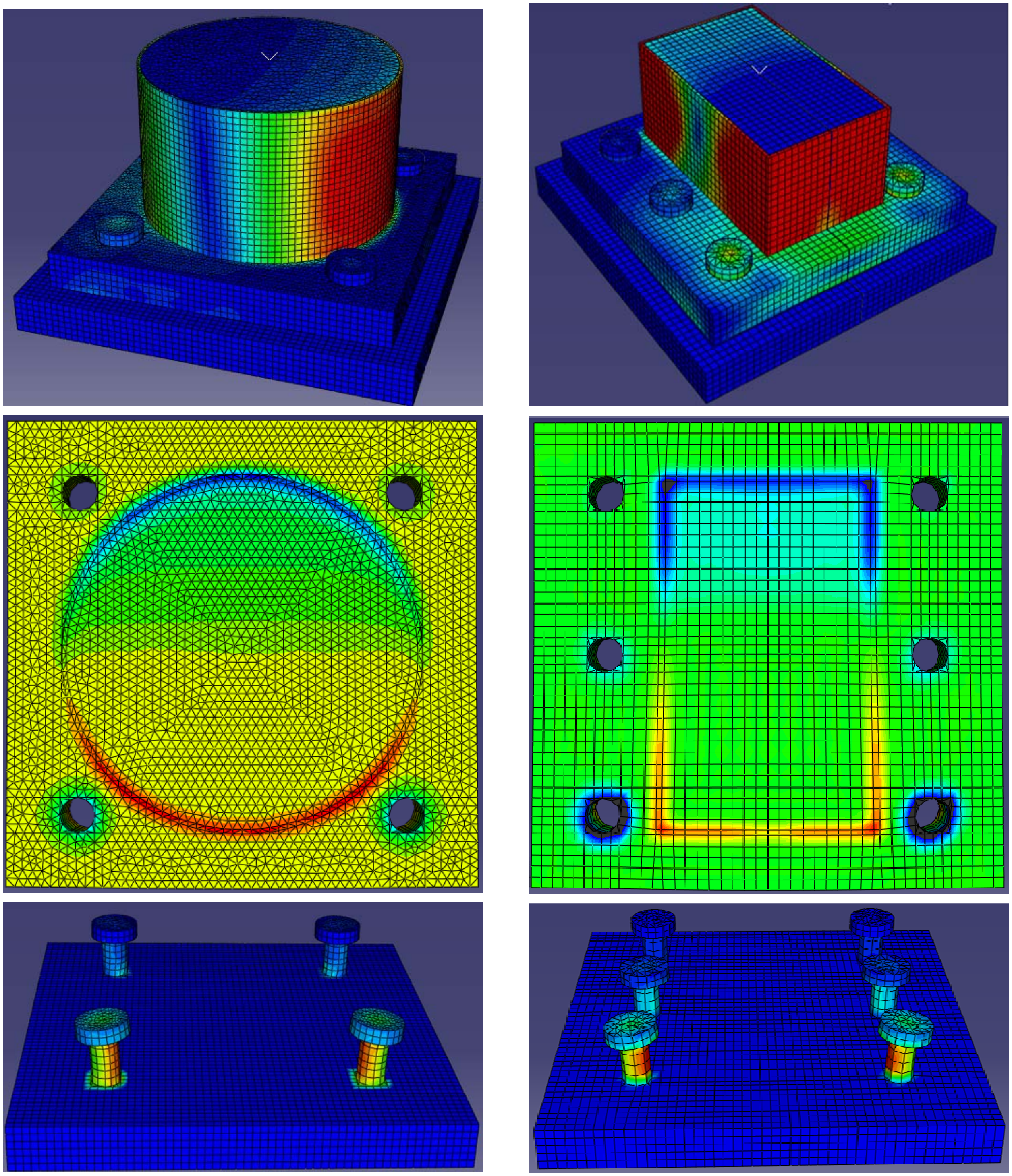

a) CCFT20x0.25 Specimen b) RCFT20x12x0.3125 Specimen

Figure 16. Finite Element Analysis performed for the base plates

The base plates will be attached to the floor using the details shown in Figure 17. Super-bolts MT-200 (with 2in diameter) will be used with the 3in and 2.5in thick base plates, while MT-150 (1.5in diameter) will be used for the remaining base and top plates. Inserts (3”-2” and 3”-1.5”) and super-nuts (≈3.6in diameter) will be used to attach the specimens to the strong-floor.

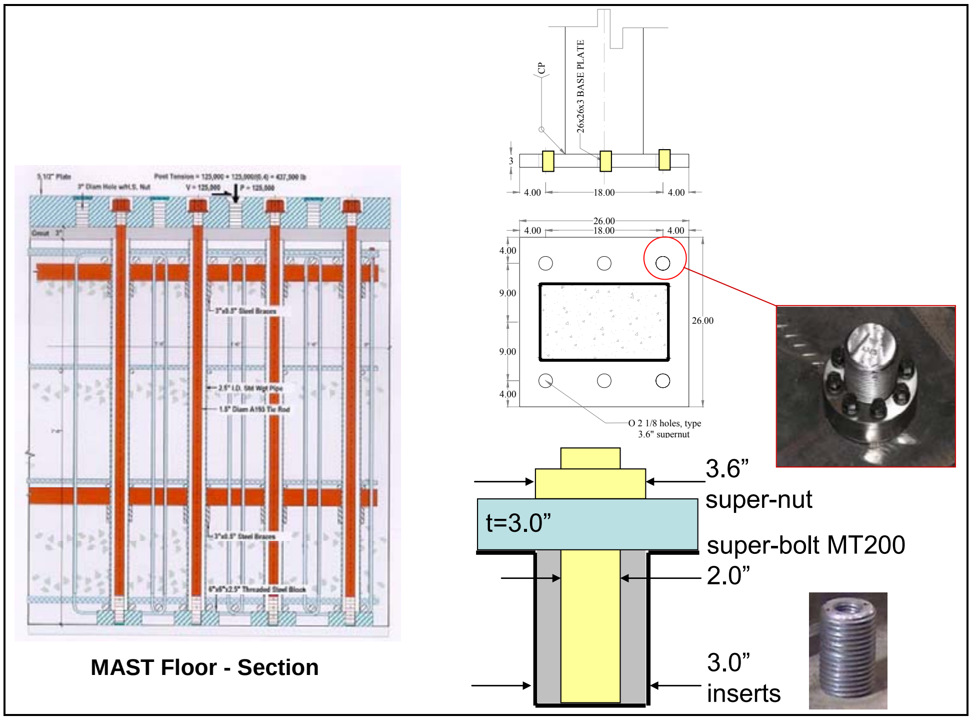

Figure 17. Super-bolts, super-nuts and inserts

The connection between the base plates and the HSS-shape is a partial joint penetration groove weld with a fillet reinforcement.

2.9 Specimen Demolition and Disposal

The specimens will be disposed off according to U. of Minnesota directives. It is anticipated that they will be treated as mixed construction refuse. The research team will be responsible for the costs of disposal, which will be managed by the U. of Minnesota. For the first two specimens, it is anticipated that the tubes may be sliced and examined before disposal; an outside construction company will be used for that purpose.

2.10 Plans of specimens

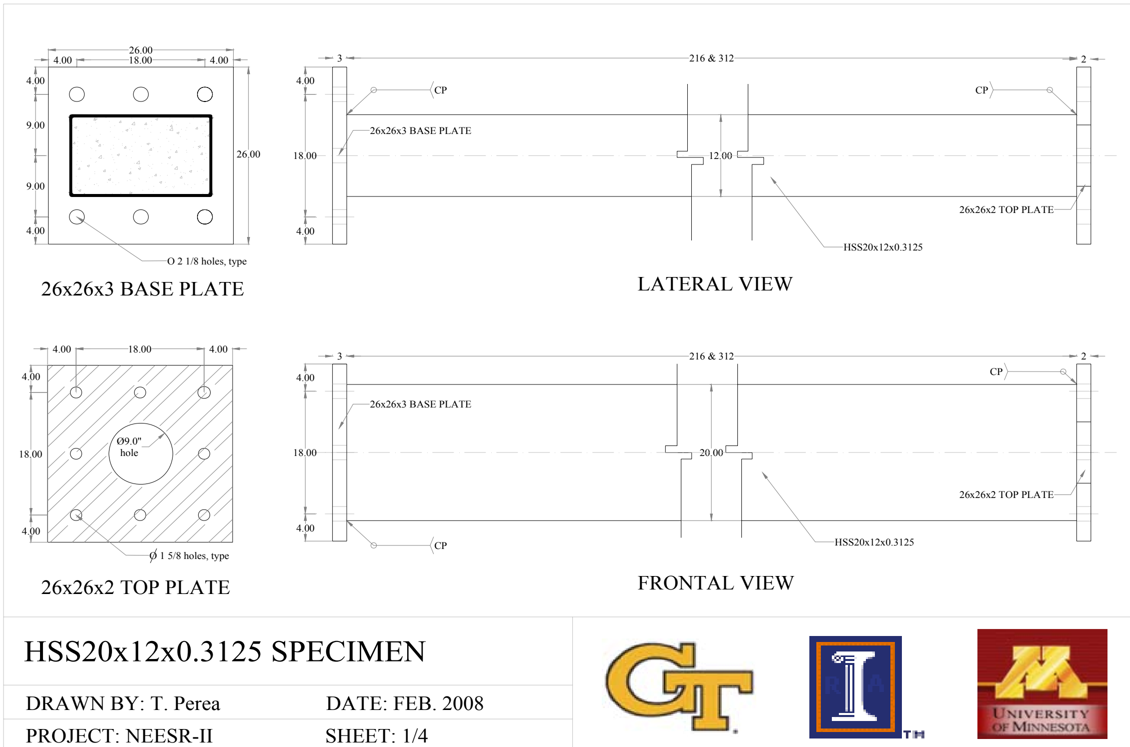

Figure 18. Details of RCFT20x12x0.3125 specimen

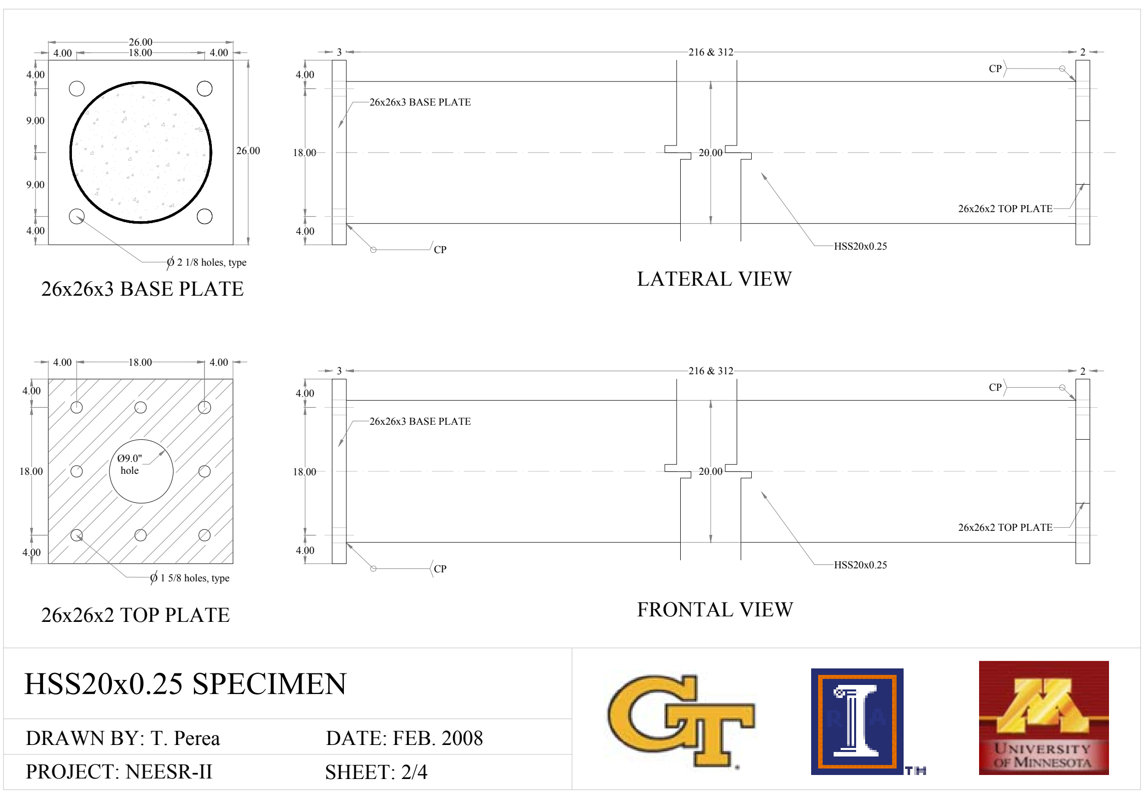

Figure 19. Details of CCFT20x0.25 specimen

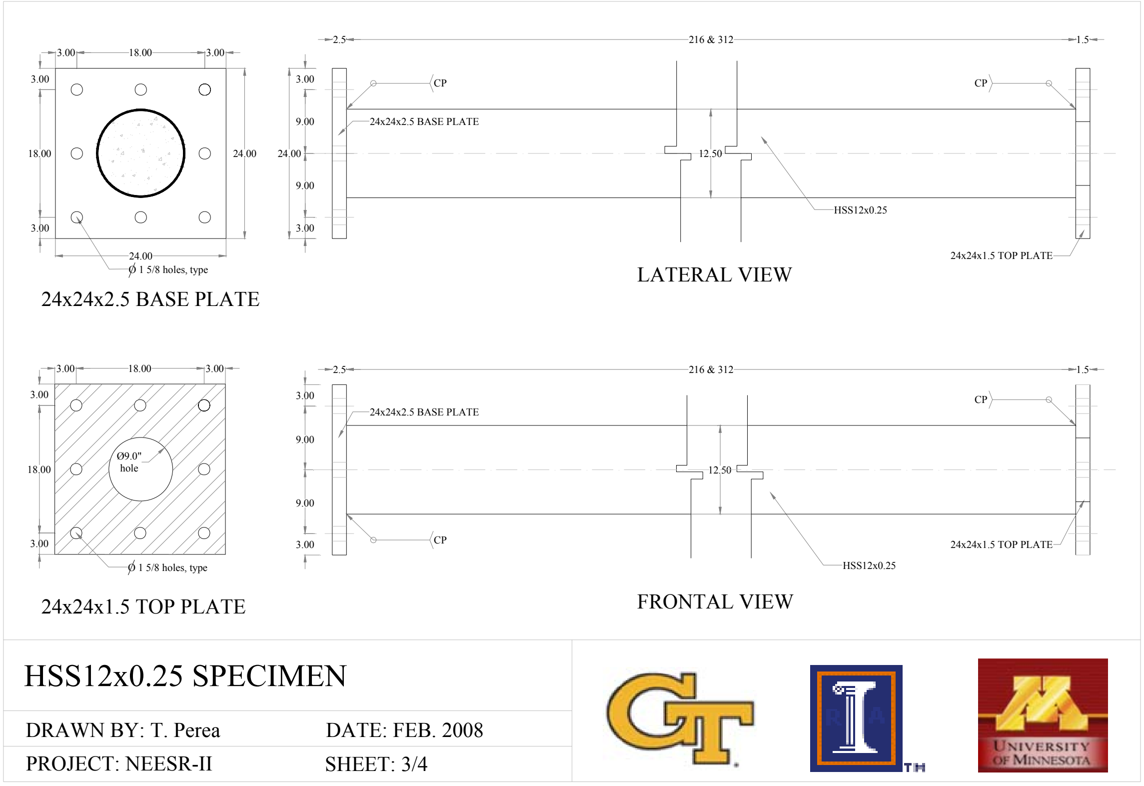

Figure 20. Details of CCFT12x0.25 specimen

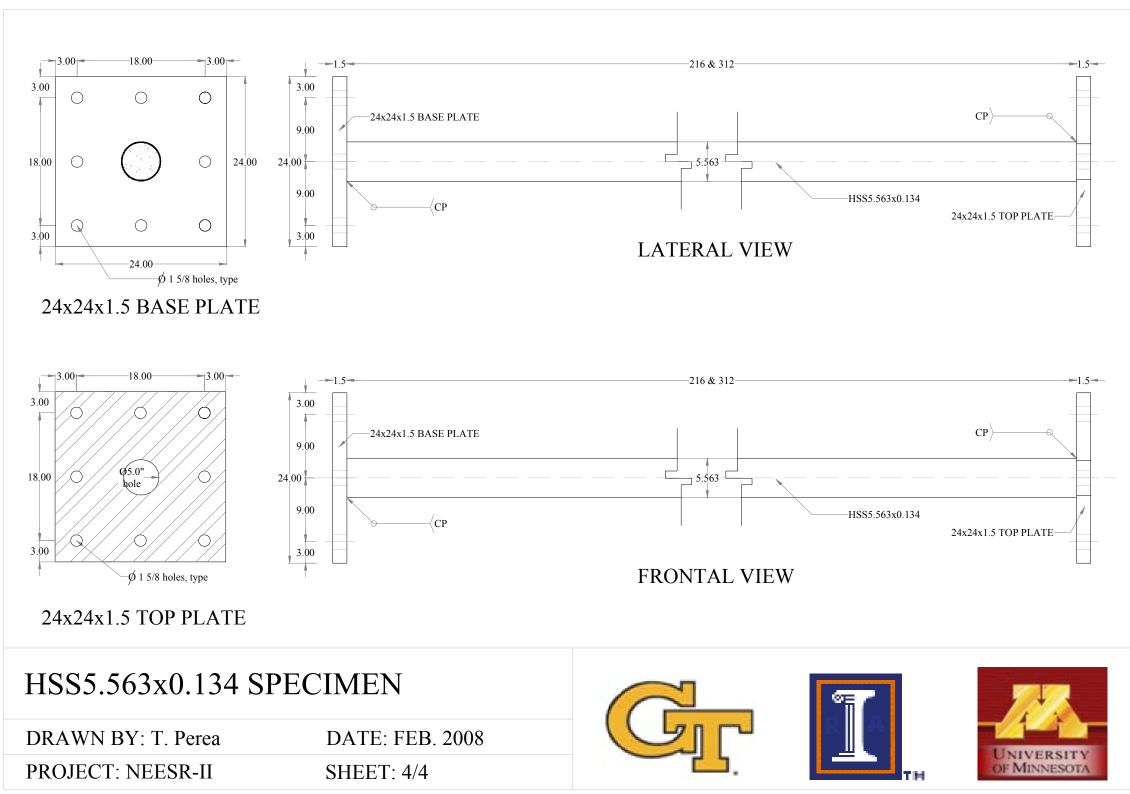

Figure 21. Details of CCFT5.563x0.134 specimen

3 Instrumentation, DAQ and Telepresence plan

Installation of instrumentation will begin with grinding surfaces and installing strain gages. This will be done away from the testing machine but will require that the specimens be in a horizontal position and accessible by the crane so they can be rotated. A working area of 30ft by 4ft should be sufficient. Cables will be bundled and connected to terminals. This will be done by GT/UIUC personnel but some help from MAST staff will be required initially with crane operation and training on lab safety procedures and operation of lab equipment. Installation of instrumentation will continue with positioning of brackets to hold LVDTs and string pots. Estimated time: it is assumed that it will take two people two days to complete this phase for each test.

Specimen will be moved to the testing machine and bolted to the bottom plate. Supervision by MAST personnel will be very desirable, at least initially. Estimated time: 2-3 hours.

Installation of instrumentation will continue by placing and connecting LVDTS and string pots. All cabling (strain ages, string pots, LVDTs, etc.) will be connected at this point and initial troubleshooting of the instrumentation will be conducted. This will be followed by the installation of the LEDs for the Krypton system. Finally, white-wash painting will be made in the specimen. Estimated time: 8 hours.

3.1 Summary of the instrumentation required

Total number and types of instrumentation to be used for each specimen is shown in Table 12.

Table 12. Instrumentation Summary

Instrument	Type/Range	Number	Owner/Supplier	Location
Strain Gages	Tokyo Sokki 10mm	102	GT	External
LVDTs	0.1in to 0.5in	28	MAST	External
String-pots	±12in	12	MAST	External
LEDs.	---	28	MAST	External
Krypton	---	1	MAST	External

3.2 Strain gages instrumentation

Up to 102 Tokyo Sokki 10mm gages (with integrated lead wires and waterproofing) will be used to measure both longitudinal and transverse strains in the specimens. Strain gages will be installed by GT personnel at MAST site, and cable lengths and connectors will be provided by MAST personnel. Details about location and layout of the strain gages on the specimens are shown in Figure 22.

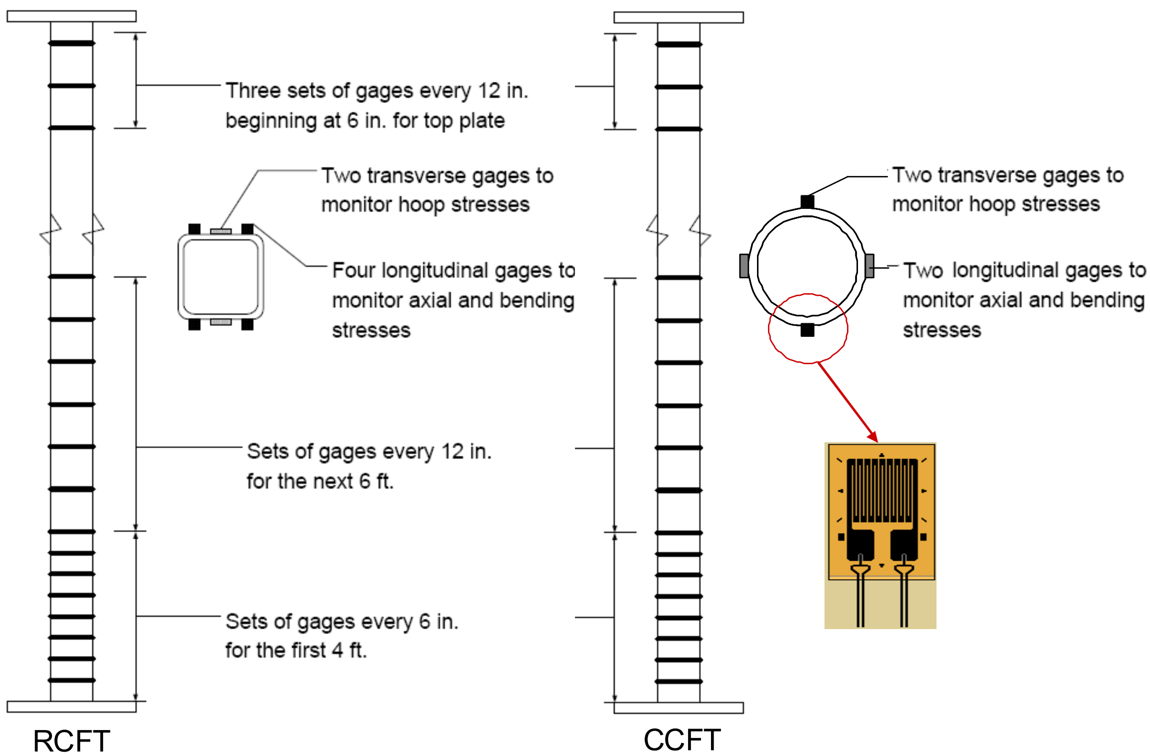

Figure 22. Details of strain gages on the specimens

3.3 LVDT instrumentation

A total of 28 LVDTs (which ranges from 0.1in to 0.5in) will be attached to each specimen to measure rotations. GT personnel will build frames to attach the instrumentation. Besides, LVDTs will be installed by GT personnel at MAST site, and cable lengths and connectors will be provided by MAST personnel. Details about location and layout of the LVDTs attached to the specimens are shown in Figure 23.

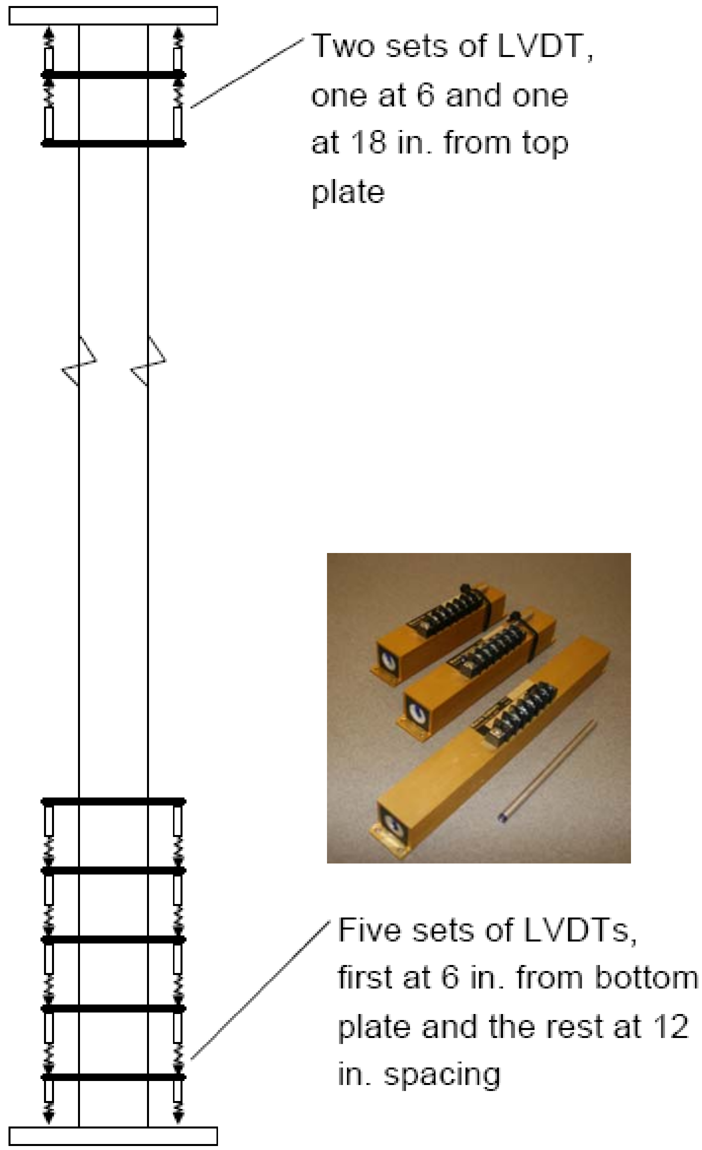

Figure 23. Details of LVDTs attached to the specimens

It is expected that to speed up the instrumentation process, all the LVDT will be attached to a single mounting frame. The mounting frame will be designed and fabricated by GT with input from MAST personnel to insure that the design will not harm the LVDTs in any way.

3.4 String-pots instrumentation

Up to 12 string-pots will be used to measure lateral displacements every 4ft. An upper limit expected for lateral displacement is about ±12 in.. String-pots will be installed by GT personnel at MAST site, and cable lengths and connectors will be provided by MAST personnel as well as an external support reference frame. Details about location and layout of the string-pots in the specimens are shown in Figure 24.

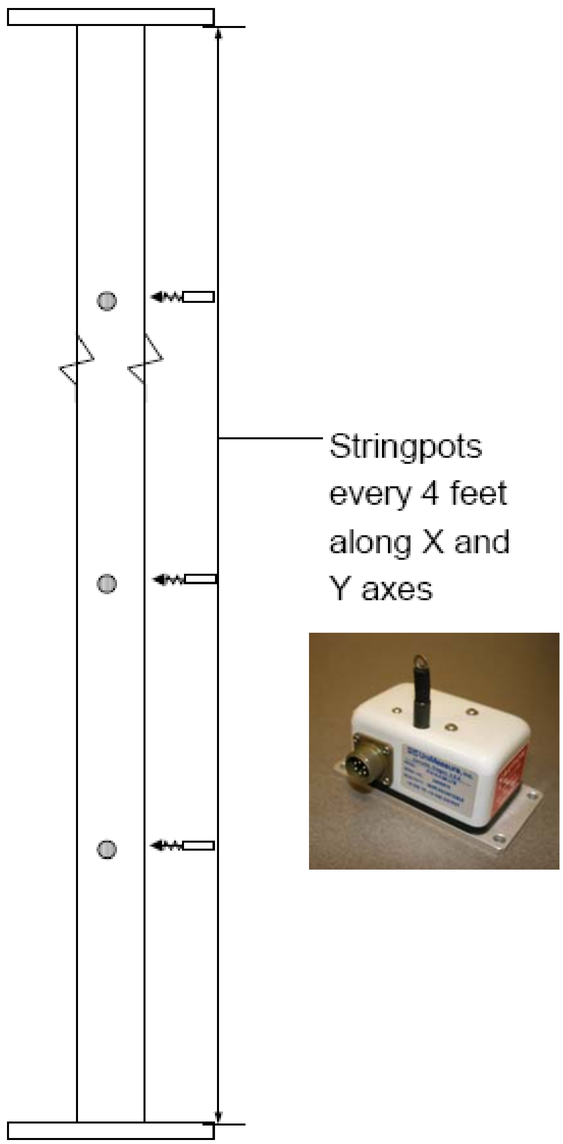

Figure 24. Details of string-pots in the specimens

3.5 Metris (Krypton) Measuring System

It is of interest to measure in-plane deformations on the specimens with the Metris K600 Dynamic Measuring Machine (DMM). The proposed layout of the LED target points on the specimens is shown in Figure 25. A total of 28 LEDs are proposed for the initial specimens. If the data appears to be off high quality, the amount of LEDs will be increased. The Metris DMM measurements are to be collected and time-stamped by the data acquisition system together with the rest of the LVDT and strain gage instruments. MAST personnel will provide the LEDs needed and assist with the initial installation.

The region to be covered by the Metris system is approximately 48” x 36”. According to the MAST Equipment Overview documents, the DMM machine could be placed approximately 60 to 72 inches away from the specimen. The measuring surface would thus be within Zone I of the K600-DMM field of vision. The exact position of the DMM machine will be decided in conunction with MAST personnel to maximize the field of view and avoid interferences with other instrumentation (LVDT mounting frame in particular). The location of the LEDs will be verified carefully before the test.

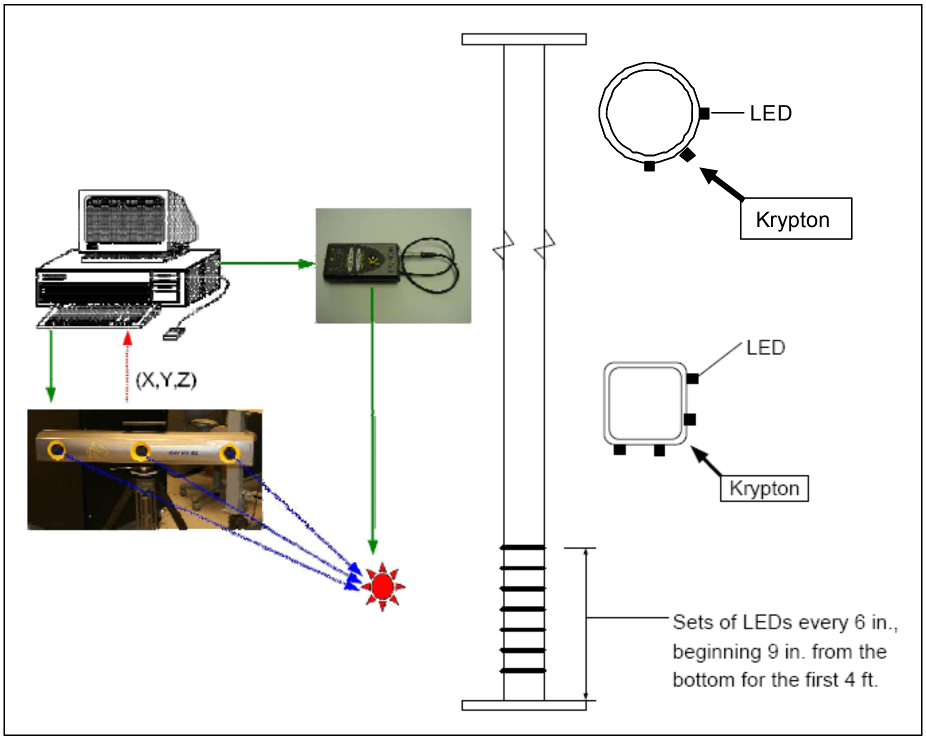

Figure 25. Details of LEDs in the specimens

3.6 Visual Data and Telepresence

MAST equipment for visual data and telepresence will be needed. MAST personnel will provide assistance regarding this issue (Figure 26).

Four robotic towers will be used. The exact location of the robotic towers will be determined with the MAST staff during the test setup. The settings regarding the shelf heights of the robotic towers will be determined with the MAST staff during the test setup. There are no specific lighting requirements. The lighting provided by the robotic towers is expected to be sufficient. Details on camera slighting and interference identification will be determined with the MAST staff during the test setup.

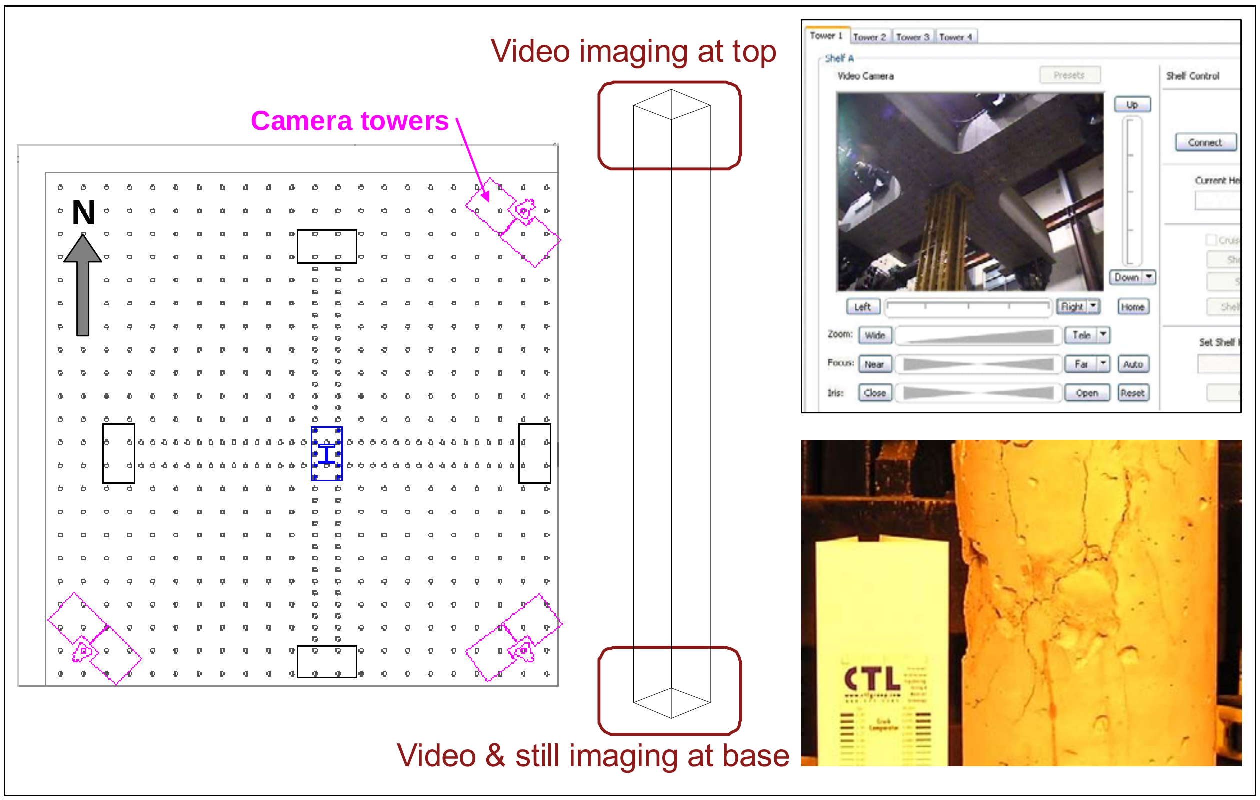

Figure 26. Visual Data and Telepresence

4 Testing plan

4.1 Pretest shakedown

The top of the column will be bolted to the MAST crosshead and initial small lateral deformations imposed in cyclic fashion (±0.25 in.) with and without axial load. Results for this short test will be processed and analyzed to ensure proper performance of the loading and data acquisition systems and instrumentation. The whole system will remain elastic. Estimated time: 4 hours.

4.2 Load histories

4.2.1 Cyclic compression force and bending moment (unlikely)

The load histories for the tests will be primarily increasing cyclic deformations along the principal axis of each specimen. The incremental axial load and fully reversed bending moments can be imposed in at least two different ways (perhaps with different resolutions).

In the first case (Figure 27), one could control the incremental axial load at the top, while maintaining the moment at the top slaved to the axial load times the fixed initial eccentricity αL. All the other out of plane DOF will be set to zero. In this case, it is expected that the MAST machine will adjust the loads in the two vertical and horizontal actuators in the plane of loading to reach the required values.

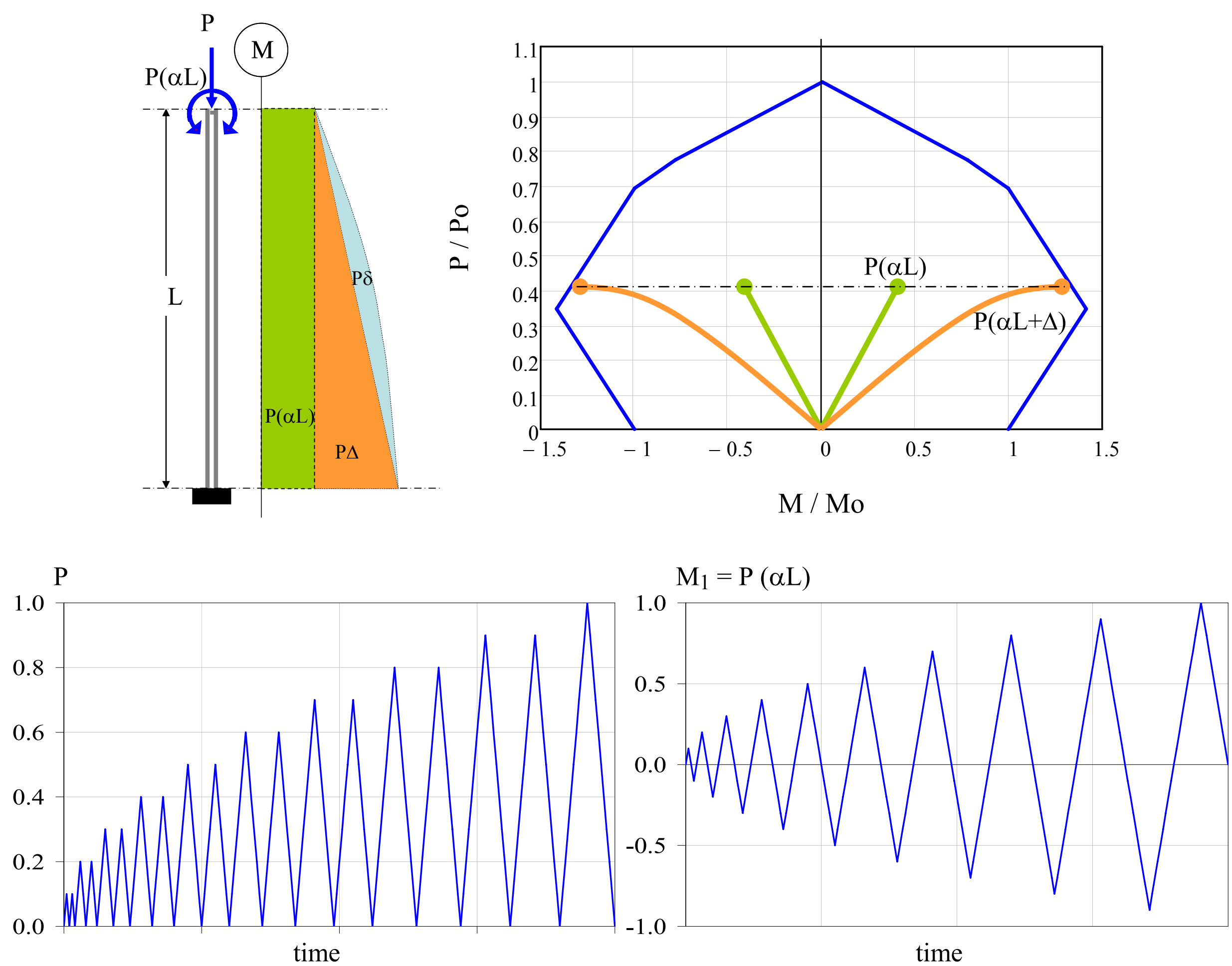

Figure 27. Loads imposed (option 1)

4.2.2 Cyclic compression and lateral forces

In the second case (Figure 28), one could envision the problem as a "nominal load" problem, and apply at the top of the specimen an incremental axial force (P) and a lateral force (αP). The value of α may range from 0.001 up to 0.10 for this and the previous case.

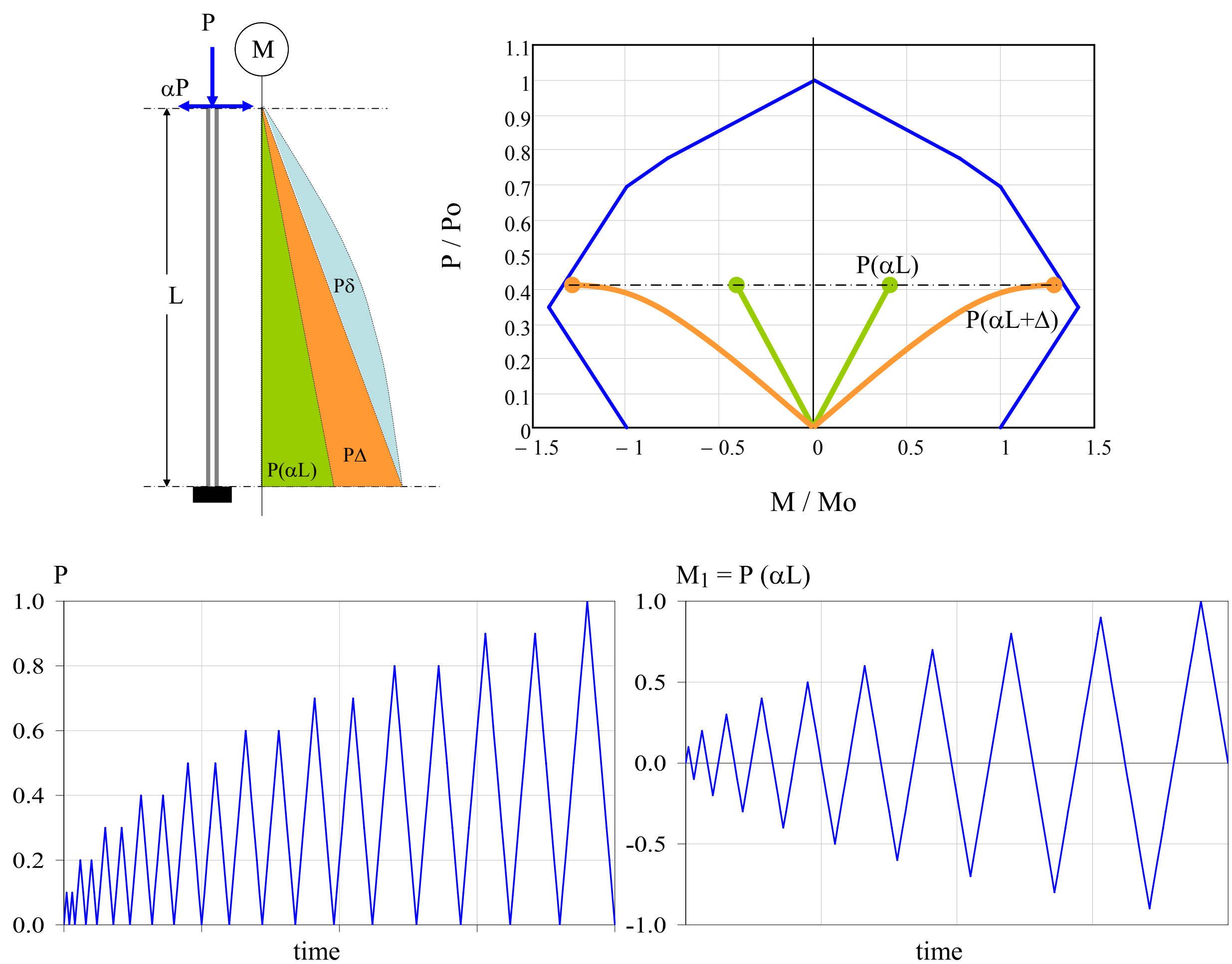

Figure 28. Loads imposed (option 2)

Regarding the limits in both axial load (P) and bending moment (M_1), in order to avoid exceeding the capacity of the MAST system and the capacity of the beam-column element, these loads will be constrained to the following limits:

$$P \le 1320kip - \frac{2 \cdot M_{crosshead}(kip \cdot ft)}{27\,ft} \le \chi P(M)$$

$$M_1 \le M_{\max}(P) - P\Delta$$

Where: $M_{\max}(P)$ is the maximum bending moment capacity in the element axially loaded with a compression P. M_1 is the first order moment, which is equal to $P(\alpha L)$. $M_{crosshead}$ is the bending moment applied at the crosshead which is zero in the first load case and M_1 in the second one. Δ is the maximum lateral displacement.

The first equation above is derived assuming uniaxial bending avoiding exceeding an axial capacity of 330kips in each one of the actuators and the maximum axial capacity in the beam column element $\chi P(M)$. The second equation intends to avoid exceeding the maximum flexural capacity ($M_{\max}=P(\alpha L+\Delta)$) of the beam column accounting for the second order effects. If conservatively $M_{crosshead}$ is assumed equal to $M_{\max}$, a conservative limit for the axial load (in terms of αL and Δ in inches) is given by:

$$P \leq \frac{1320kip}{1-\frac{2(\alpha \cdot L+\Delta)}{324in}} = \frac{213840kip}{\left(\frac{\alpha \cdot L+\Delta}{in}\right)+162}$$

It is estimated that, initially, each test may take up to a week. It is expected that later tests will take less time, as some instrumentation for the next test will be installed while the current test is being tested. It is expected that a three-day turnaround can be achieved as the project advances.

4.2.3 Cyclic lateral displacement with constant compression force

A third alternative (Figure 29) consists in the application of a constant axial load, which can be fixed with values from $0.1P_o$ to $0.6P_o$, and a lateral displacement or drift acting cyclically, which can be proportional to the elastic displacement (Δ_y). As seen in the displacement history, once the analytical Δ_y is reached, elastic cycles will be performed just after each cycle for validation and calibration purposes.

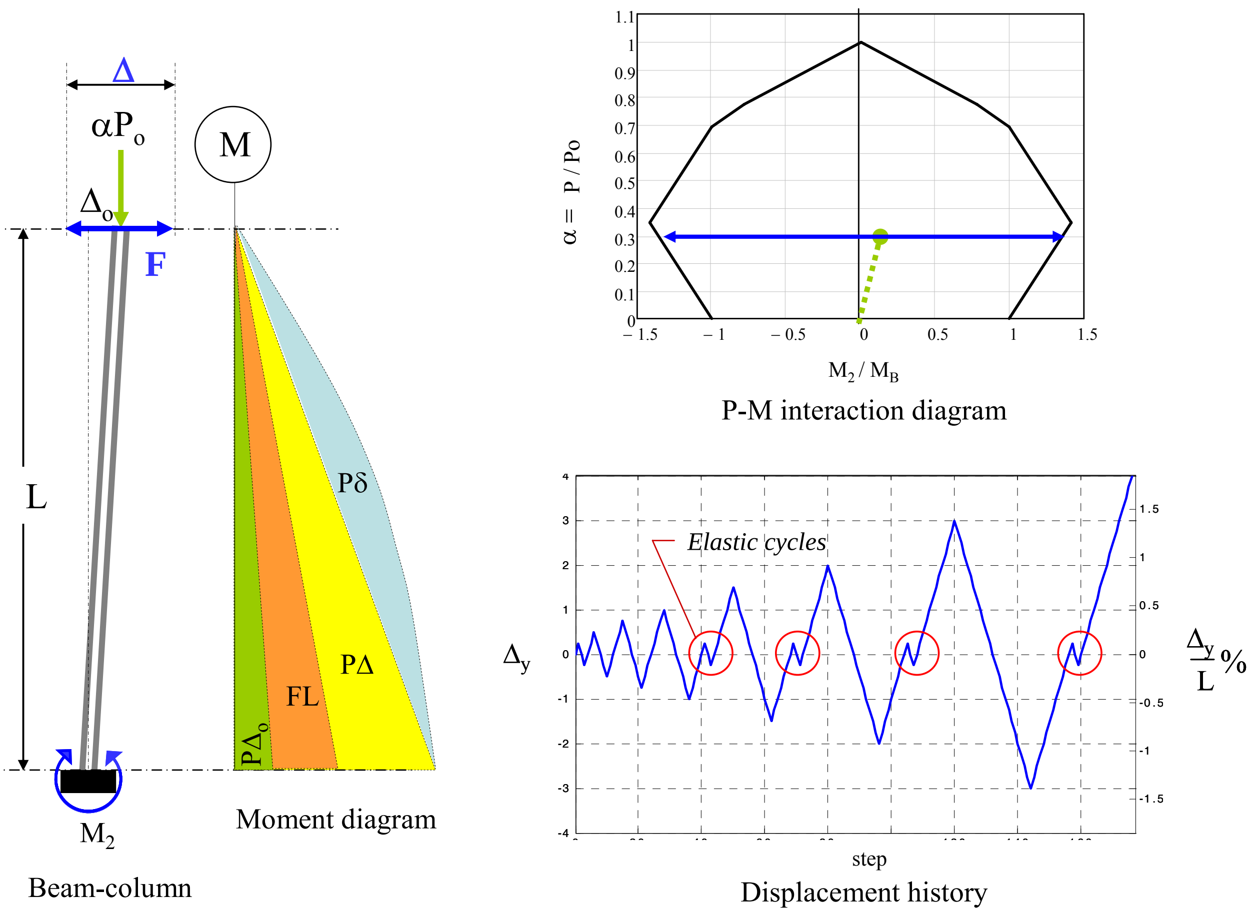

Figure 29. Displacement control (option 3)

4.3 MAST 6-DOF loads and displacements

4.3.1 Analysis with variable eccentric compression load

The intent is to apply a series of progressively larger axial loads that will subject the column to a P-M loading as shown upper-right corner in Figure 27 and Figure 28. It is assume that for most of the tests the loading history will be applied slowly and on a principal plane. Two of the testes on the RCFT will feature loading along a plane connecting the corners of the column. If at the end of some of the tests the specimen is still relatively undamaged, some more complicated load histories will be imposed to collect data on changes in EI with unusual load histories.

The following sections summarize the results for a fiber-based analysis for each specimen (From Table 13 to Table 16, and from Figure 30 to Figure 45).

Table 13. Summary of Fiber-based analysis for the CCFT20x0.25

L (ft)	f_c' (ksi)	e (in)	P_{max} (kip)	F_{max} (kip)	M_{1_max} (k-ft)	M_{2_max} (k-ft)	Δ_{x_max} (in)	Δ_{y_max} (in)	θ_{z_max} (deg)
18	5	0	1250.9	2.50	45.0	91.6	0.45	0.17	0.18
		1	1250.9	8.29	149.3	307.6	1.52	0.18	0.62
		5	818.8	20.59	370.6	587.5	3.18	0.13	1.23
		10	523.1	25.26	454.7	600.3	3.34	0.08	1.28
	12	0	1280.2	2.56	46.1	59.8	0.13	0.08	0.05
		1	1280.2	8.49	152.8	198.1	0.43	0.08	0.17
		5	1280.2	32.19	579.5	915.3	3.15	0.09	1.18
		15	469.4	33.54	603.7	731.3	3.26	0.01	1.21
26	5	0	978.0	1.96	50.9	271.4	2.71	0.20	0.77
		1	818.8	4.26	110.8	327.4	3.18	0.17	0.89
		5	545.8	9.84	255.8	569.6	6.90	0.16	1.86
	12	0	1280.2	2.56	66.6	134.3	0.64	0.11	0.18
		1	1280.2	6.66	173.3	352.5	1.68	0.12	0.47
		5	768.1	13.85	360.0	729.8	5.78	0.09	1.51
		15	341.4	17.10	444.5	605.0	5.64	0.02	1.47

Table 14. Summary of Fiber-based analysis for the CCFT12.75x0.25

L (ft)	f_c' (ksi)	e (in)	P_{max} (kip)	F_{max} (kip)	M_{1_max} (k-ft)	M_{2_max} (k-ft)	Δ_{x_max} (in)	Δ_{y_max} (in)	θ_{z_max} (deg)
18	5	0	418.6	0.84	15.1	87.9	2.09	0.13	0.86
		1	341.5	2.26	40.8	148.0	3.77	0.13	1.52
		5	220.3	5.54	99.7	203.0	5.63	0.13	2.22
		10	154.2	7.45	134.1	211.6	6.04	0.11	2.36
	12	0	680.3	1.36	24.5	120.2	1.69	0.11	0.70
		1	510.3	3.38	60.9	164.9	2.45	0.09	0.97
		5	264.6	6.65	119.8	209.4	4.06	0.06	1.56
26	5	0	209.3	0.42	10.9	59.3	2.78	0.10	0.79
		1	165.3	0.86	22.4	63.6	3.00	0.08	0.84
		5	121.2	2.18	56.8	135.8	7.82	0.14	2.15
	12	0	340.2	0.68	17.7	76.3	2.07	0.07	0.59
		1	245.7	1.28	33.2	76.9	2.13	0.05	0.59
		5	151.2	2.73	70.9	159.7	7.05	0.08	1.90

Table 15. Summary of Fiber-based analysis for the RCFT20x12x0.3125s

L (ft)	f_c' (ksi)	e (in)	P_{max} (kip)	F_{max} (kip)	M_{1_max} (k-ft)	M_{2_max} (k-ft)	Δ_{x_max} (in)	Δ_{y_max} (in)	θ_{z_max} (deg)
18	5	0	1271.9	2.54	45.8	83.9	0.36	0.20	0.15
		1	1271.9	8.43	151.8	280.1	1.21	0.21	0.49
		5	932.7	23.46	422.2	640.2	2.81	0.17	1.10
	12	0	1272.5	2.54	45.8	58.7	0.12	0.10	0.05
		1	1272.5	8.44	151.9	194.7	0.40	0.10	0.16
		5	1272.5	32.00	576.0	784.7	1.97	0.11	0.76
		15	619.0	44.23	796.1	965.6	3.29	0.04	1.24
26	5	0	1102.3	2.20	57.3	357.2	3.27	0.27	0.93
		1	953.9	4.97	129.1	427.8	3.76	0.24	1.06
		5	657.2	11.85	308.0	635.9	5.99	0.20	1.64
	12	0	1272.5	2.54	66.2	128.1	0.58	0.14	0.16
		1	1272.5	6.62	172.2	334.4	1.53	0.15	0.43
		5	928.6	16.74	435.2	853.7	5.41	0.13	1.44
		15	481.5	24.11	626.9	900.7	6.83	0.07	1.80

Table 16. Summary of Fiber-based analysis for the RCFT20x12x0.3125w

L (ft)	f_c' (ksi)	e (in)	P_{max} (kip)	F_{max} (kip)	M_{1_max} (k-ft)	M_{2_max} (k-ft)	Δ_{x_max} (in)	Δ_{y_max} (in)	θ_{z_max} (deg)
18	5	0	996.3	1.99	35.9	261.9	2.72	0.18	1.13
		1	826.8	5.48	98.7	344.0	3.56	0.16	1.44
		5	551.2	13.86	249.5	512.1	5.72	0.16	2.26
	12	0	1272.5	2.54	45.8	122.0	0.72	0.10	0.29
		1	1203.7	7.98	143.6	393.0	2.49	0.11	1.00
		5	687.8	17.30	311.4	597.3	4.99	0.09	1.93
26	5	0	487.6	0.98	25.4	116.4	2.24	0.11	0.64
		1	424.0	2.21	57.4	215.6	4.48	0.12	1.25
		5	318.0	5.73	149.0	408.9	9.81	0.22	2.71
	12	0	791.0	1.58	41.1	192.8	2.30	0.09	0.66
		1	584.6	3.04	79.1	183.5	2.14	0.07	0.60
		5	378.3	6.82	177.3	419.3	7.68	0.11	2.07

The following assumptions were made in the analyses:

- Steel elastic-perfectly plastic: F_y'$=R_yF_y=1.4F_y$, E_s=29000ksi,
- Concrete01: $E_c=0.033w^{1.5}\sqrt{fc'}$, ε_y=0.002, ε_u=0.01
- Eccentricity and initial imperfection: $e=\alpha L-\Delta_o=(F/P)L-\Delta_o$, $\Delta_o=L/500$, K=2 (fix-free)
- Load history as shown in Figure 28

Table 17 shows the crosshead check for both translation and rotation and for two of the most critical values (shown from Table 13 to Table 16). This table shows the desired crosshead displaced shape and the actuator swivel to swivel lengths. As seen, any of these two upper limit values are exceeding the MAST capacity in displacement. The total vertical displacement reaches up to 8 inches, which includes the specimen shortening and rotation of both crosshead and vertical actuators.

Table 17. Check of the crosshead with the some critical values

a) CCFT12.75x0.25, L=18, f_c'=5ksi, e=10in

Desired Crosshead Translations/Rotations		
delta - X	6.04	inches
delta - Y	0.00	inches
delta - Z	-0.11	inches
theta - X	0.00	degrees
theta - Y	2.36	degrees
theta - Z	0.00	degrees

Actuator Swivel to Swivel Lengths

Actuator	Length after move (in)	Min length possible (in)	Max length possible (in)	Okay?	% of Extension Capacity Used
X1	164.14	141.37	173.37	OK	71%
X2	164.14	141.37	173.37	OK	71%
Y3	157.63	141.37	173.37	OK	51%
Y4	157.63	141.37	173.37	OK	51%
Z1	174.10	154.12	194.12	OK	50%
Z2	174.10	154.12	194.12	OK	50%
Z3	167.44	154.12	194.12	OK	33%
Z4	180.76	154.12	194.12	OK	67%

b) RCFT20x12x0.3125w, L=26, f_c'=5ksi, e=5in

Desired Crosshead Translations/Rotations		
delta - X	9.81	inches
delta - Y	0	inches
delta - Z	-0.22	inches
theta - X	0	degrees
theta - Y	2.71	degrees
theta - Z	0	degrees

Actuator Swivel to Swivel Lengths

Actuator	Length after move (in)	Min length possible (in)	Max length possible (in)	Okay?	% of Extension Capacity Used
X1	168.03	141.37	173.37	OK	83%
X2	168.03	141.37	173.37	OK	83%
Y3	157.90	141.37	173.37	OK	52%
Y4	157.90	141.37	173.37	OK	52%
Z1	174.14	154.12	194.12	OK	50%
Z2	174.14	154.12	194.12	OK	50%
Z3	166.47	154.12	194.12	OK	31%
Z4	181.81	154.12	194.12	OK	69%

Figure 30 to Figure 45 show the interaction paths (P-M, P-Δ_x-θ_z) for different specimens loaded with an incremental axial load under different eccentricities. The left sides show the second order P-M_2 path (blue-continuous line) and the first order P-M_1 path (red-dashed line); as a reference, the P-M interaction diagrams (whole or part) are also shown for the cross section (AISC anchor points) and the slender column (AISC P-M simplified). Double axes are included showing normalized P-M loads with reference to maximum cross-section values (P_o, M_b). The right sides show load displacement/rotation paths P-Δ_x-θ_z.

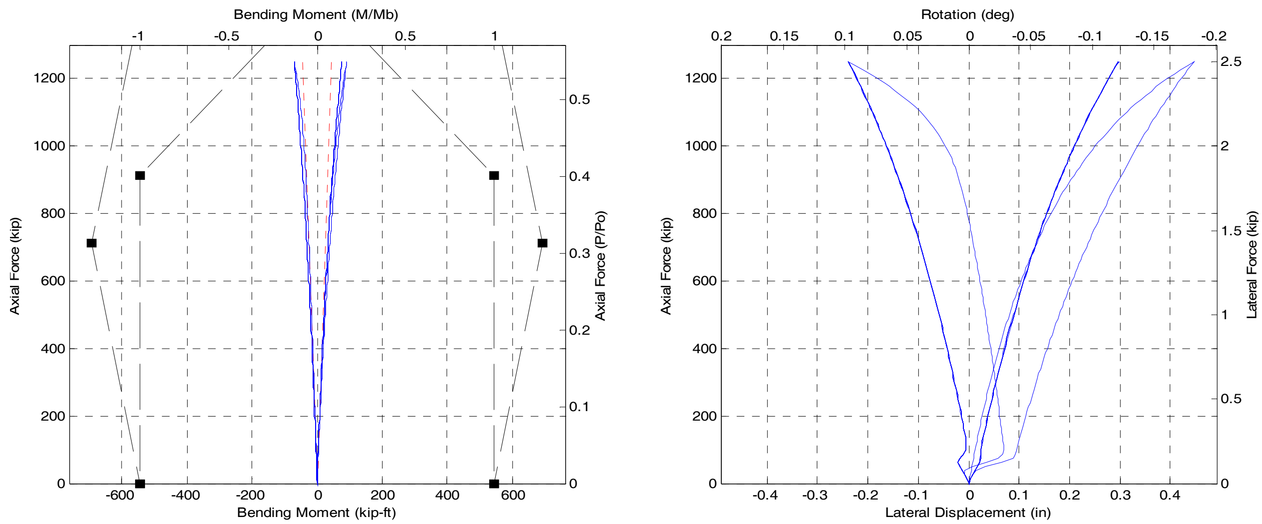

i) no eccentricity

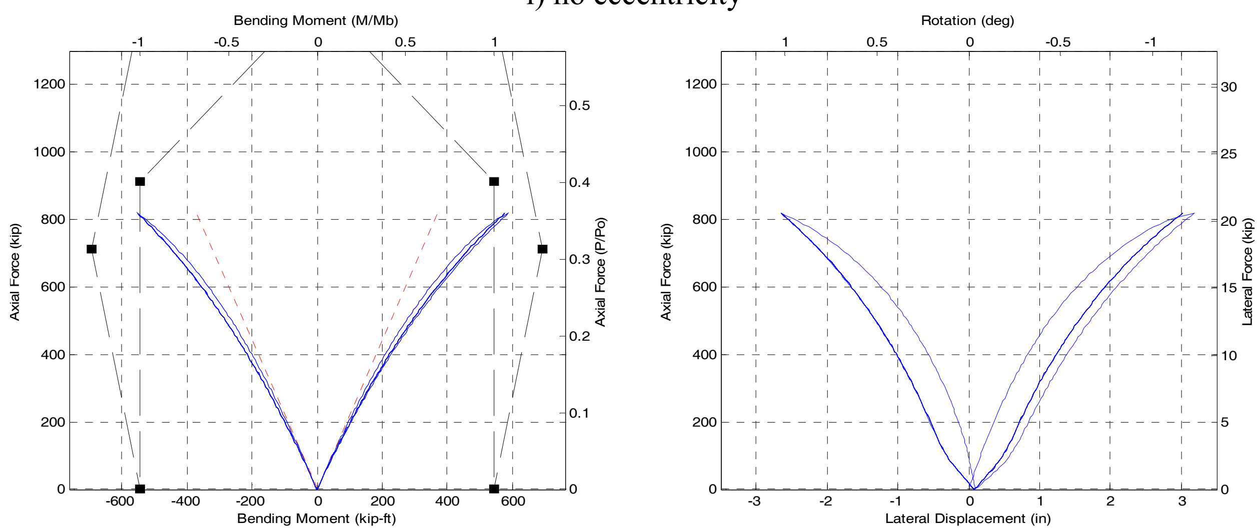

ii) 5in eccentricity

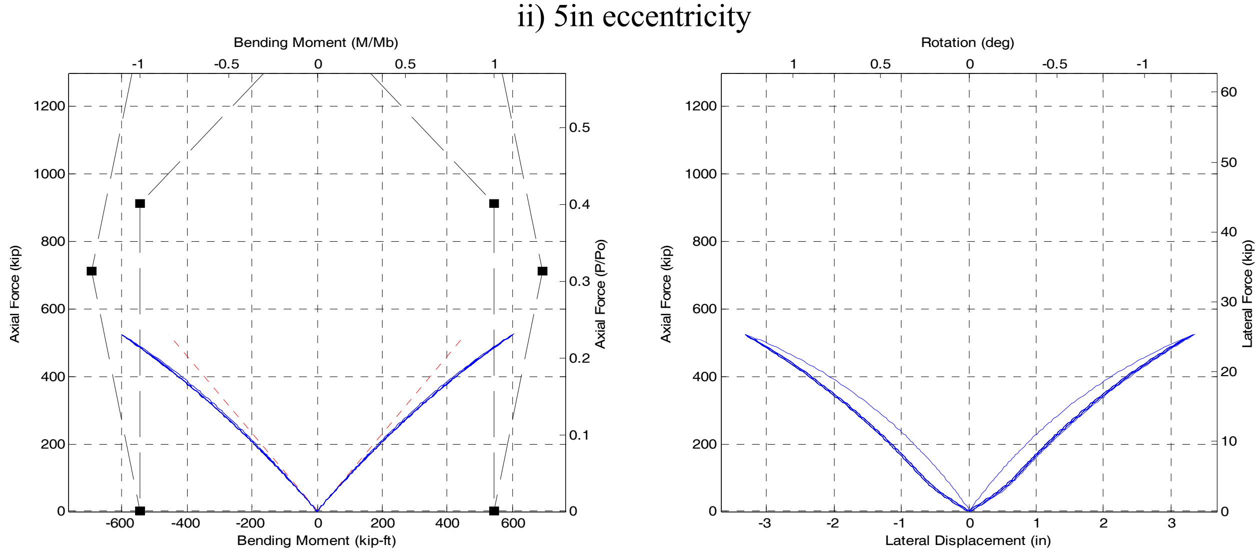

iii) 10in eccentricity

Figure 30. CCFT20x0.25 Specimen (K=2, L=18ft, f'c=5ksi)

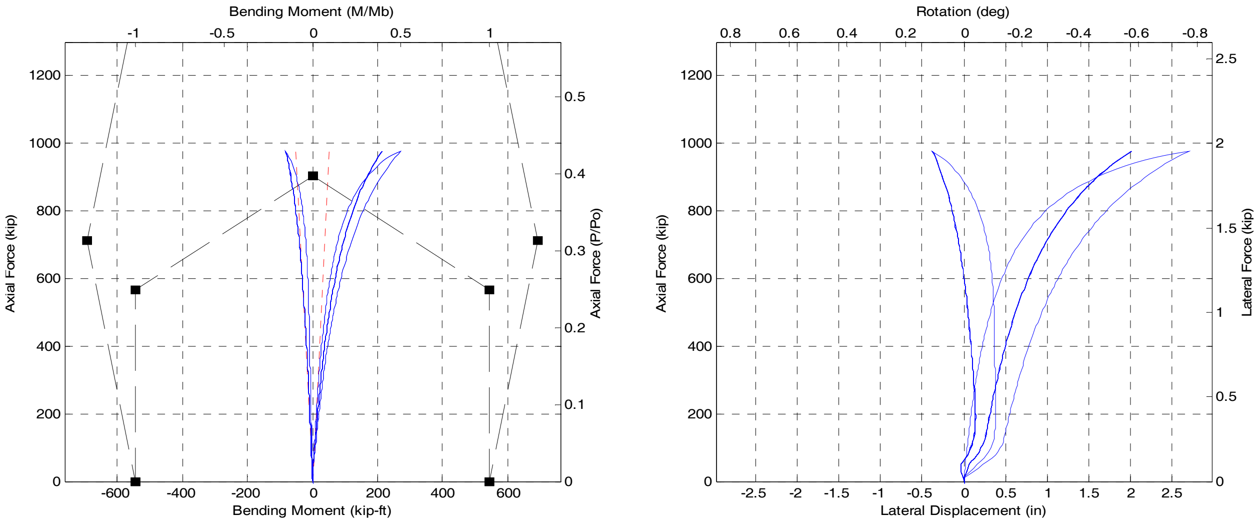

i) no eccentricity

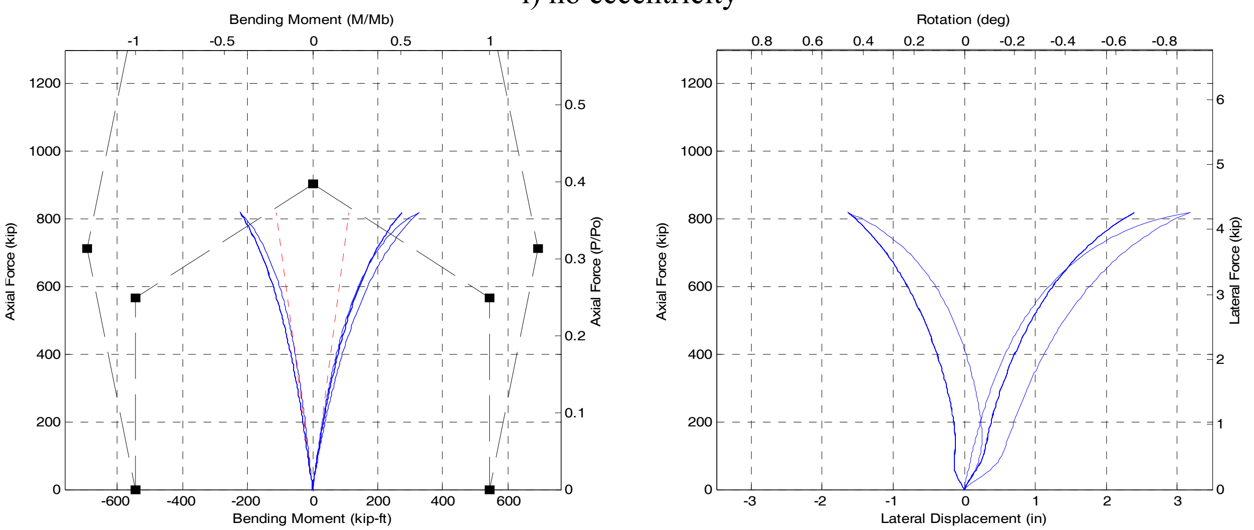

ii) 1in eccentricity

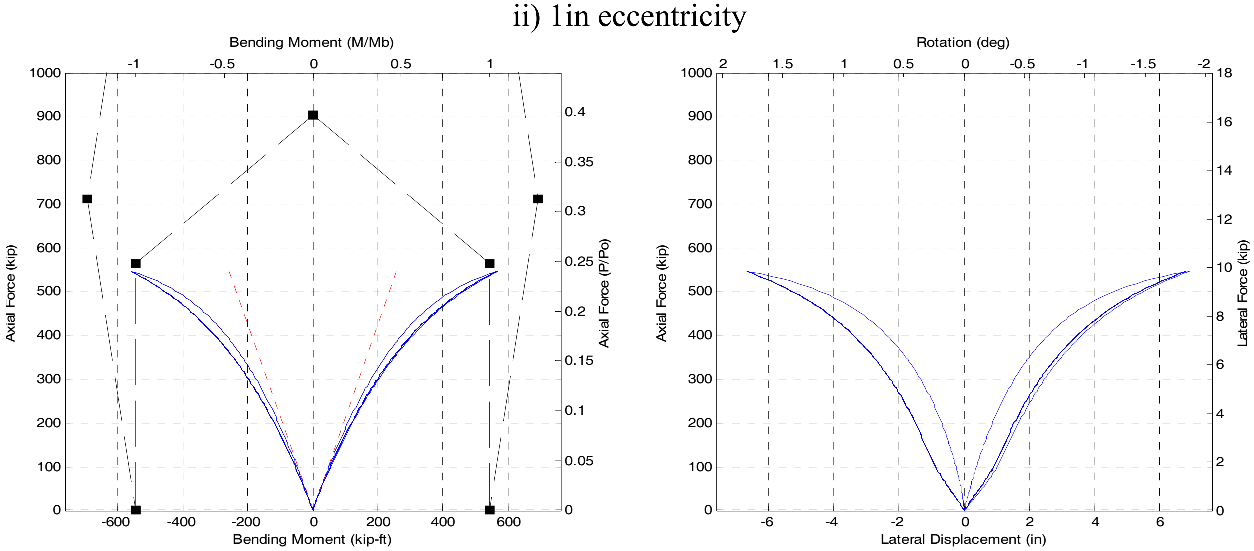

iii) 5in eccentricity

Figure 31. CCFT20x0.25 Specimen (K=2, L=26ft, f'c=5ksi)

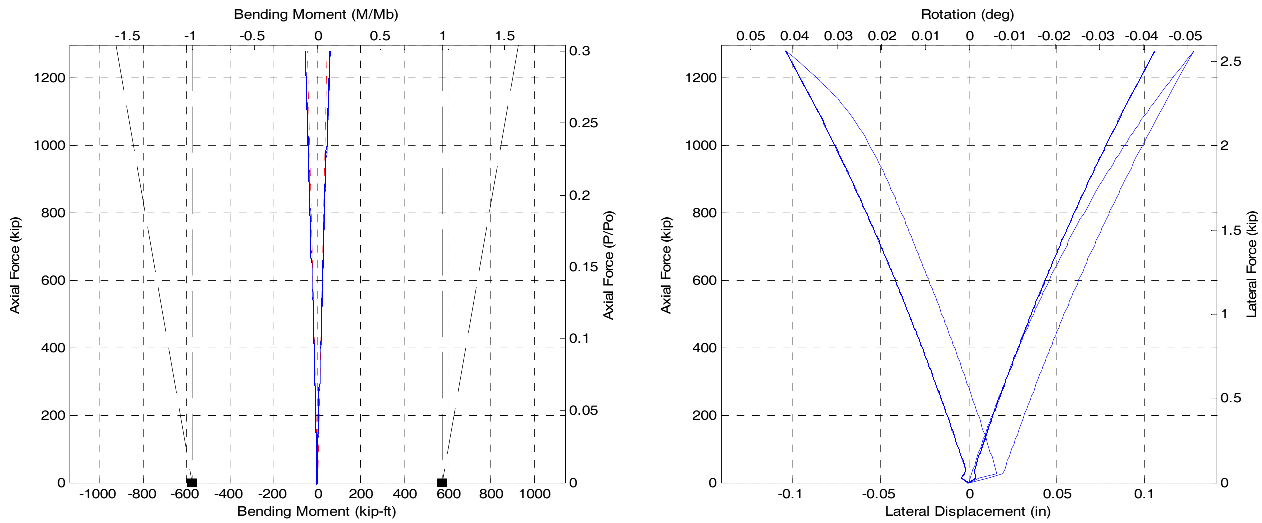

i) no eccentricity

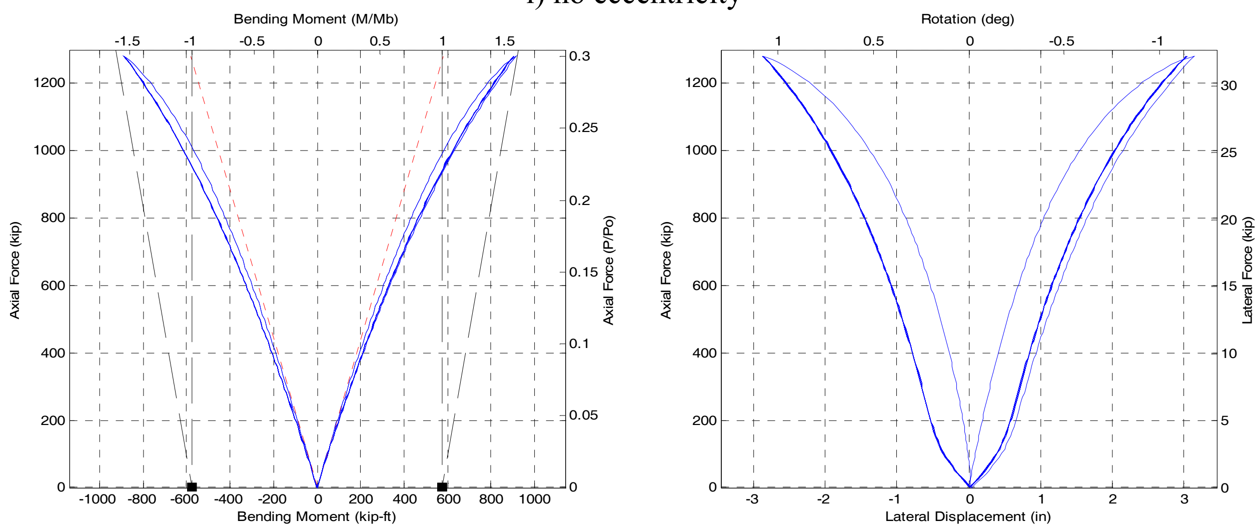

ii) 5in eccentricity

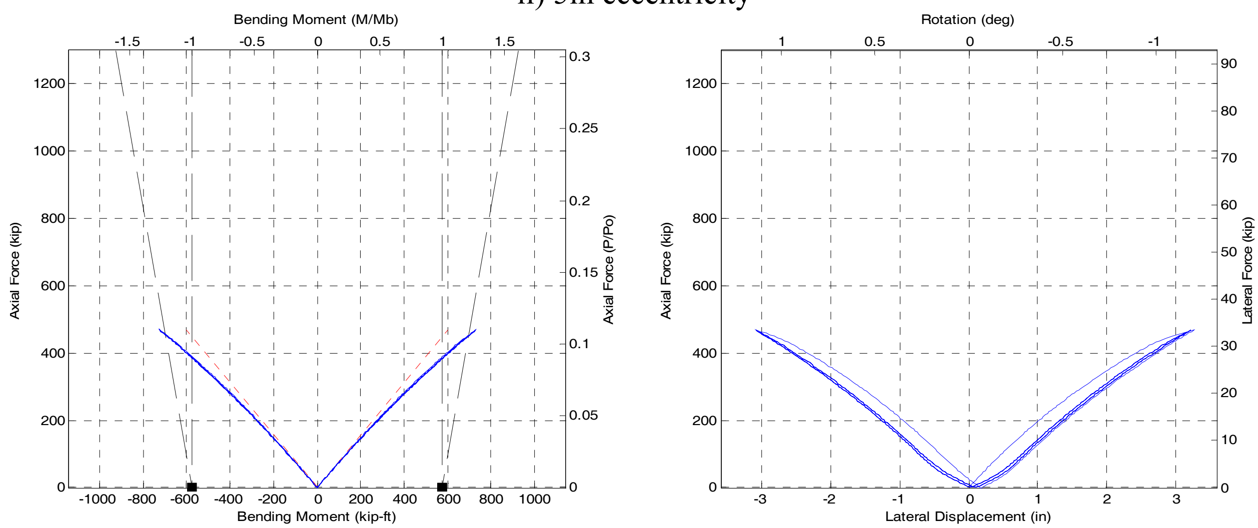

iii) 15in eccentricity

Figure 32. CCFT20x0.25 Specimen (K=2, L=18ft, f'c=12ksi)

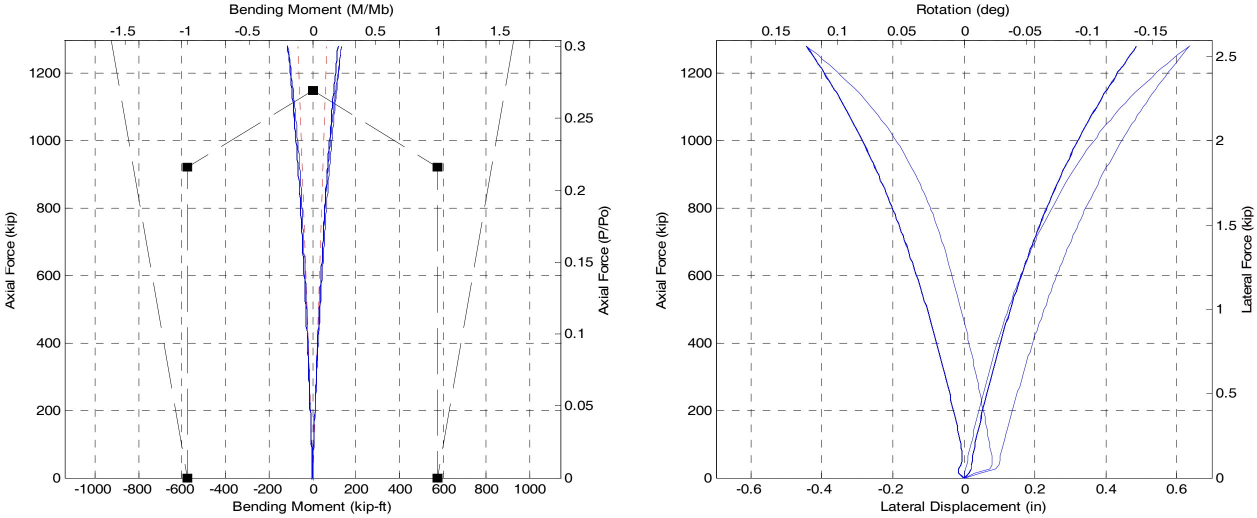

i) no eccentricity

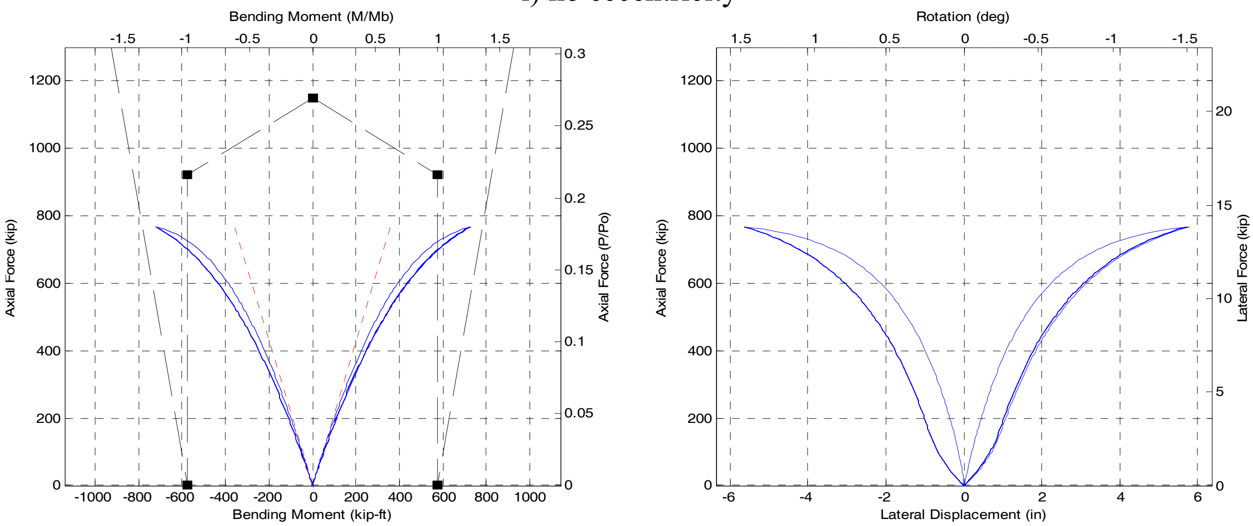

ii) 5in eccentricity

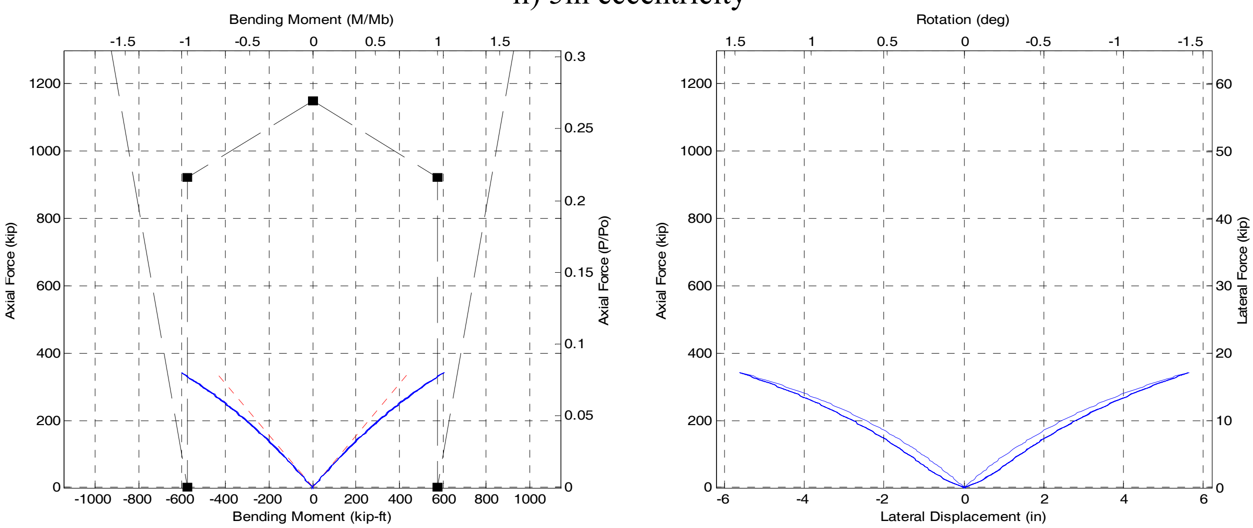

iii) 15in eccentricity

Figure 33. CCFT20x0.25 Specimen (K=2, L=26ft, f'c=12ksi)

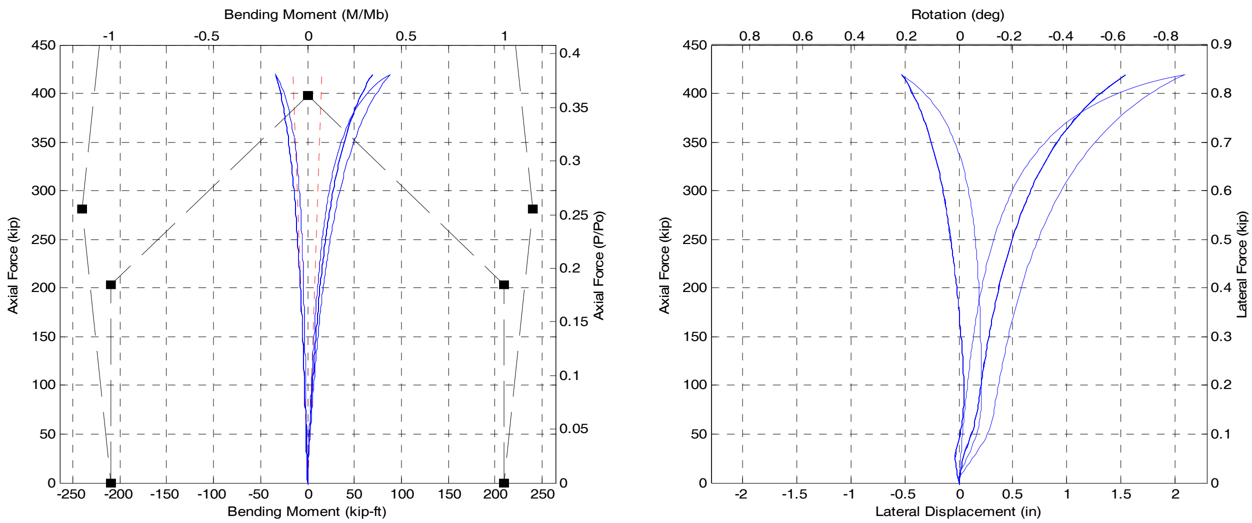

i) no eccentricity

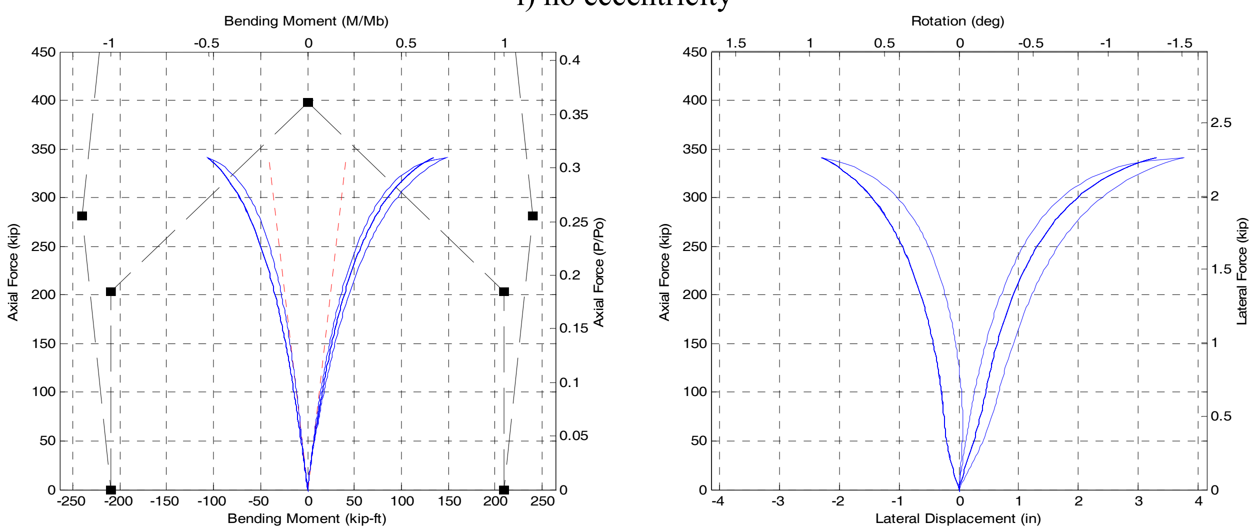

ii) 1in eccentricity

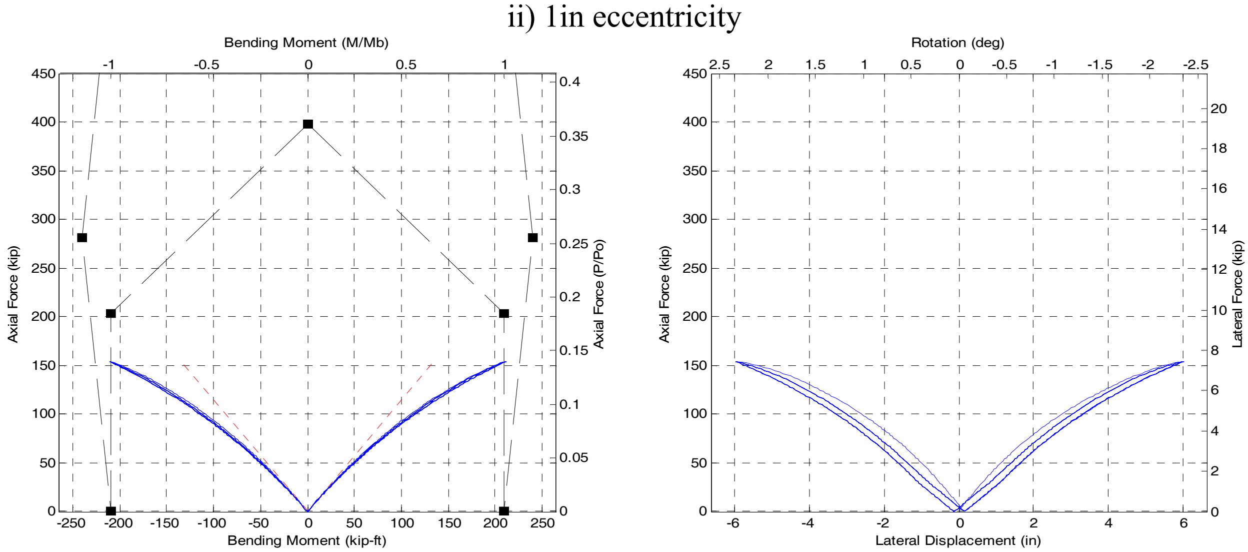

iii) 10in eccentricity

Figure 34. CCFT12.75x0.25 Specimen (K=2, L=18ft, f'c=5ksi)

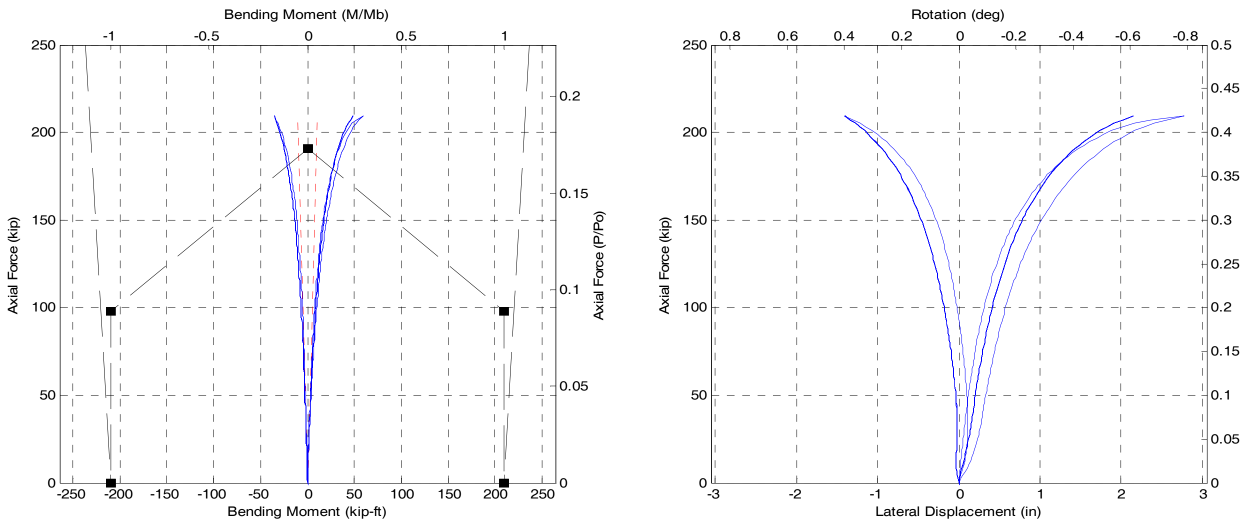

i) no eccentricity

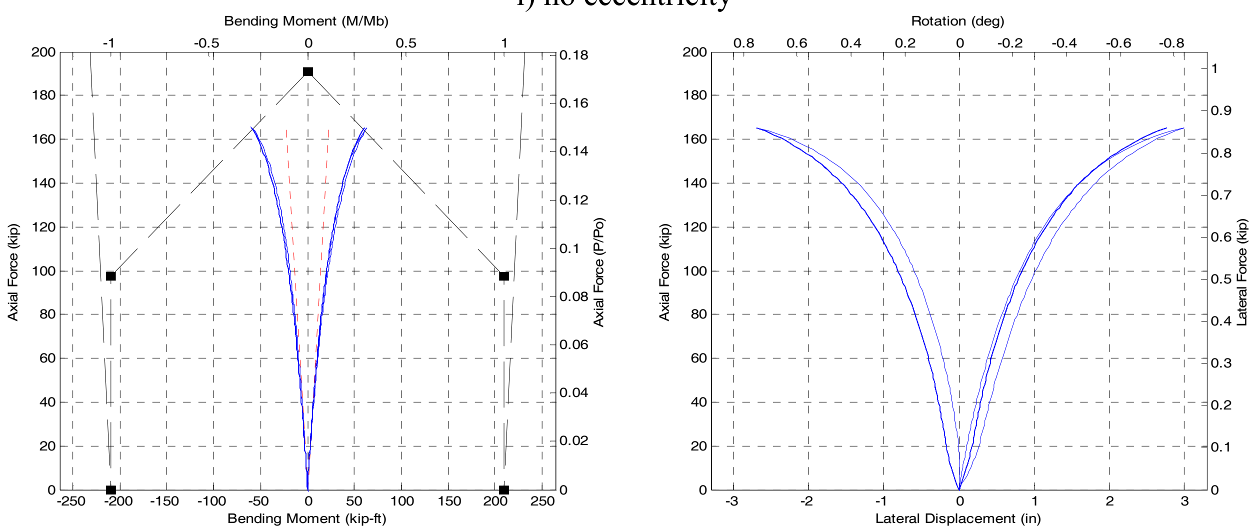

ii) 1in eccentricity

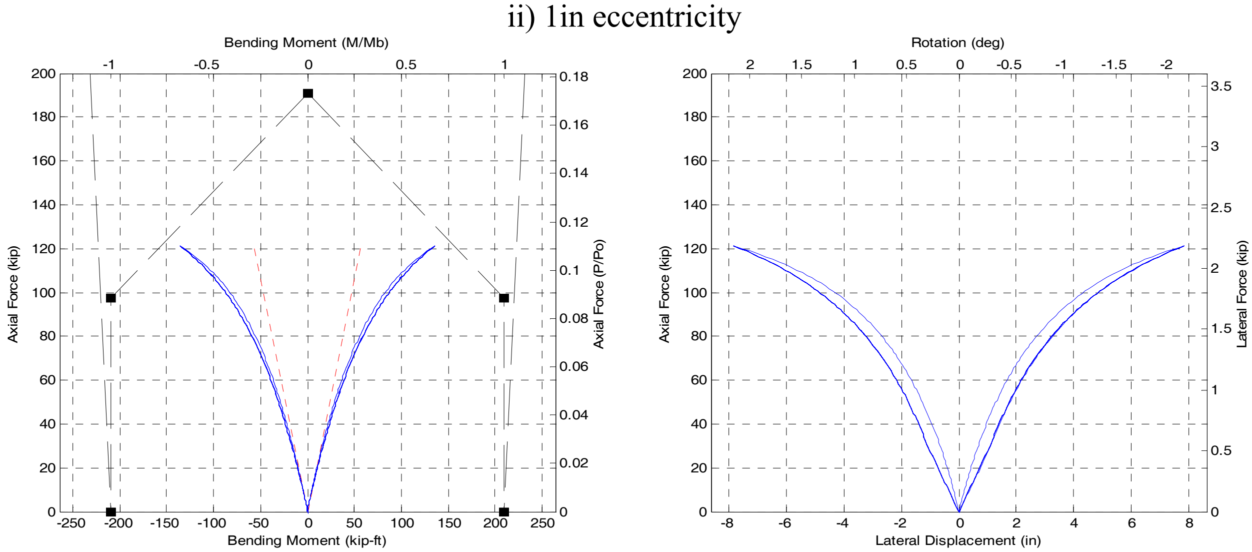

iii) 5in eccentricity

Figure 35. CCFT12.75x0.25 Specimen (K=2, L=26ft, f'c=5ksi)

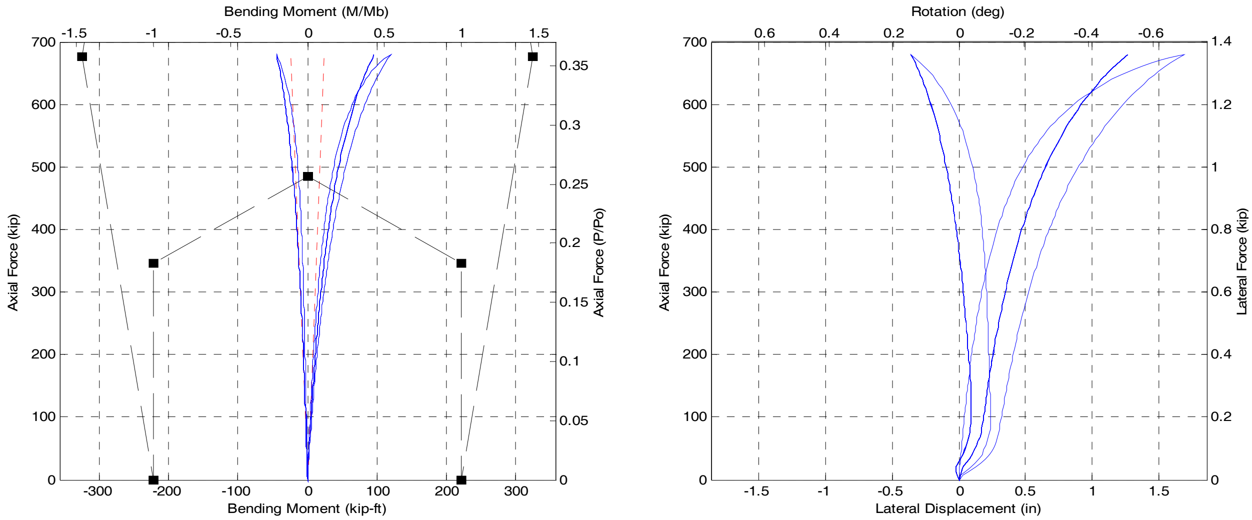

i) no eccentricity

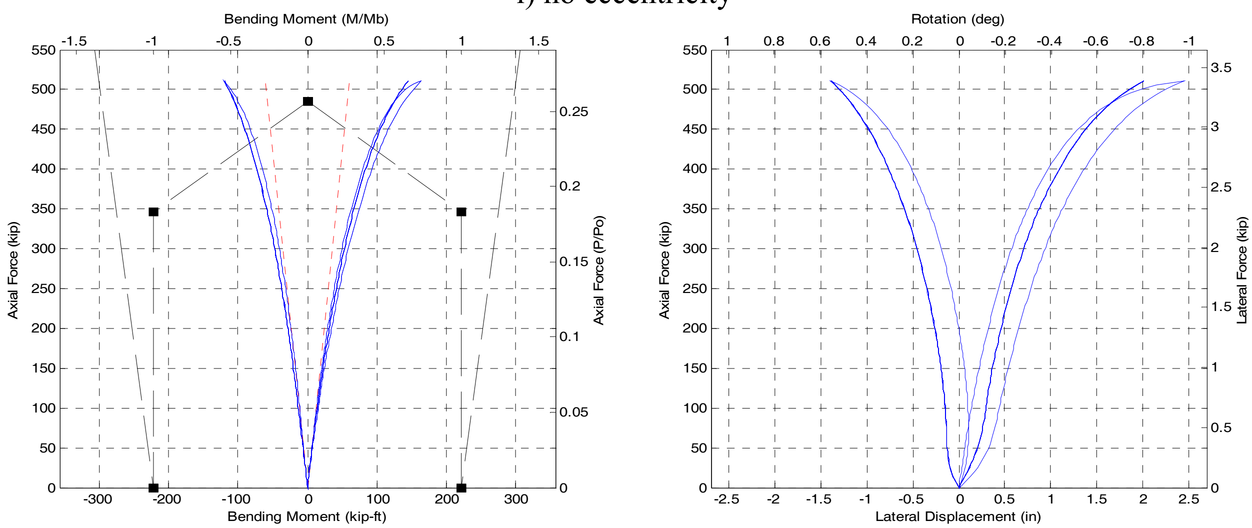

ii) 1in eccentricity

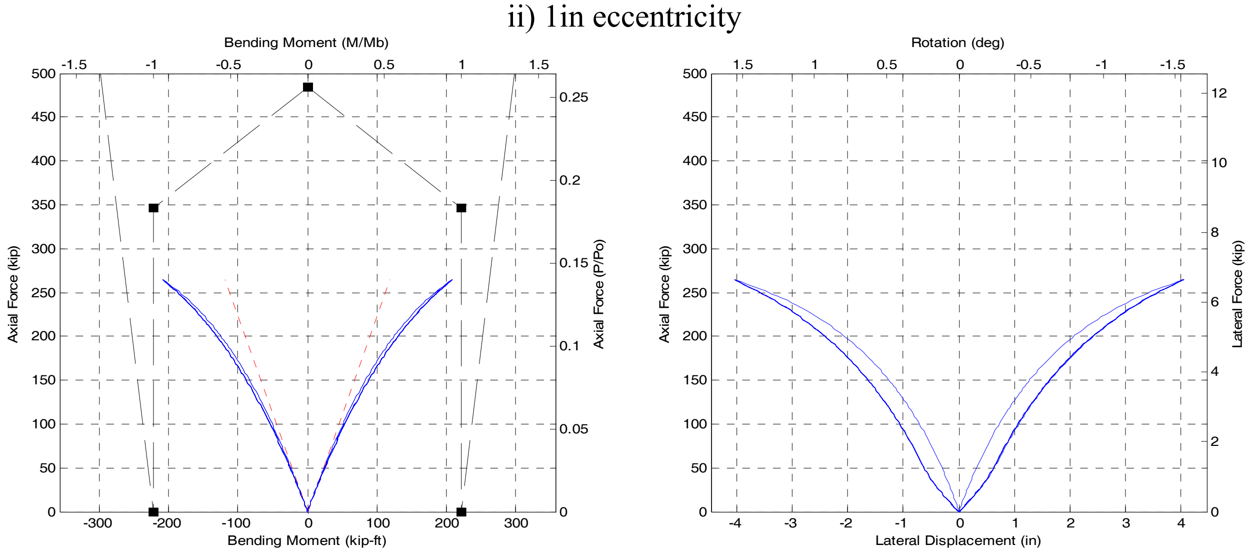

iii) 5in eccentricity

Figure 36. CCFT12.75x0.25 Specimen (K=2, L=18ft, f'c=12ksi)

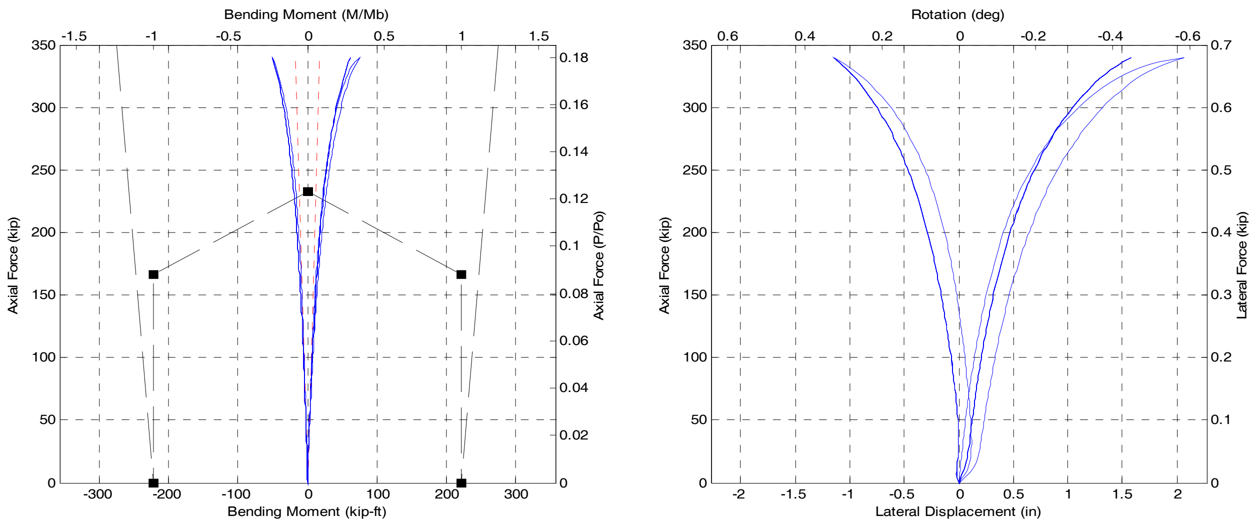

i) no eccentricity

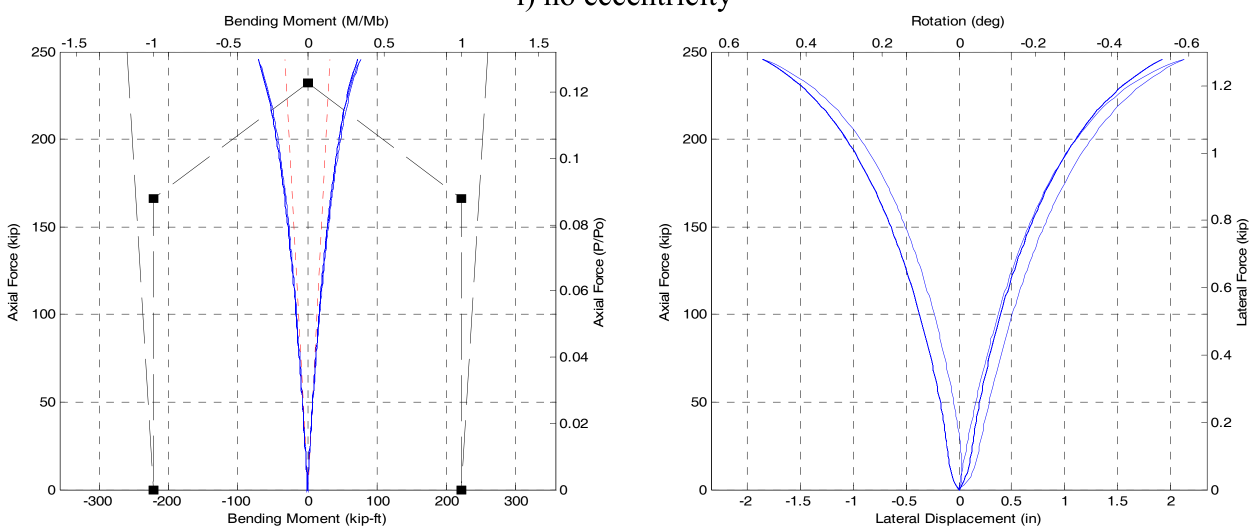

ii) 1in eccentricity

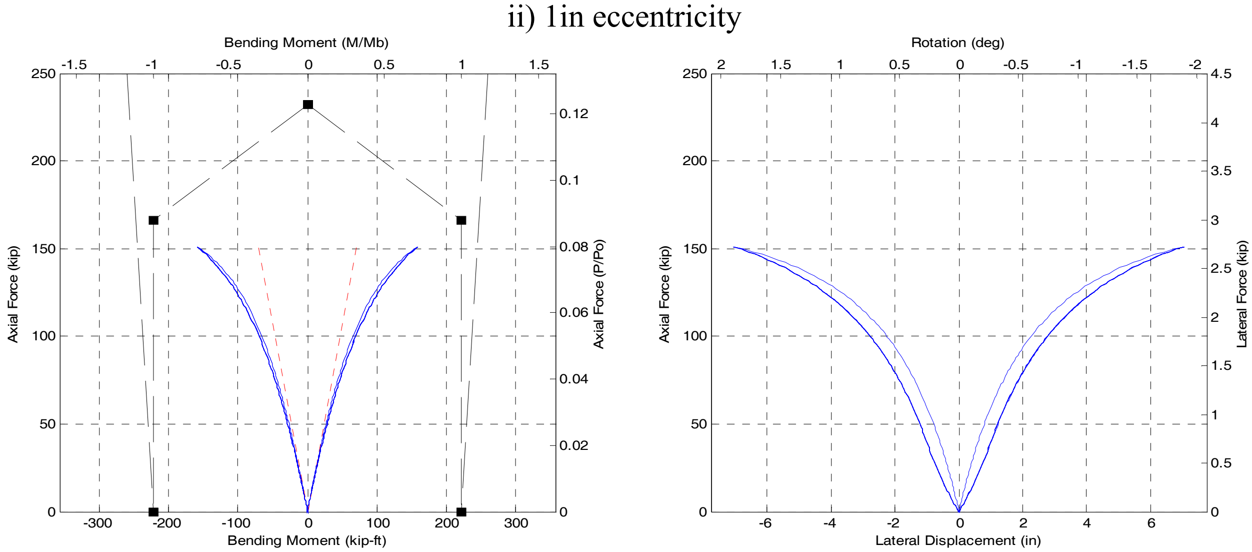

iii) 5in eccentricity

Figure 37. CCFT12.75x0.25 Specimen (K=2, L=26ft, f'c=12ksi)

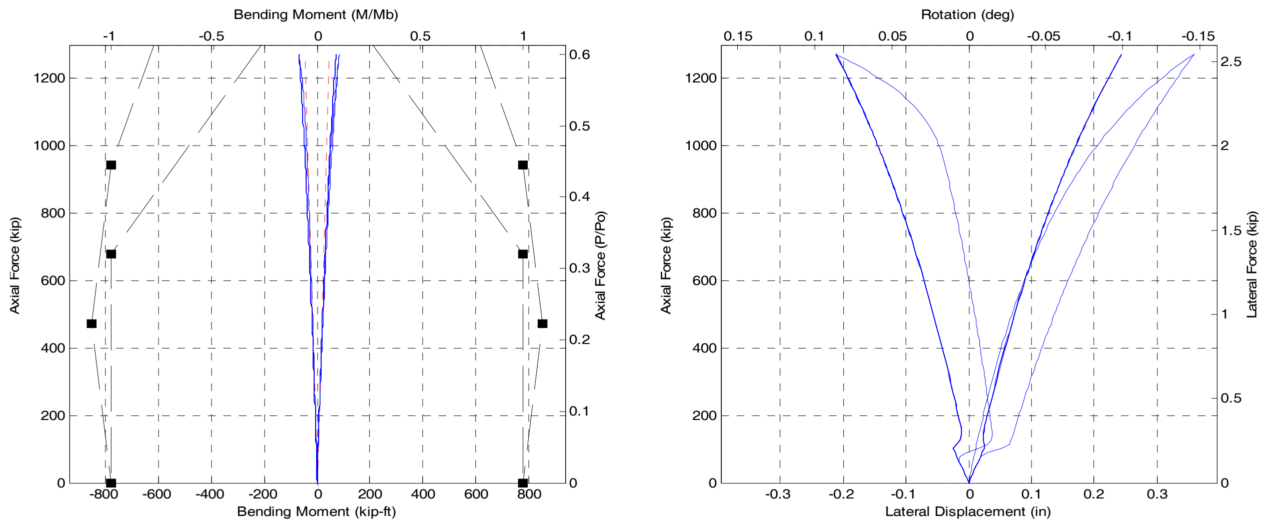

i) no eccentricity

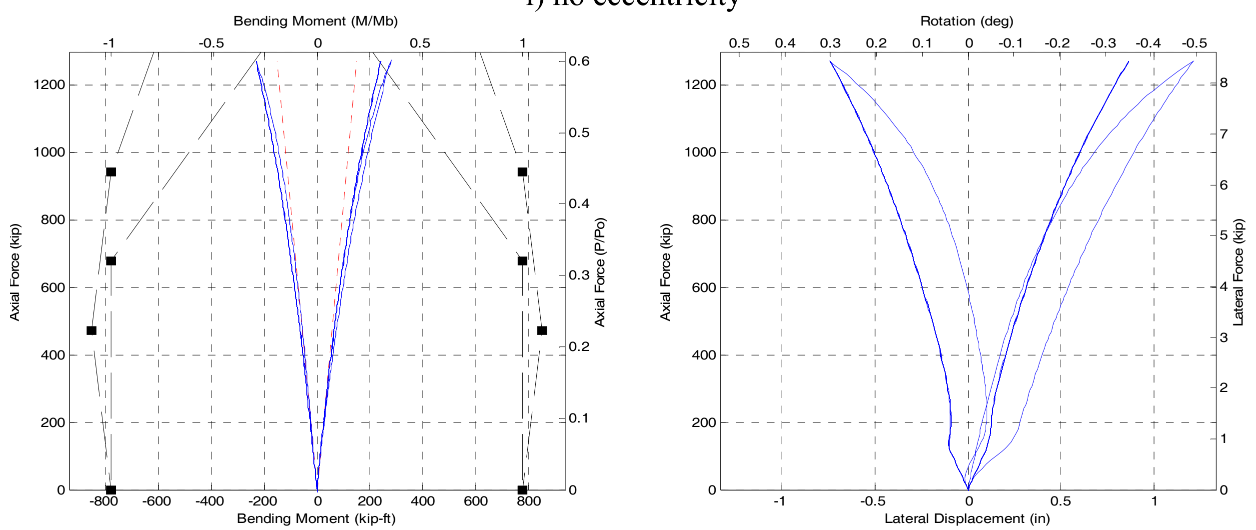

ii) 1in eccentricity

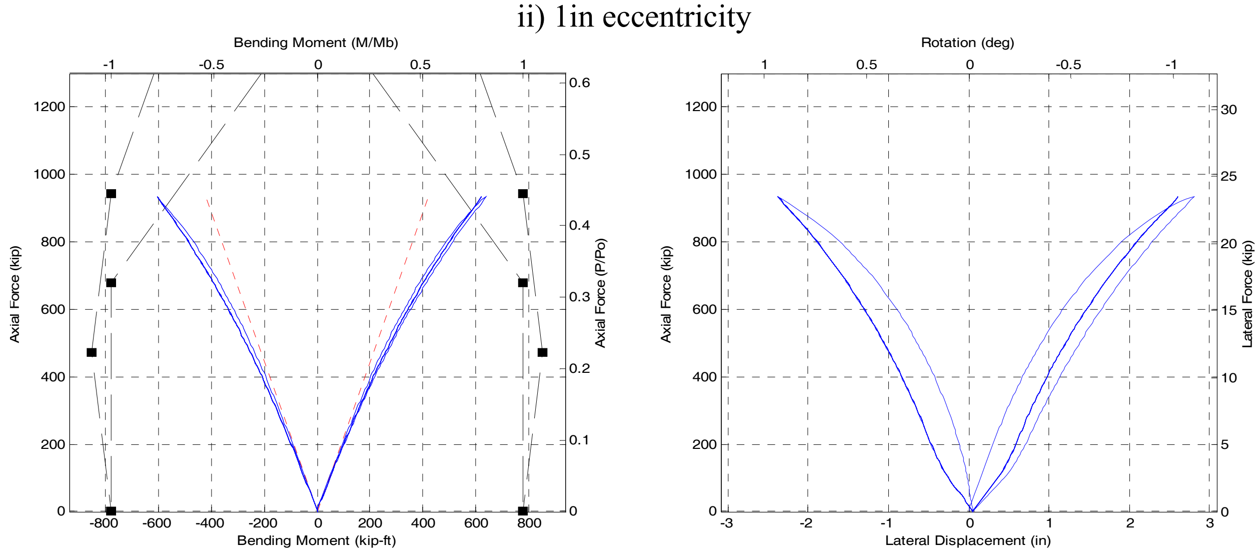

iii) 5in eccentricity

Figure 38. RCFT20x12x0.3125s Specimen (K=2, L=18ft, f'c=5ksi)

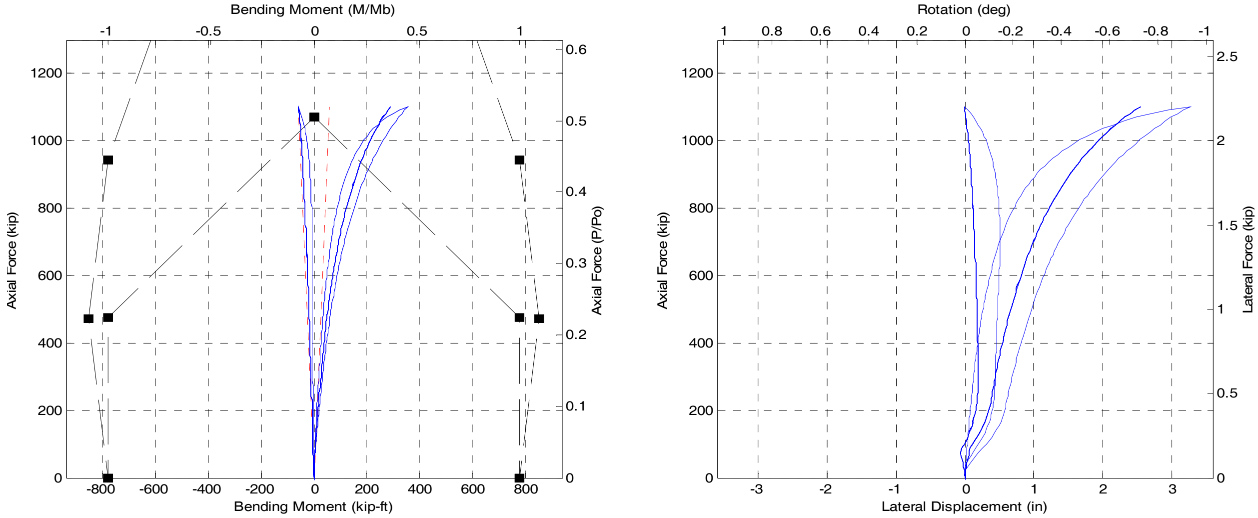

i) no eccentricity

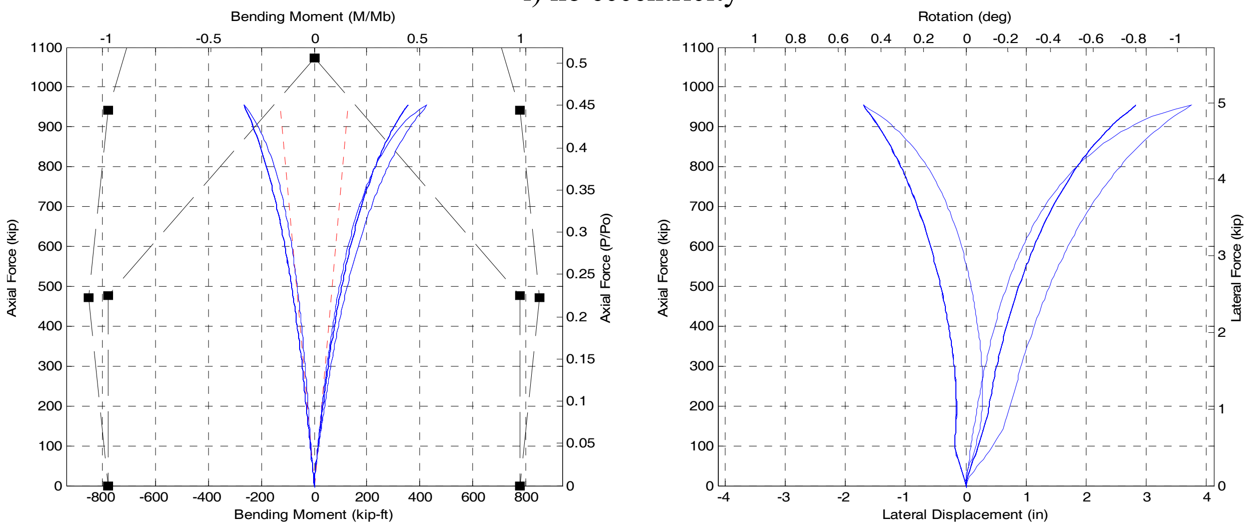

ii) 1in eccentricity

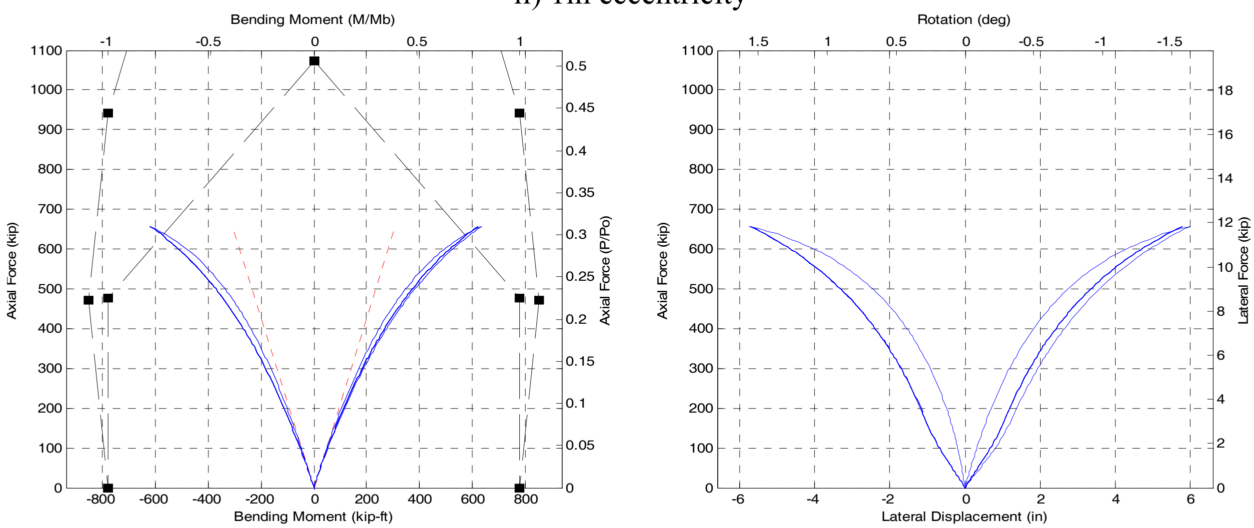

iii) 5in eccentricity

Figure 39. RCFT20x12x0.3125s Specimen (K=2, L=26ft, f’c=5ksi)

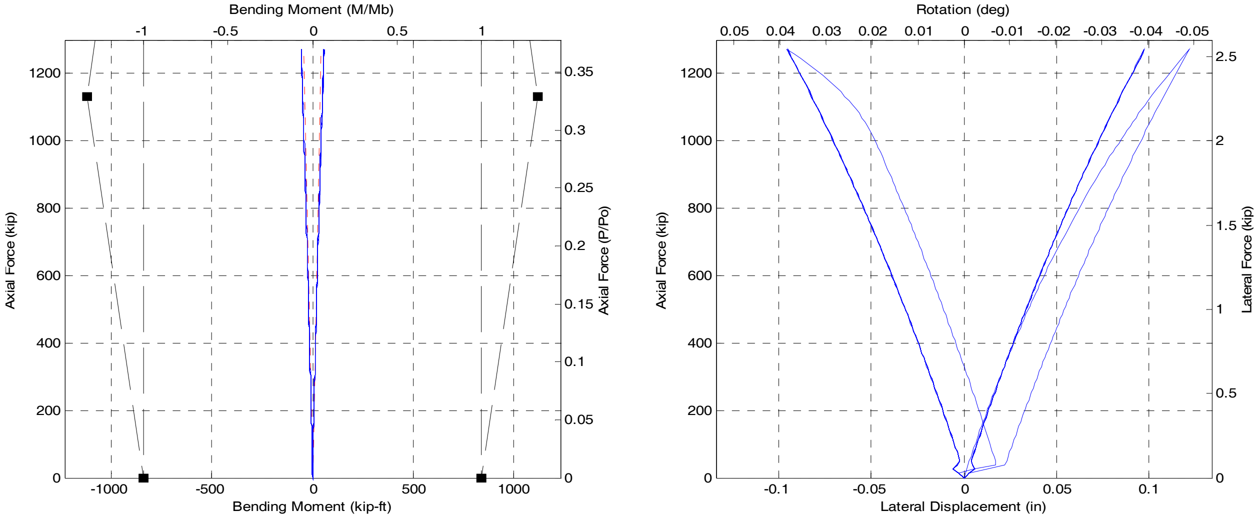

i) no eccentricity

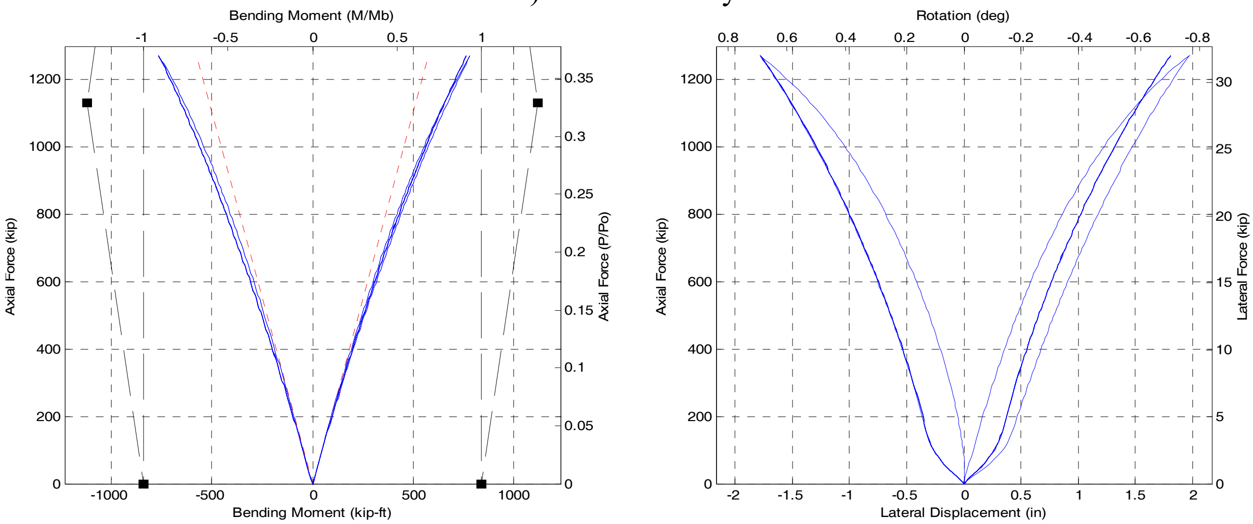

ii) 5in eccentricity

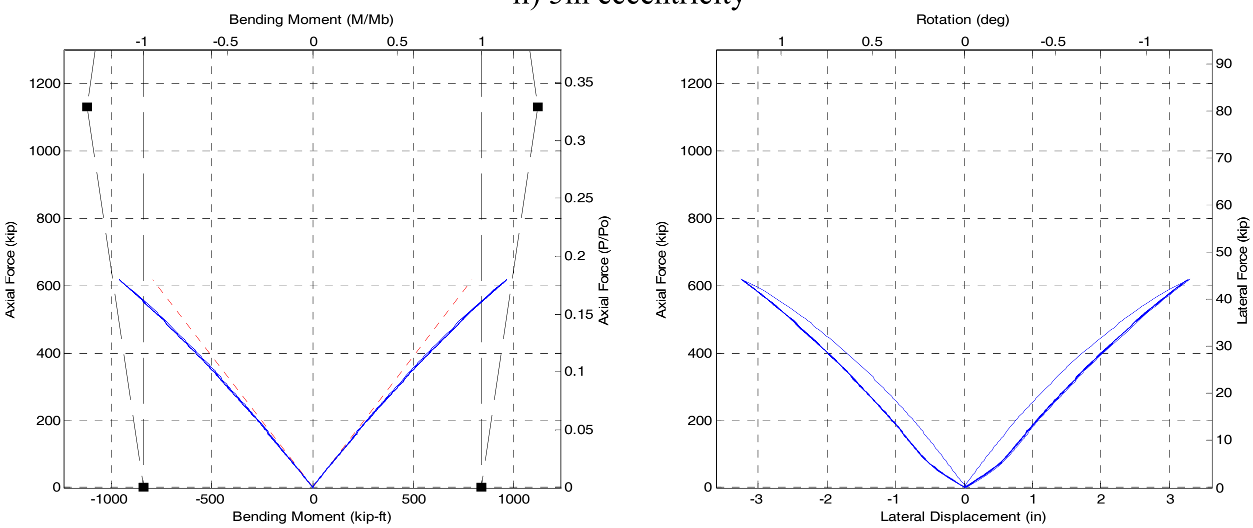

iii) 15in eccentricity

Figure 40. RCFT20x12x0.3125s Specimen (K=2, L=18ft, f'c=12ksi)

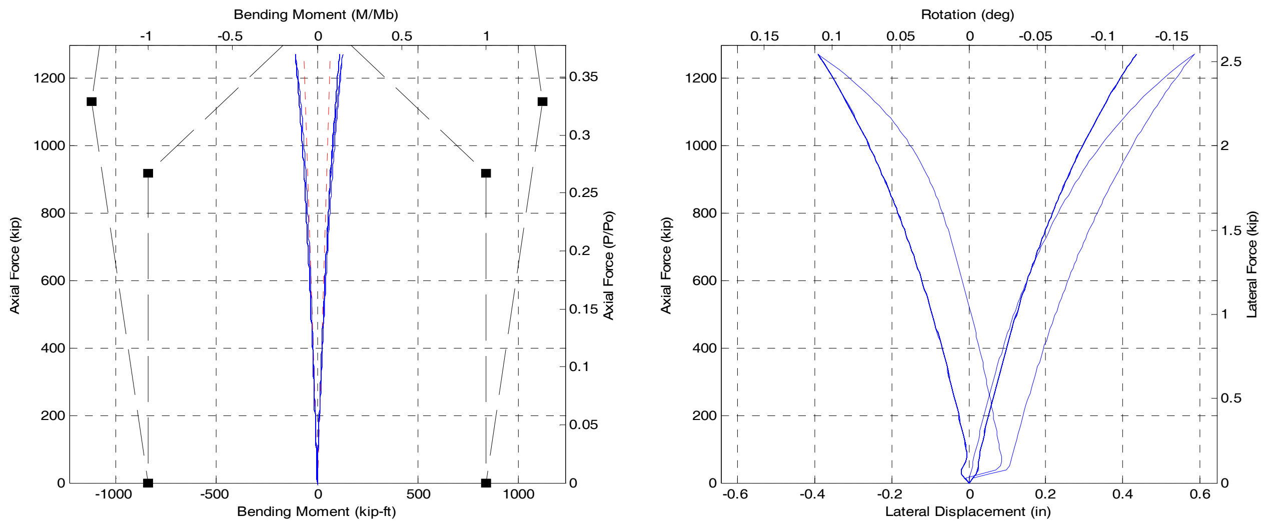

i) no eccentricity

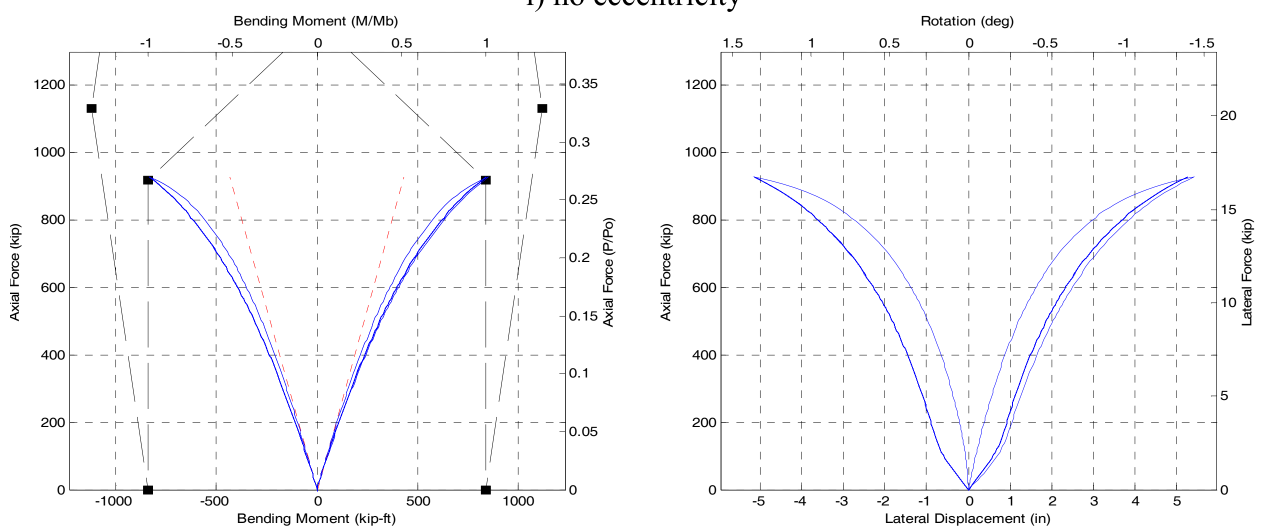

ii) 5in eccentricity

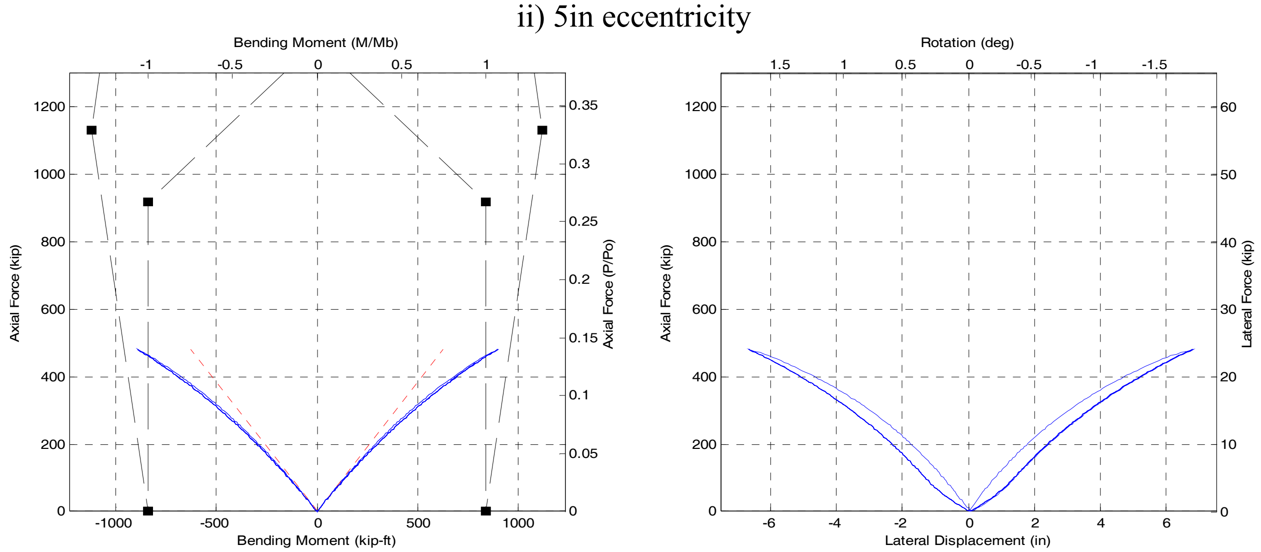

iii) 15in eccentricity

Figure 41. RCFT20x12x0.3125s Specimen (K=2, L=26ft, f’c=12ksi)

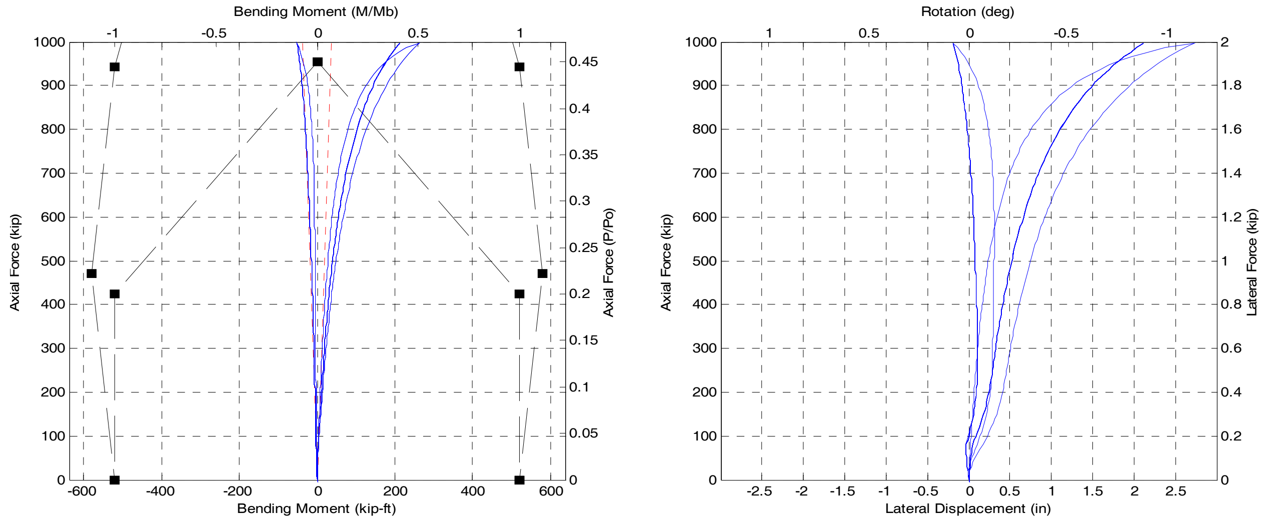

i) no eccentricity

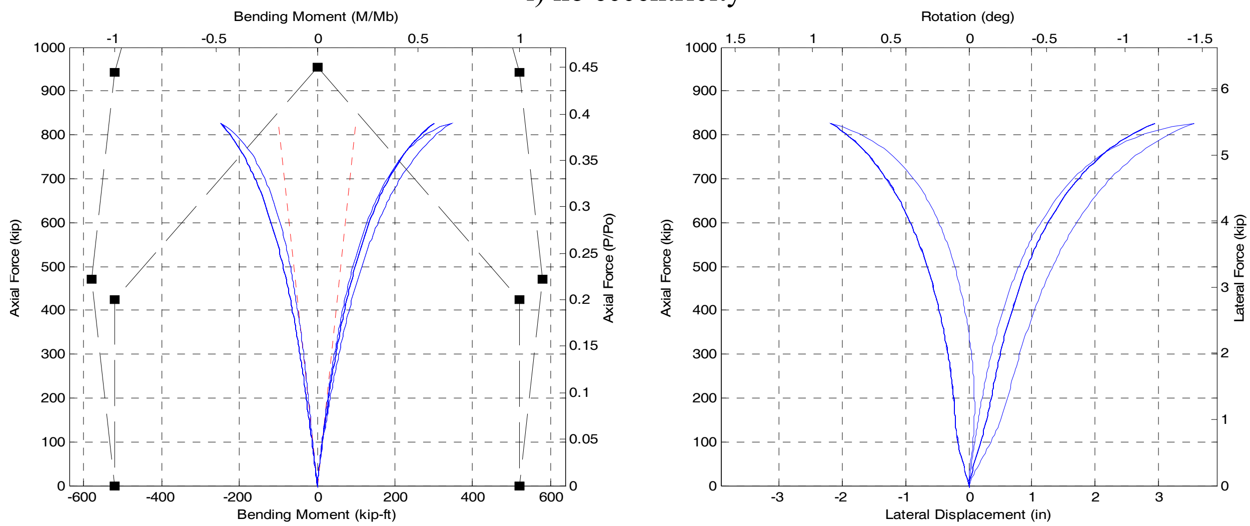

ii) 1in eccentricity

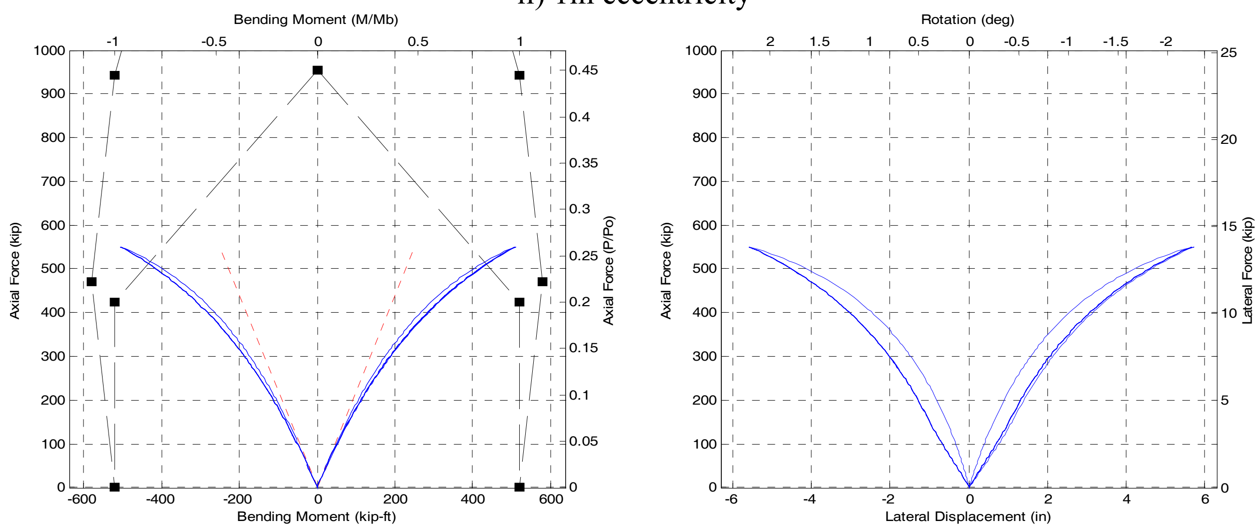

iii) 5in eccentricity

Figure 42. RCFT20x12x0.3125w Specimen (K=2, L=18ft, f'c=5ksi)

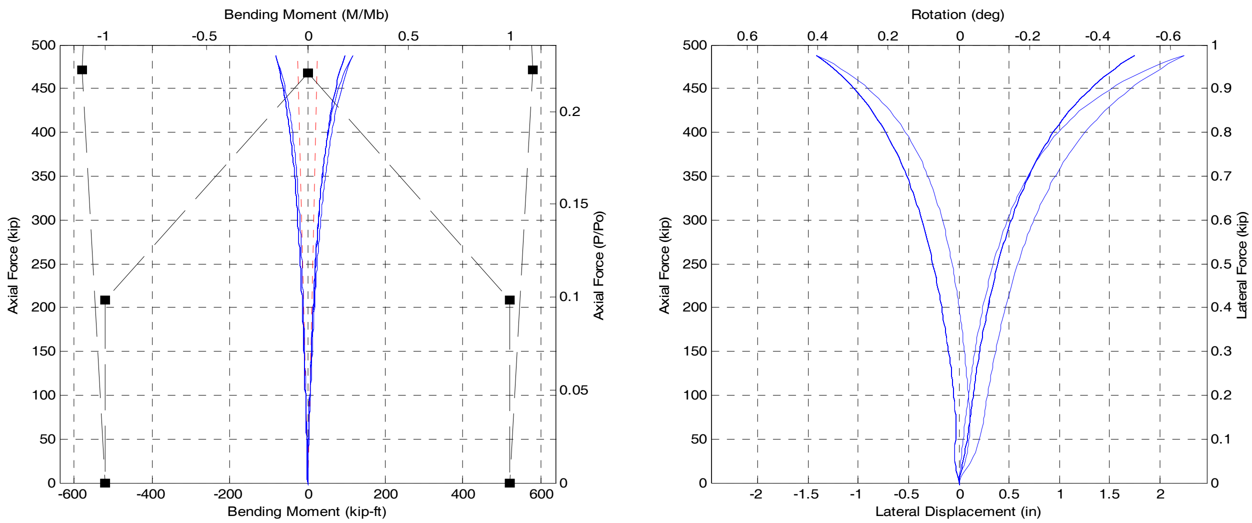

i) no eccentricity

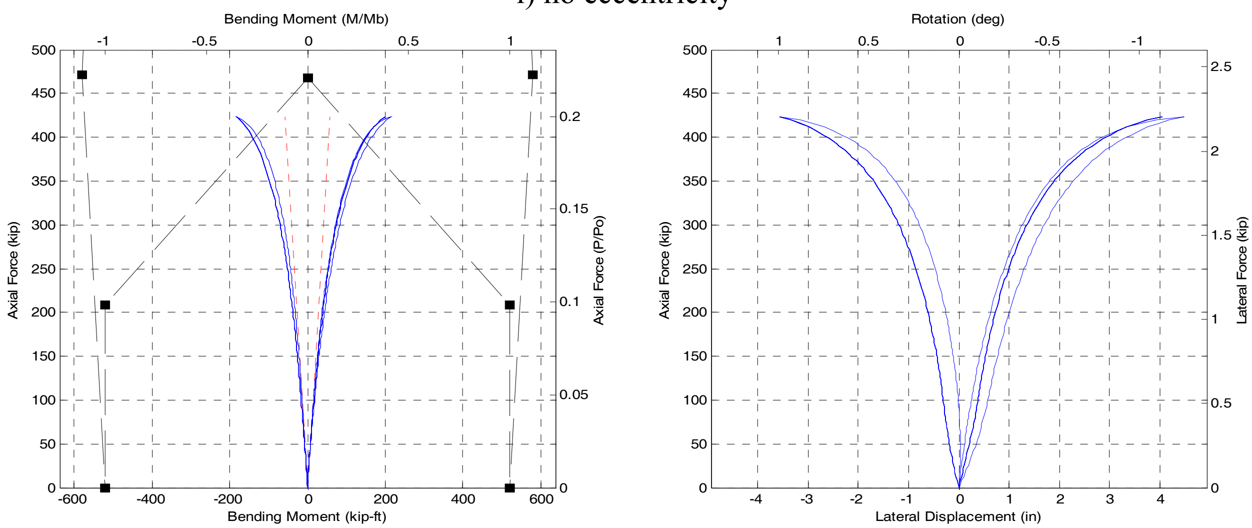

ii) 1in eccentricity

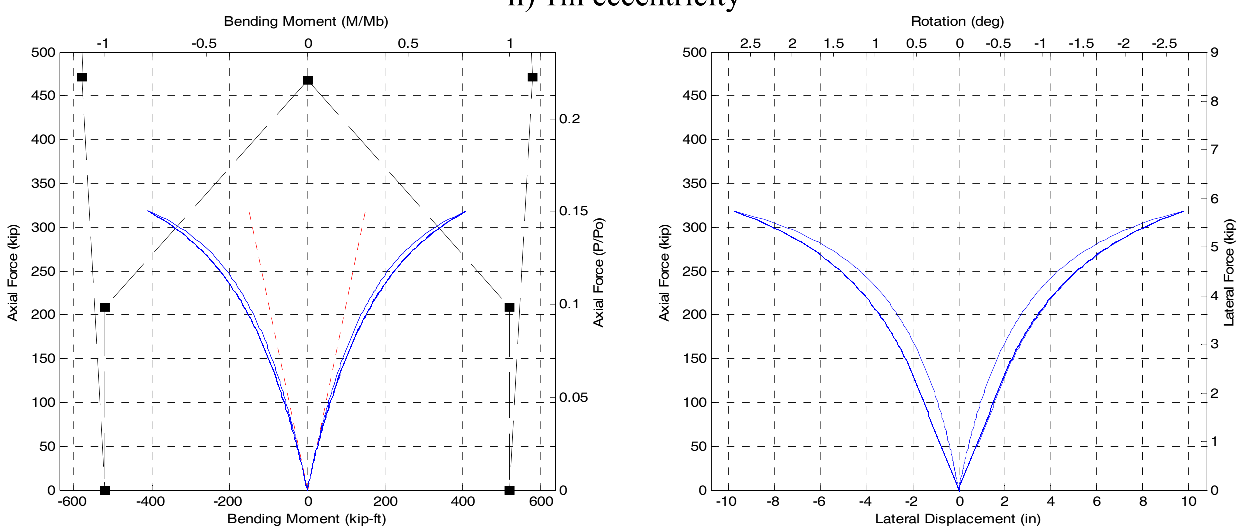

iii) 5in eccentricity

Figure 43. RCFT20x12x0.3125w Specimen (K=2, L=26ft, f'c=5ksi)

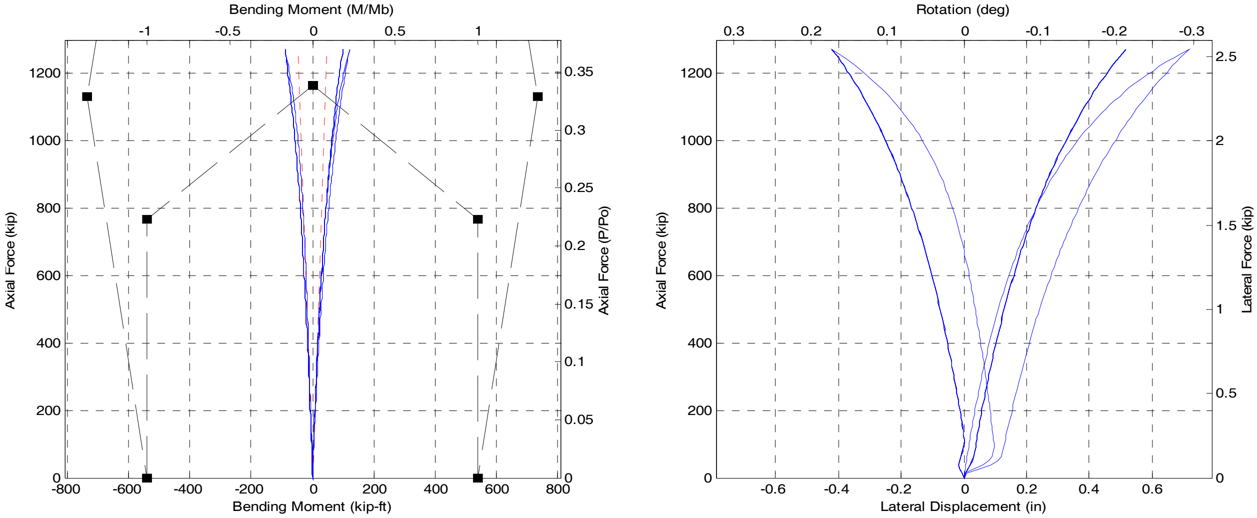

i) no eccentricity

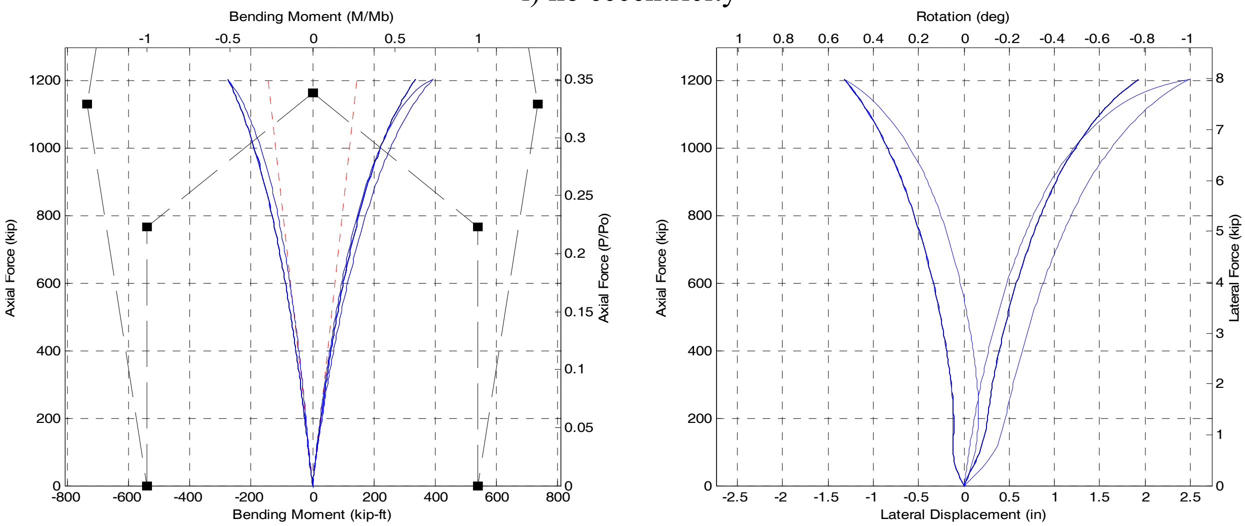

ii) 1in eccentricity

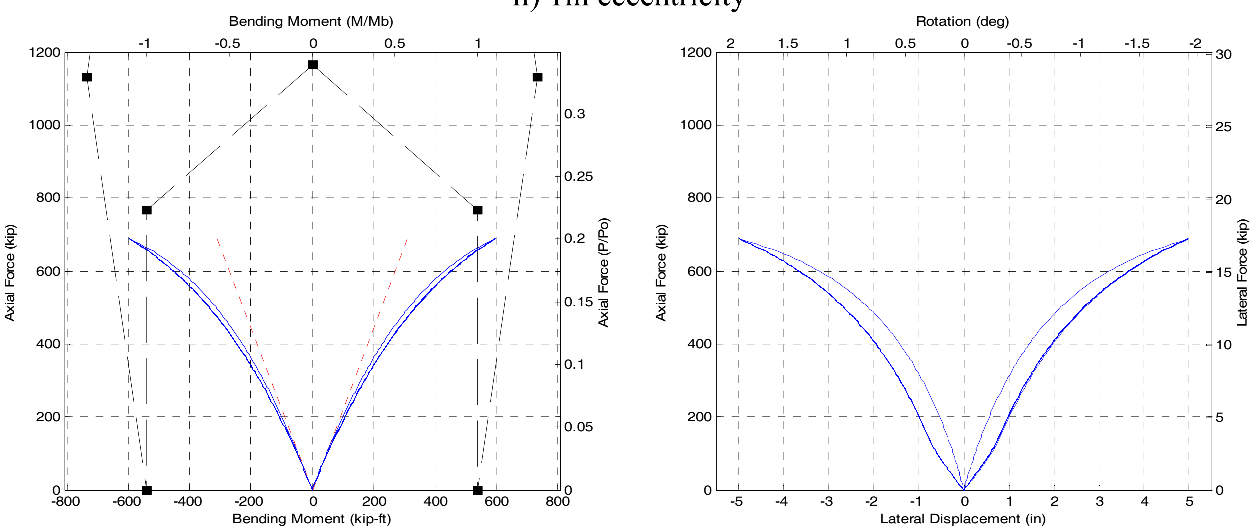

iii) 5in eccentricity

Figure 44. RCFT20x12x0.3125w Specimen (K=2, L=18ft, f'c=12ksi)

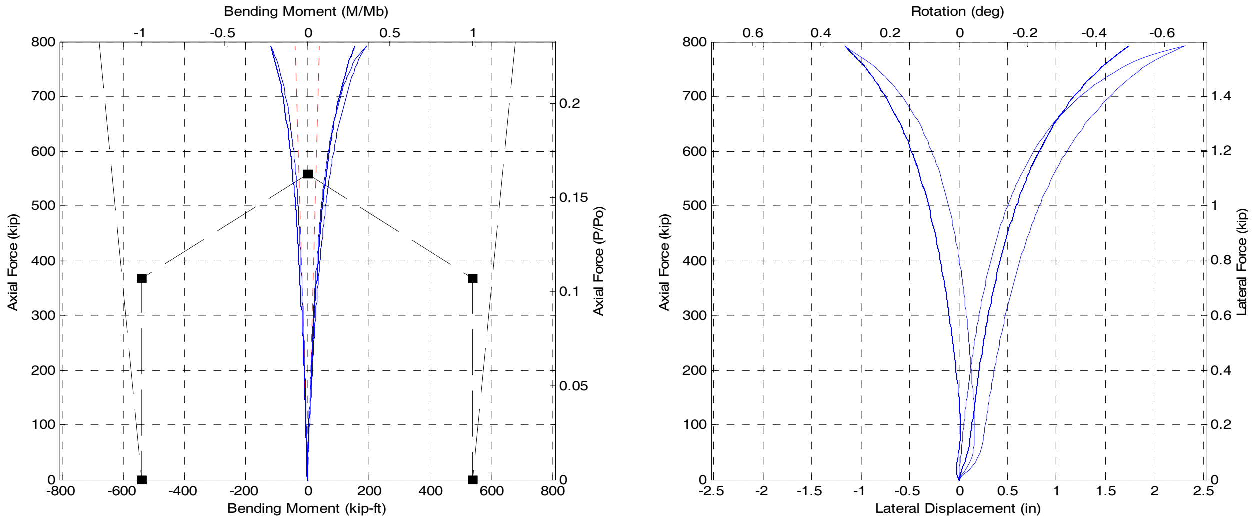

i) no eccentricity

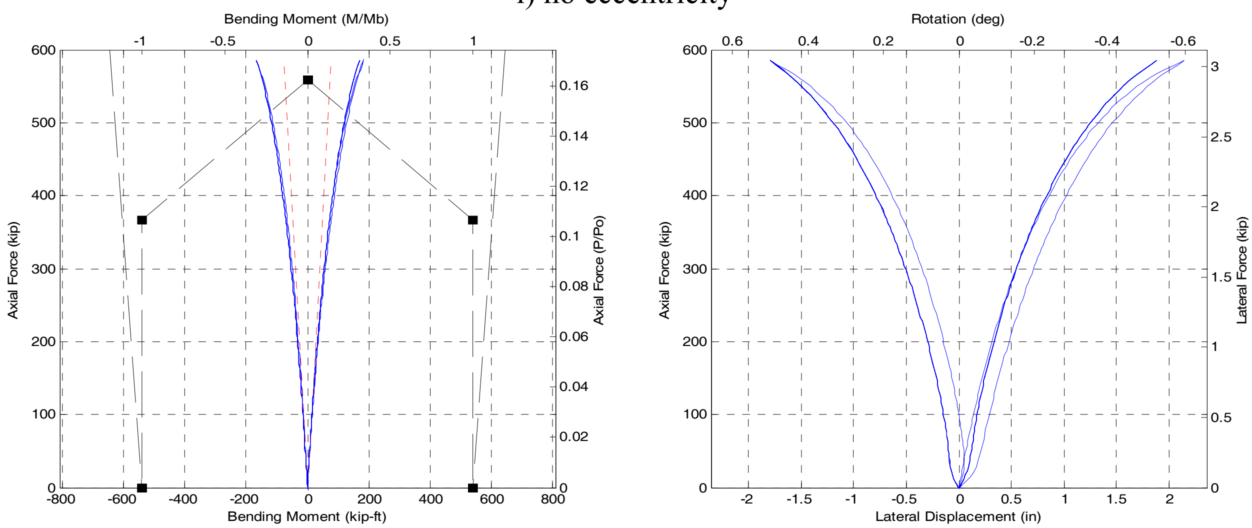

ii) 1in eccentricity

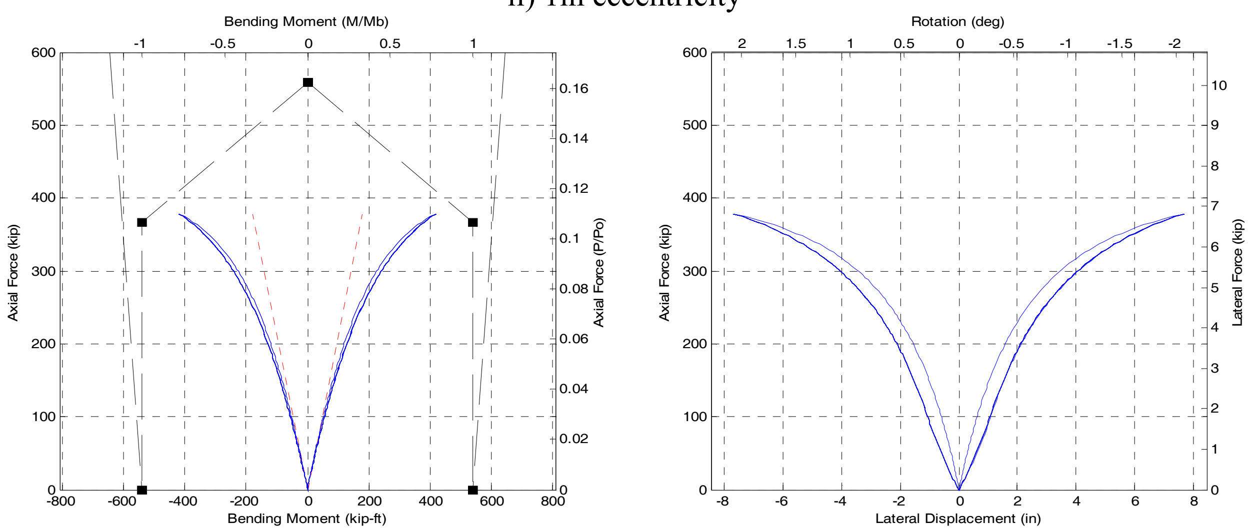

iii) 5in eccentricity

Figure 45. RCFT20x12x0.3125w Specimen (K=2, L=26ft, f'c=12ksi)

4.3.2 Analysis with constant compression load and variable lateral load

As previously described in Figure 29, a third alternative consists in the application of a constant axial load, which can be fixed with values from $0.1P_o$ to $0.6P_o$, and a lateral (monotonic or cyclic) displacement at the top, which may be proportional to lateral drift.

Results of fiber analysis on the CCFT20x0.25x18 specimen are shown in this section. This specimen assumed L/1000 of initial our-of-plumbness, $0.2P_o$ of constant compression load, and both monotonic (Figure 46) and cyclic (Figure 47) loads. These analyses were performed in OpenSees, and "Concrete04" behavior was used for modeling the confined concrete (f_c'=5ksi, f_{cc}'=6ksi, ε_o=0.002, ε_{cc}=0.0055, $ft=7\sqrt{f_c'}$, $\varepsilon_{uc}=80\varepsilon_o=29\varepsilon_{cc}=0.16$), while "hysteretic" behavior was used for modeling the steel ($+1.08R_yF_y$, $-0.89R_yF_y$, $+1.08R_uF_u$, $-0.89R_uF_u$, $\varepsilon_u=80\varepsilon_y$).

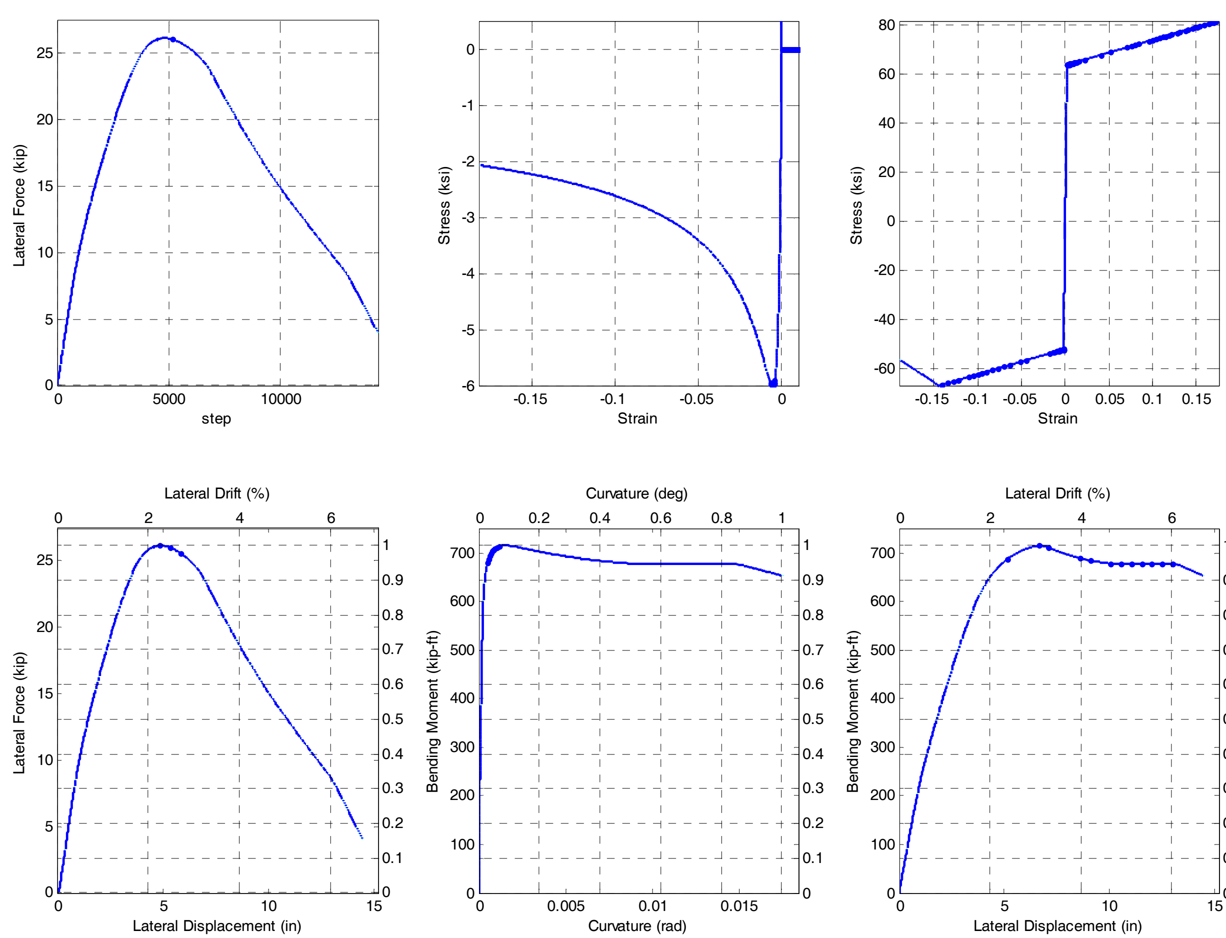

Figure 46. Fiber analysis on CCFT20x0.25x18 with monotonic load

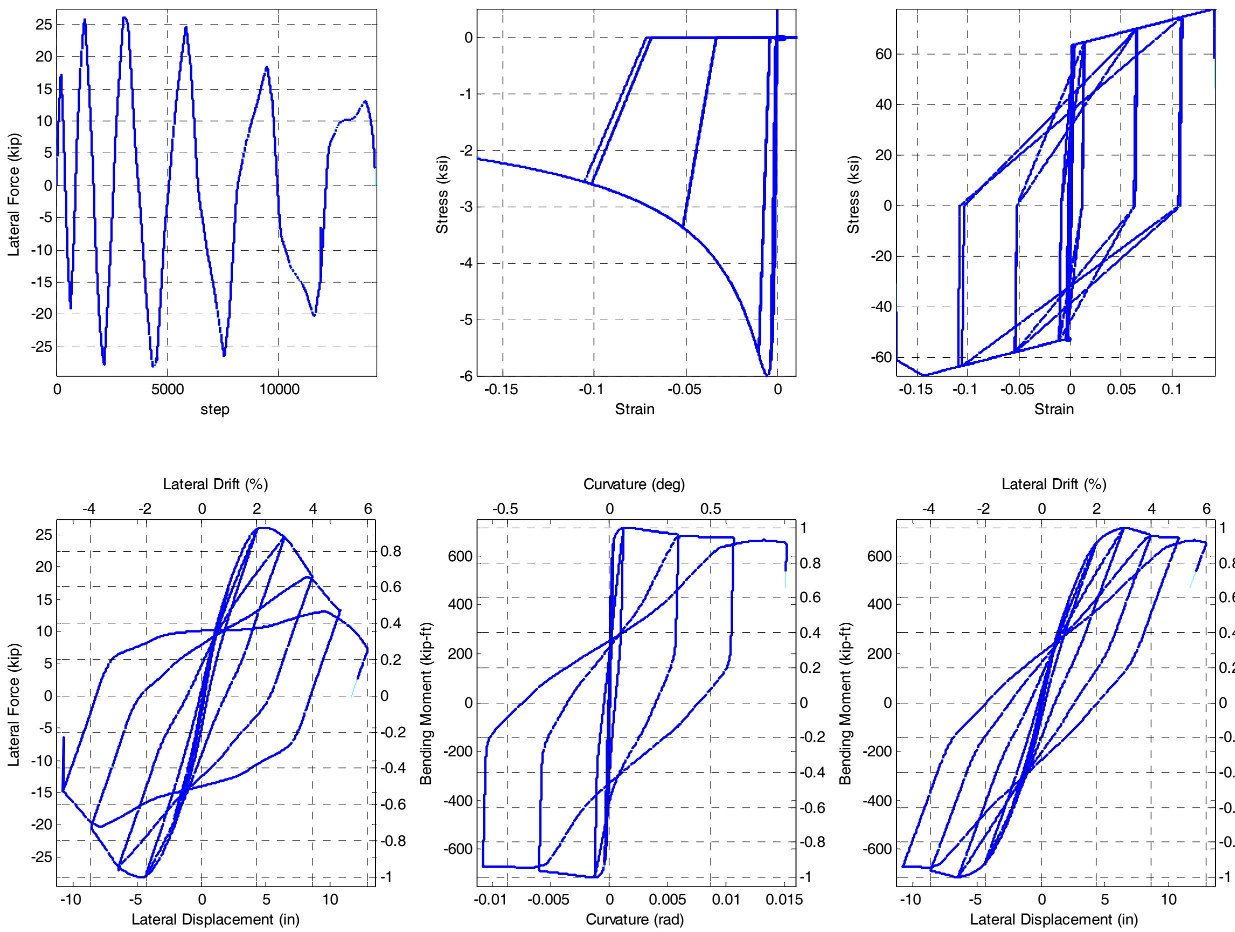

Figure 47. Fiber analysis on CCFT20x0.25x18 with cyclic load

4.4 Specimen Observation

Specimen observations during testing will be done in the following manner:

- Continuous observation will be done from the control room windows and through the video and still cameras in the robotic towers.
- Physical observation by the researchers will be done upon reaching the desired peak force and/or displacement targets.
- Photographs may be taken during the loading pauses after reaching peak levels.
- Overall pictures of damage and deformation will be taken during the loading pauses before and after reaching peak levels.

5 Data Management Plan

5.1 NEES Central Project Folder

A NEES Central project folder exists. The formal project folder name is: *NEESR-II: Inelastic NEESR-II: system behavior factors for composite and mixed structural systems*. The project folder nickname is: *NEESR-II CC*.

MAST personnel who are members of the project are: Carol Shield, Paul Bergson, Drew Daugherty, Jonathan Messier, and Angela Kingsley.

5.2 Data Transfer and Timing

The researchers will be responsible for transferring the data to NEES Central. The data transfer will be done within 1 month from the completion of the experiment.

5.3 Local Storage

Local storage at MAST has been requested and appropriate storage space has been created.

5.4 MAST IT Staff Assistance with NEES Central

At this time, no specific MAST IT assistance with NEES Central is envisioned.

5.5 NEES-IT Contact

The project's NEES-IT contact is:

Justin Fitzgerald
NEESit Support Specialist
justin@sdsc.edu
858-822-3602

6 Risk Management and Hazard Identification

6.1 Risk Management

6.1.1 Schedule

The following are events that may pose a risk on the schedule:

- Untimely delivery of the specimens to MAST
- Unavailability of the MAST testing space as anticipated due to other testing activities.
- Underestimation of the time to setup the experiment.
- Delays in the dismantling of the test setup after a test or for final clean-up.

The research team will work with the U. of Minnesota personnel to minimize the impact of these problems. The PIs are well aware that it is likely that some disruptions of this type will occur.

6.1.2 Moving Specimens

- Moving of the specimen poses safety risks during the lifting and rigging operations since they are very slender. Inappropriate lifting or rigging of the specimens could cause injury to workers and/or damage to items on the laboratory. The U. of Minnesota personnel will have the final say in any of these operations.

- The risk of damaging the columns is small. No damage is expected to happen to the specimens during the normal lifting and righting procedures. However, the specimen may be damaged if it is dropped; this is considered highly unlikely.

6.1.3 Damage to Internal Instrumentation

A very few strain gage cables will be protruding from the specimen. This cables run the risk of being cut off during rigging and moving. An effort will be made to protect the cables by attaching them to the specimen with duct-tape and snap ties.

6.1.4 Specimen Connection to Crosshead

Uplift between the crosshead bottom flange and the top plate of the specimen should be avoided. Some limited shimming (less than or equal to ¼ in.) may be needed. This movement will be monitored by knowing the rotation of the crosshead. If full contact is maintained between these two surfaces, the rotations should be the same.

6.1.5 Specimen Connection to Strong Floor

Uplift between the footing and the strong floor should be avoided. The base plate thicknesses and the vicinity of the bolts of the column will insure that this problem is minimized. The extensive FE analyses run do not show uplift. This will be visually and digitally monitored during the test. Some limited shimming (less than or equal to ¼ in.) may be needed.

6.1.6 Material (concrete) Quality Control

The major risk is improper consolidation of the concrete; proper admixtures to help fluidize and stabilize the mixture will be used. An experienced contractor recommended by MAST will be contacted to help with this process.

6.1.7 Testing Plan

The potential risks associated with the testing plan are:

- Difficulties on the application of the desired load/deformations due to the large number of degrees of freedom in force-control during the initial part of the test.

- Ensuring that the MAST staff is fully aware of the testing plan.

6.2 Hazard Identification

6.2.1 Working at Heights

Work at heights will be mostly during casting, instrumentation, assembly and disassembly. The following tasks carry risks:

- Loss of connection between the specimen and the support frame during casting. Extreme care will be taken before casting to ascertain the stability of the specimens
- Damaging of some instrumentation in the higher portions of the column during casting and moving. The risk is low as there is comparatively little instrumentation near the top of the specimen.
- White-wash painting of the top of the specimens when in position in the testing machine. This will be minimized by using a scissor-lift truck for this operation..

6.2.2 Power Equipment

Minimal power equipment will be used during the assembly/disassembly of the specimen. Proper training on the use of this equipment is expected to be provided by MAST and careful use of the equipment should be exercised at all times.

6.2.3 Demolition Activities

Demolition of the columns is simple, as we intend to dispose of the specimens in one piece.

6.2.4 Rigging/Moving Specimens

The specimen are very heavy and care should be taken during their rigging and moving as they may injure people and/or damage items in the laboratory.

6.2.5 Hand Tool Usage

Please see Section 6.2.2.

6.2.6 Structure Load Shedding

The failure of the specimens is presumed to be ductile and gradual. The robust control, provided by MAST should preclude any problems in this area. The major risk is a sudden fracture of the weld connecting the tube to the base plate. Even in this case, however, the specimen will not move appreciably.

6.2.7 Installation of Equipment underneath Specimen

Please see section 6.2.1.

6.2.8 Electrical

No electrical risks are foreseen. However, it is clear that care should be taken when dealing with electrically powered tools to make sure that they are used according to the manufacturers recommendations.